

For Reference

NOT TO BE TAKEN FROM THIS ROOM

Ex LIBRIS
UNIVERSITATIS
ALBERTAENSIS



For Reference

NOT TO BE TAKEN FROM THIS ROOM

THE UNIVERSITY OF ALBERTA

THE EFFECT OF TEMPERATURE AND VARYING SALT
CONCENTRATIONS ON THE STRUCTURE OF WATER

BY



NOEL MICHAEL BURNS

A THESIS

SUBMITTED TO THE FACULTY OF GRADUATE STUDIES
IN PARTIAL FULFILMENT OF THE REQUIREMENTS FOR THE DEGREE
OF DOCTOR OF PHILOSOPHY

DEPARTMENT OF CHEMISTRY

EDMONTON, ALBERTA

JULY, 1968



Digitized by the Internet Archive
in 2020 with funding from
University of Alberta Libraries

<https://archive.org/details/NMBurns1968>

Thesis
1968 (E)
13 D

UNIVERSITY OF ALBERTA
FACULTY OF GRADUATE STUDIES

The undersigned hereby certify that they have
read, and recommend to the Faculty of Graduate Studies
for acceptance, a thesis entitled

THE EFFECT OF TEMPERATURE AND VARYING
SALT CONCENTRATIONS ON THE STRUCTURE OF WATER

submitted by NOEL MICHAEL BURNS, in partial fulfilment
of the requirements for the degree of Doctor of
Philosophy.

Abstract

An examination of published data on a number of the physical properties of water was carried out in an effort to determine the minimum number of distinct species necessary to explain the physical behaviour of water. A consideration of the excess acoustical absorbance of ultrasound by water and the partial molal heat capacities of salts at infinite dilution led to the conclusion that the existence of at least three species of water aggregates is necessary to explain these two phenomena.

An analysis of the specific volumes of water over the temperature range 0° - 100° led to the postulate that a low concentration (mole fraction = 0.043 at 0°) of a truly ice-like species of water, H_2O_I , exists at temperatures below 60° . A careful analysis of the specific heat of water from 0 to 100° , together with the assumption that only one relatively unassociated species of water exists above 180° , led to the postulation of the existence of a second species of water, H_2O_{II} , which decreases linearly in concentration with temperature from a mole fraction of 0.57 at 0° to 0.23 at 100° . H_2O_{II} is thought to transform into a third species of water, H_2O_{III} , as the temperature is increased. It is considered that H_2O_I has 2.0 hydrogen bonds per molecule, H_2O_{II} has 1.8

hydrogen bonds per molecule and $\text{H}_2\text{O}_{\text{III}}$ has 1.2 hydrogen bonds per molecule.

With this model of water it was possible to predict the heat capacity of water from 100° to 20° to within 1% and from 20° to 0° to within 3%. The specific volumes and isothermal compressibilities of various concentrations of KF and KI solutions (0.0 m to 2.0 m between 0° and 100°) were determined to see whether the water in these solutions behaved in a manner predicted by the model of water constructed here.

An analysis of the measured specific volumes of the salt solutions led to the conclusion that the postulate regarding the existence of $\text{H}_2\text{O}_{\text{I}}$ is correct and that $\text{H}_2\text{O}_{\text{I}}$ is more strongly broken down in solutions by KI than by KF. In order to explain the specific volume findings, it was also necessary to postulate the existence of $\text{H}_2\text{O}_{\text{II}}$ and that it breaks down into $\text{H}_2\text{O}_{\text{III}}$ increasingly with increasing temperature. It was also concluded that the F^- ion breaks down $\text{H}_2\text{O}_{\text{II}}$ more strongly than the I^- ion in dilute solution but that this effect is reversed at concentrations above 0.6 m.

A consideration of the isothermal compressibility measurements led to the same conclusions as those of the specific volume measurements except that it was not

necessary to postulate the existence of $\text{H}_2\text{O}_\text{I}$ to explain the compressibility results. Both the specific volume and compressibility studies indicated the existence of $\text{H}_2\text{O}_\text{II}$ at concentrations above 2.0 m at all temperatures.

Acknowledgements

It is a pleasure to acknowledge the support of the director of this work, Dr. H. B. Dunford.

The help of other graduate students, particularly in regard to the assistance given with computer programming, is much appreciated.

The financial assistance of the University of Alberta and the Province of Alberta is most gratefully acknowledged.

Table of Contents

	Page
Chapter I - Introduction	1
Chapter II - Pure Water	
Experimental Data	6
Results	8
Discussion	20
Conclusions	60
Chapter III - Specific Volumes of Salt Solutions	
Introduction	62
Experimental	63
Results	69
Discussion	74
Conclusions	103
Chapter IV - Compressibilities of Salt Solutions	
Introduction	104
Experimental	107
Calculations	112
Results	114
Discussion	125
Conclusions	132
Bibliography	134

List of Tables

Table		Page
I	Temperature of Minimum Compressibility vs. Temperature	14
II	Mole % Bulky Species at Various Temperatures .	23
III	Observed and Calculated Heat Capacities of Water; Enthalpy Differences between H_2O_{II} and H_2O_{III} at Different temperatures	39
IV	Concentration of Each Species of Water with Temperature, Comparison of Observed and Predicted Heat Capacities	45
V	Variation of Volume and Concentration of Each Species of Water with Temperature . . .	48
VI	Variation of Excess Acoustic Absorbance by H_2O_I and H_2O_{II} with Temperature	55
VII	Specific Volumes of KI Solutions at Various Temperatures	70
VIII	Specific Volumes of KF Solutions at Various Temperatures	72
IX	Adiabatic Compressibilities of KI Solutions at Various Temperatures	115
X	Adiabatic Compressibilities of KF Solutions at Various Temperatures	117
XI	Isothermal Compressibilities of KF Solutions at Various Temperatures	119

Table	Page
XII	
Isothermal Compressibilities of KI	
Solutions at Various Temperatures	121

List of Figures

1.	(a) Specific Volume, V , vs. Temperature	8
	(b) dV/dt vs. Temperature	9
2.	(a) Specific Heat, C , vs. Temperature	10
	(b) dC/dt vs. Temperature	11
3.	(a) Isothermal Compressibility, K , vs Temperature	12
	(b) dK/dt vs. Temperature	13
4.	Log n vs $1/T$	16
5.	Excess acoustical Absorption vs. Temperature. . .	17
6.	Integrated Raman Intensities of Water	
	without Filter vs. Temperature	19
7.	Integrated Raman Intensities of Water	
	with Filter vs. Temperature	19
8.	Variation of Enthalpies of Bulky and Dense Species with Temperature	24
9.	Partial Molar Heat Capacities of Alkali Halides at Infinite Dilution	29
10.	Specific Heat of Ice vs. Temperature	36
11.	dV/dt vs. Temperature ($0^\circ - 240^\circ$)	41
12.	Comparison of Observed and Calculated heat Capacities	46
13.	Energy Level Diagram for Three Species of Water	50

	Page
14. Excess Acoustic Absorbance due to $\text{H}_2\text{O}_\text{I}$ vs. Concentration	56
15. Excess Acoustic Absorbance due to $\text{H}_2\text{O}_\text{II}$ vs. Concentration	57
16. Fisher Density Bottle	63
17. Expansivity of KF Solutions (0.0 to 0.2m) vs. Temperature	75
18. Expansivity of KF Solutions (0.4 to 0.8m) vs. Temperature	76
19. Expansivity of KF Solutions (1.0 to 1.4m) vs. Temperature	77
20. Expansivity of KF Solutions (1.6 to 2.0m) vs. Temperature	78
21. Expansivity of KI Solutions (0.0 to 0.2m) vs. Temperature	79
22. Expansivity of KI Solutions (0.4 to 0.8m) vs. Temperature	80
23. Expansivity of KI Solutions (1.0 to 1.4m) vs. Temperature	81
24. Expansivity of KI Solutions (1.6 to 2.0m) vs. Temperature	82
25. Expansivity of KI and KF solutions vs. Concentration	83
26. Temperature of Disappearance of $\text{H}_2\text{O}_\text{I}$ vs. Concentration	85

	Page
27. (a) Partial Molal Volumes of KF vs. Temperature	91
(b) Partial Molal Volumes of KF vs. Temperature	92
28. (a) Partial Molal Volumes of KI vs. Temperature	94
(b) Partial Molal Volumes of KI vs. Temperature	95
29. Expansivity at 0° if no H ₂ O _I were Present vs. Concentration	98
30. Wave Length of Central Relaxation vs. Concentration for Various Electrolytes	99
31. Piezometer for measuring adiabatic compressibilities	108
32. Isothermal Compressibilities of Water, 2m KI and 2m KF Solutions vs. Temperature	124
33. Partial Molal Isothermal Compressibilities of KF vs. Temperature	126
34. Partial Molal Isothermal Compressibilities of KI vs. Temperature	127

CHAPTER I

Introduction. On the Structure of Water

For many years there has been considerable interest in the nature of liquid water, yet even now there is little unanimous agreement among scientists on the matter, as revealed by the reviews of Frank ⁽¹⁾ and Kavanau. ⁽²⁾

Röntgen ⁽³⁾ in 1892 proposed that liquid water was a solution of ice in a denser, fluid water species. In 1933, Bernal and Fowler ⁽⁴⁾ proposed that water was; 1) ice-like at temperatures below 4°C; 2) quartz-like between 4° - 200°; 3) ammonia-like and close-packed between 200° - 340°. They said that the forms are not distinct and pass continuously from one into another. Leonard-Jones and Pople ⁽⁵⁾ in 1951 suggested a different model. They proposed that, 1) the molecules in liquid water have essentially the same number of bonds as in ice but that these bonds are more flexible than in ice and are able to bend independently, which is not possible in the ice lattice; 2) when ice melts, some of the molecules move into the formerly unoccupied regions of the tridymite-like ice lattice, leading to the observed volume diminution. This model still has wide acceptance.

Another widely accepted model is the 'flickering-cluster' model of Frank and Wen, ^(6,7) proposed in 1957. Their theory takes into account the fact that the polarization of a water molecule increases with the formation of a

hydrogen bond and this increased polarization facilitates further bond formation. Thus a cluster of molecules which are highly hydrogen bonded builds up rapidly. Similarly, the breaking of a bond in a cluster leads to its rapid breakdown. These clusters are mixed with non-hydrogen bonded molecules. This model envisages that water consists of an equilibrium mixture of single molecules and clusters thereof.

Pauling ⁽⁸⁾ in 1959 suggested that water could consist, in part, of structures which are found in the gas-hydrate crystals. In these structures, pentagonal dodecahedra consisting of 20 water molecules, each of which participates in 3 hydrogen bonds, link together to enclose a gas molecule. Pauling proposed that water consists of a labile arrangement of gas hydrate structures in which the enclosed regions are occupied by unbonded water molecules.

The previously mentioned flickering clusters could have the form of Pauling's hydrate structures and in 1961 Frank and Quist ⁽⁹⁾ analysed the Pauling model. They found that they could account for the heat capacity of water only by considering that their model contained 3 species; framework water, interstitial water (freely rotating monomers) and a third class of water molecules which was neither framework nor interstitial water.

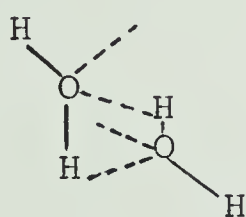
Wada ⁽¹¹⁾ has published a simplified model for the structure of water based on the assumption that at 100°, 20% of the water is in the form very similar to ice and the remainder of the water is in a state similar to that of unassociated liquids. He obtained good agreement between measured thermodynamic quantities and those predicted by his model in the range 0° - 20°.

Grjotheim and Krogh-Moe ⁽¹⁰⁾ have proposed a similar model in which they assume that 25% of the water is icelike at 100° and that this fraction disappears completely at 170°. Good agreement was obtained between measured and calculated values of the heat of fusion of ice and magnetic susceptibility of water in the range 0 to 70°.

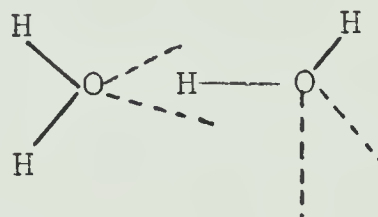
Davis and Litovitz ⁽¹²⁾ in 1965 proposed a two state theory of liquid water, in which one of the states was described as water molecules linked together with straight hydrogen bonds forming an ice-like lattice of puckered hexagonal rings. They proposed that the second state consisted of the same puckered hexagonal rings but that these rings were linked together in a more compact arrangement than in the first state. This compact arrangement, however, requires a number of bent hydrogen bonds and non-hydrogen-bonded neighbors.

In 1966 Wicke, ⁽¹³⁾ after considering the transformation of normal bulky ice I into the much denser

ice III (2050 atm pressure and -22°) and the even denser ice II (2100 atm, -34.5°) both of which contain shortened and bent hydrogen bonds, proposed that water consists of clusters of molecules in the bulky ice I arrangement and aggregates of molecules linked together with bent or dipolar hydrogen bonds, together with non-hydrogen bonded molecules. The types of dipolar hydrogen bonds between water molecules are (14,15);



(a)



(b)

From the results of two recent spectroscopic studies^(16,17) it has been suggested that water is a continuum either in the sense of the model of Pople⁽⁵⁾ or in the sense of an infinite number of distinct structures.

This brief summary of the literature on the structure of liquid water shows that there are a diversity of opinions on the subject. There appears an obvious need for further work of possible relevance to liquid water structure and the results of three approaches used in this laboratory are summarized in the following chapters. Chapter II summarizes a re-analysis of existing data on

physical properties of water as a function of temperature. New experimental measurements of the specific volumes of aqueous solutions of potassium fluoride and potassium iodide as a function of temperature and salt concentration are described in Chapter III, along with an interpretation of the experimental results. In a similar fashion, Chapter IV describes results on the compressibilities of aqueous solutions of KI and KF as a function of temperature and salt concentration.

CHAPTER II

The Effect of Temperature on the Structure of Water

1. - Experimental Data

The experimental values which are quoted in the literature for specific volume,⁽¹⁸⁾ specific volume as a function of temperature and pressure,⁽¹⁹⁾ specific heat,⁽²⁰⁾ excess acoustic absorbance⁽²¹⁾ and specific viscosity,⁽²²⁾ were analysed here in a number of different ways in an attempt to obtain the most relevant information on the nature of the structure of water.

The values of dx/dt vs t were examined, where t represents temperature in degrees Celsius and x represents specific volume,^(18,19) specific heat⁽²⁰⁾ and isothermal compressibility.⁽¹⁹⁾ The isothermal compressibility of water, K , was calculated for temperatures from 0° to 150° and pressures from 0.0 bar to 1000 bar from the data of Kell and Whalley.⁽¹⁹⁾ The values of K at each temperature for a given pressure were fitted to a polynomial expression of the form,

$$K = \sum_{i=1}^5 \sum_{j=0}^4 C_i t^j$$

to within 1 part in 10^4 , where t = temperature in degrees Celsius and C_i are constants. This expression was then differentiated to obtain values for dK/dt at each pressure and temperature.

The accuracy of the equation for the best-fit straight line segment of Fig. (1b) was checked against the original V vs t data by integration:

$$V = \frac{1}{2} at^2 + bt + k$$

The constant k was evaluated by inserting values for V into eqn. (1) at temperatures of 60°, 70°, 80°, 90°, 100° and was found to be invariant. The resulting equation is

$$V = (3.11 t^2 + 162 t) 10^{-6} + 0.99613 \text{ ml/gm} \quad (1)$$

where t is the temperature in degrees Celsius. From 100° to 59° eqn. (1) predicts the experimental values to the sixth significant figure. Below 59°, the difference, D_V , between the observed volume, V_{obs} and that calculated from eqn. (1), $D_V = V_{\text{obs}} - V$ increased steadily with decreasing temperature.

Our analysis of the specific volume data of Kell and Whalley ⁽¹⁹⁾ shows that this data can be more easily fit to a quadratic equation than to a cubic or quartic equation in the range of 50° to 140°, showing that dV/dt is linear in this range.

In addition excess acoustical absorbance ⁽²¹⁾ and the log of specific viscosity ⁽²²⁾ were examined as a function of temperature. The recent Raman spectra of water obtained by Walrafen ⁽²³⁾ were carefully considered.

2 - Results

Fig. (1a) shows the plot of specific volume V vs temperature, t . The derivative curve, of dV/dt vs t ,

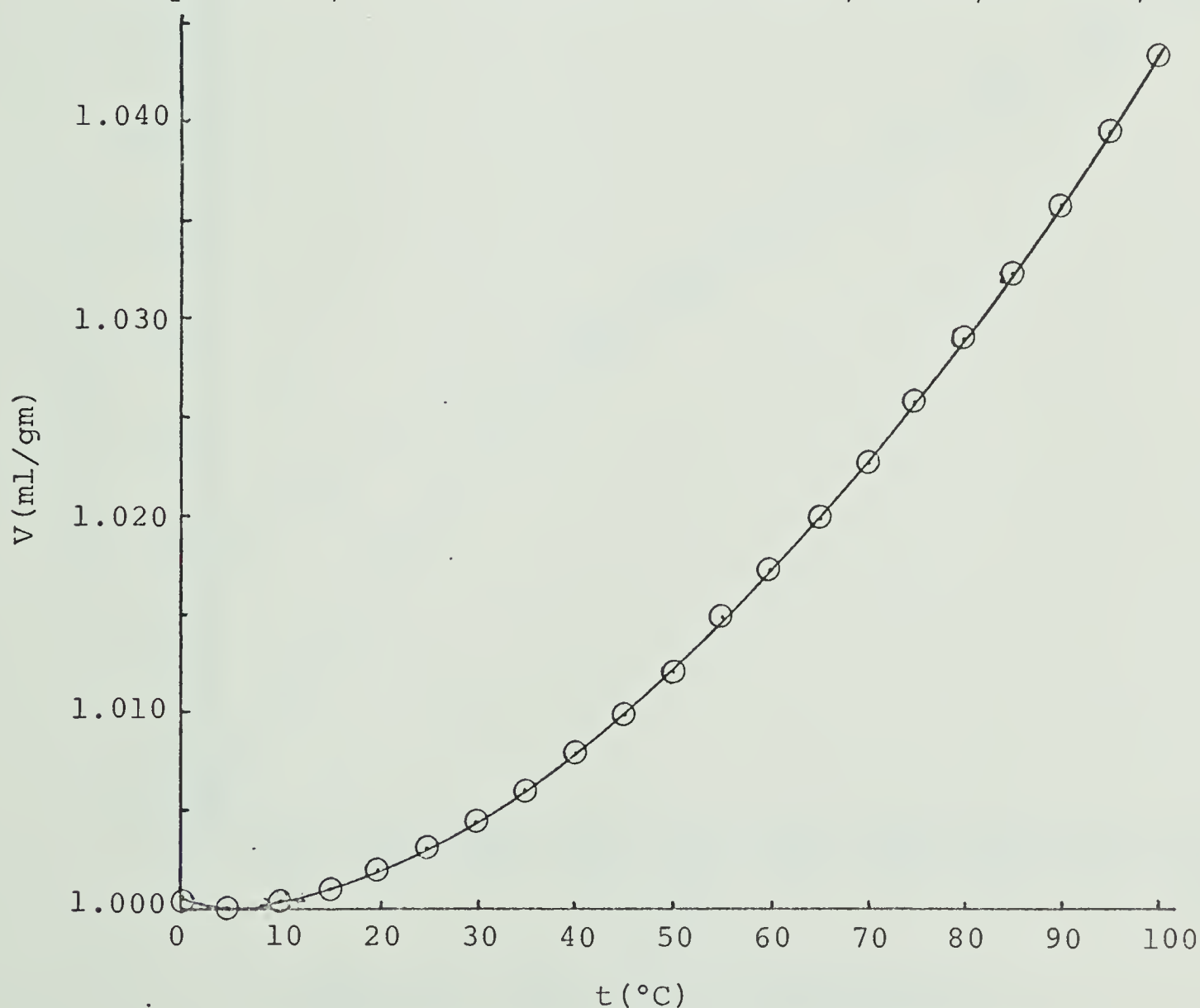


Fig. 1a. Specific Volume, V vs Temperature, t .

obtained from the data in Fig. (1a), is shown in Fig. (1b). It consists of two distinct sections: one from 0° to 58° is curved and the other from 58° to 100° is a straight line.

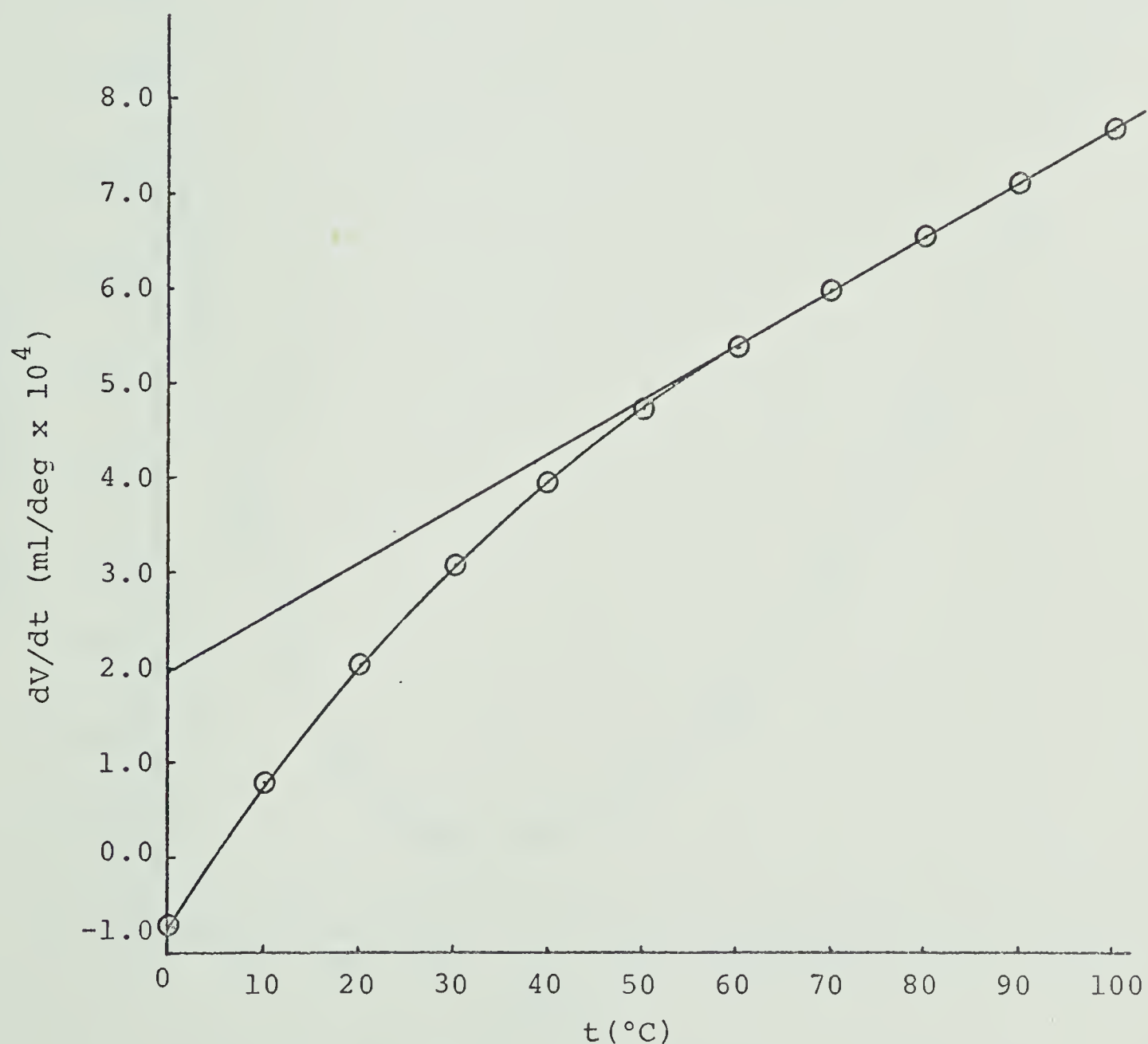


Fig. 1b. DV/dt , V' vs Temperature, t .

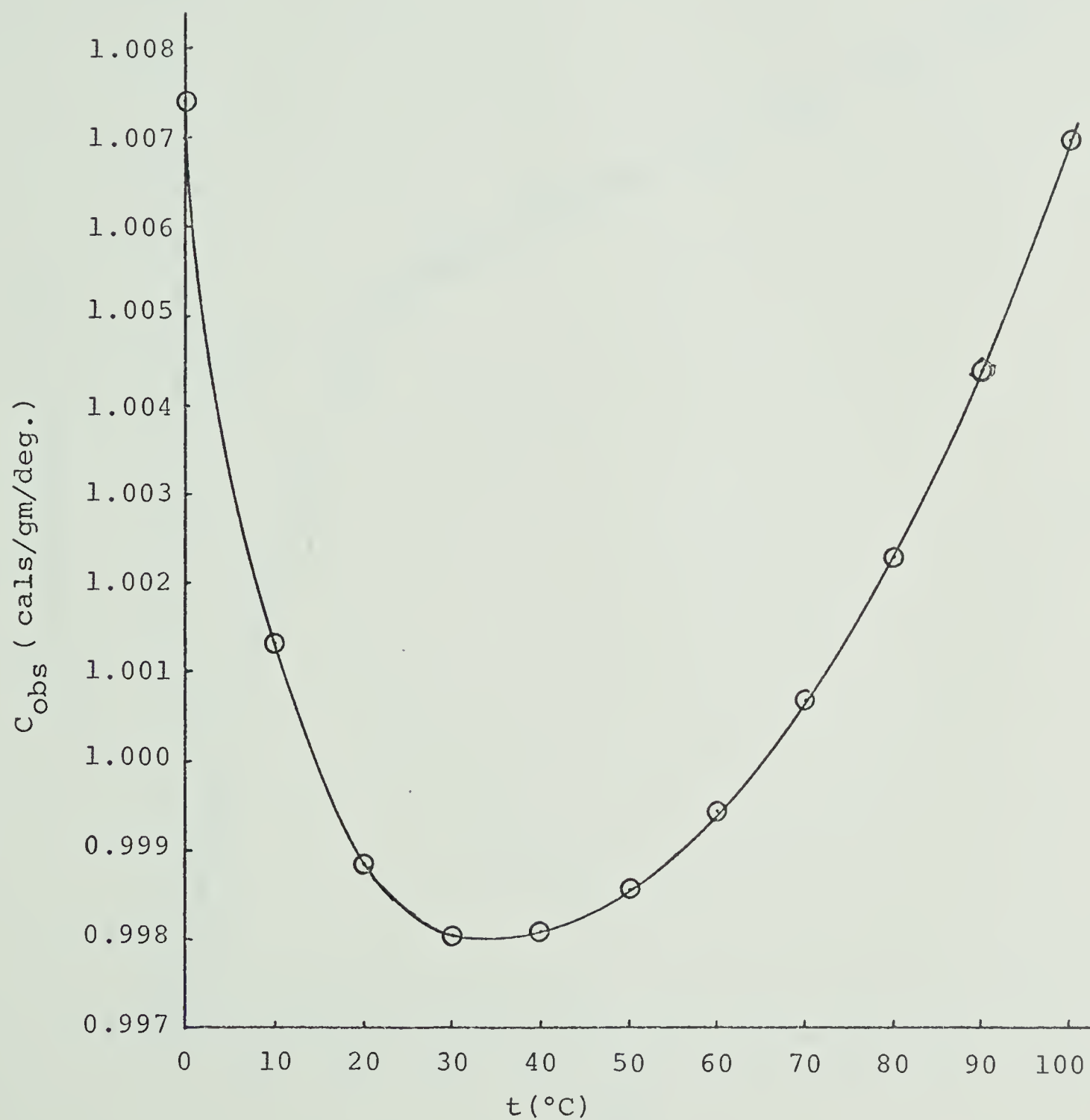


Fig. 2a. Specific Heat, C vs Temperature, t .

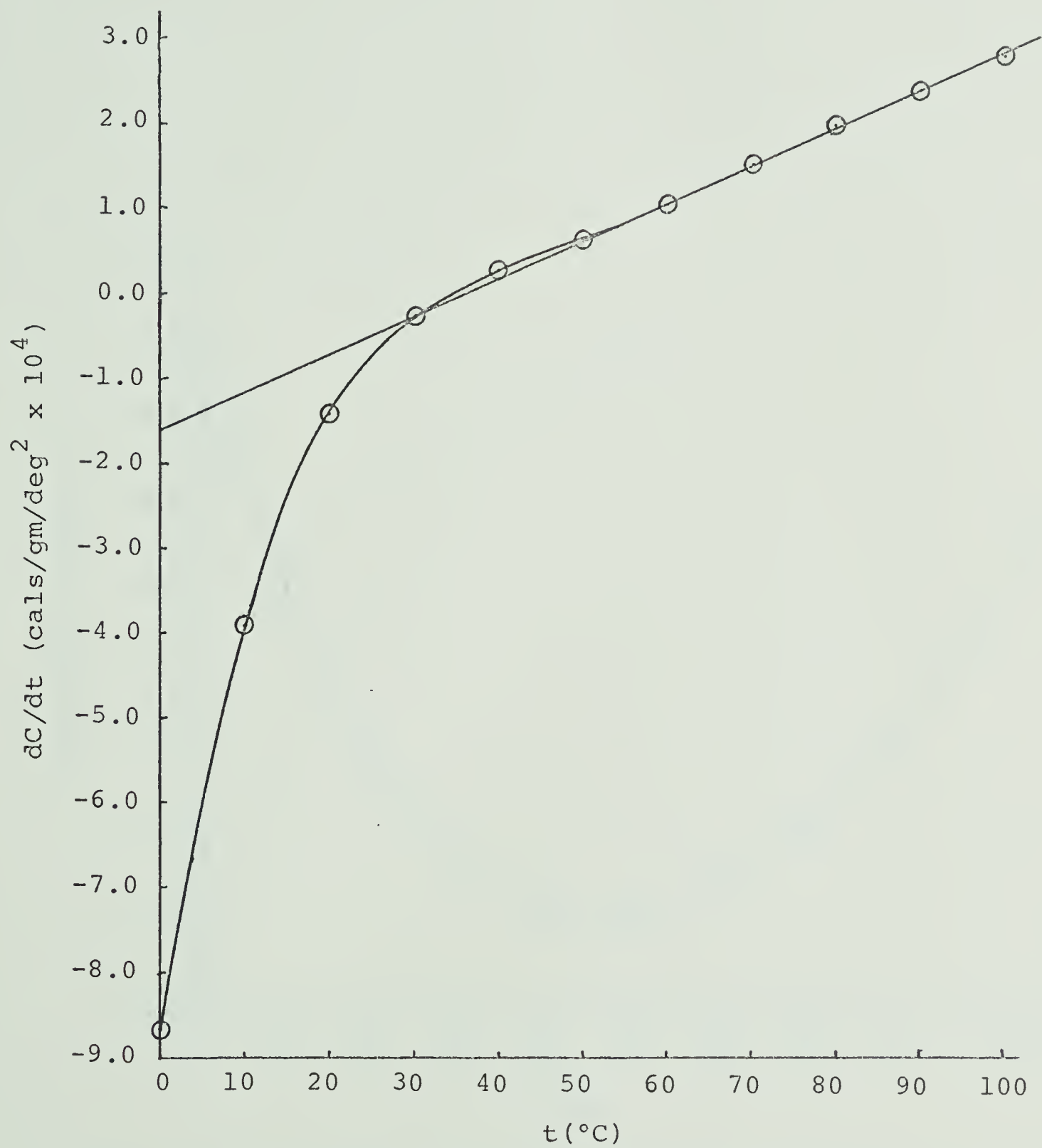


Fig. 2b. DC/dt , vs Temperature, t .

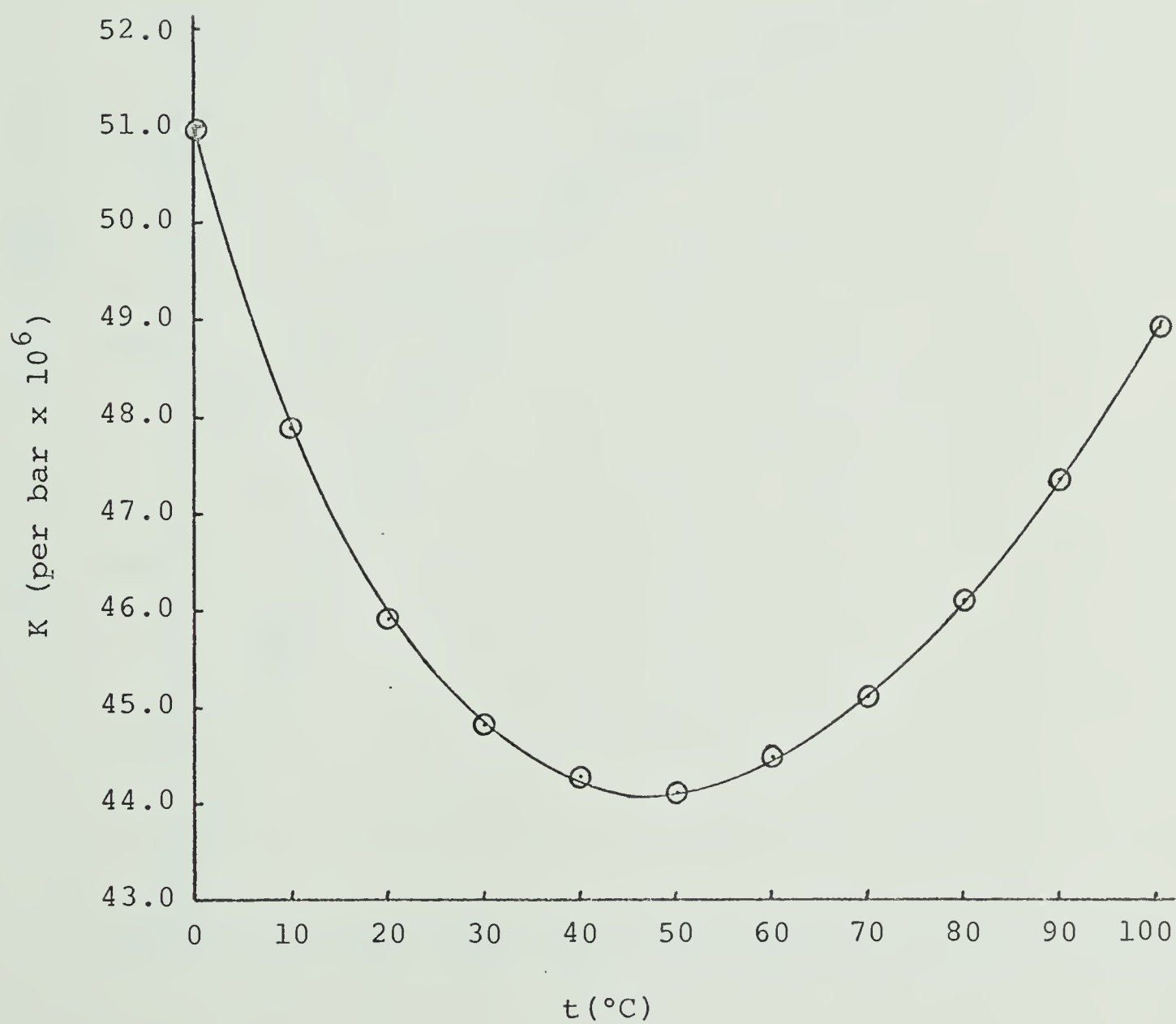


Fig. 3a. Isothermal Compressibility, K vs Temperature, t,
at one atmosphere pressure.

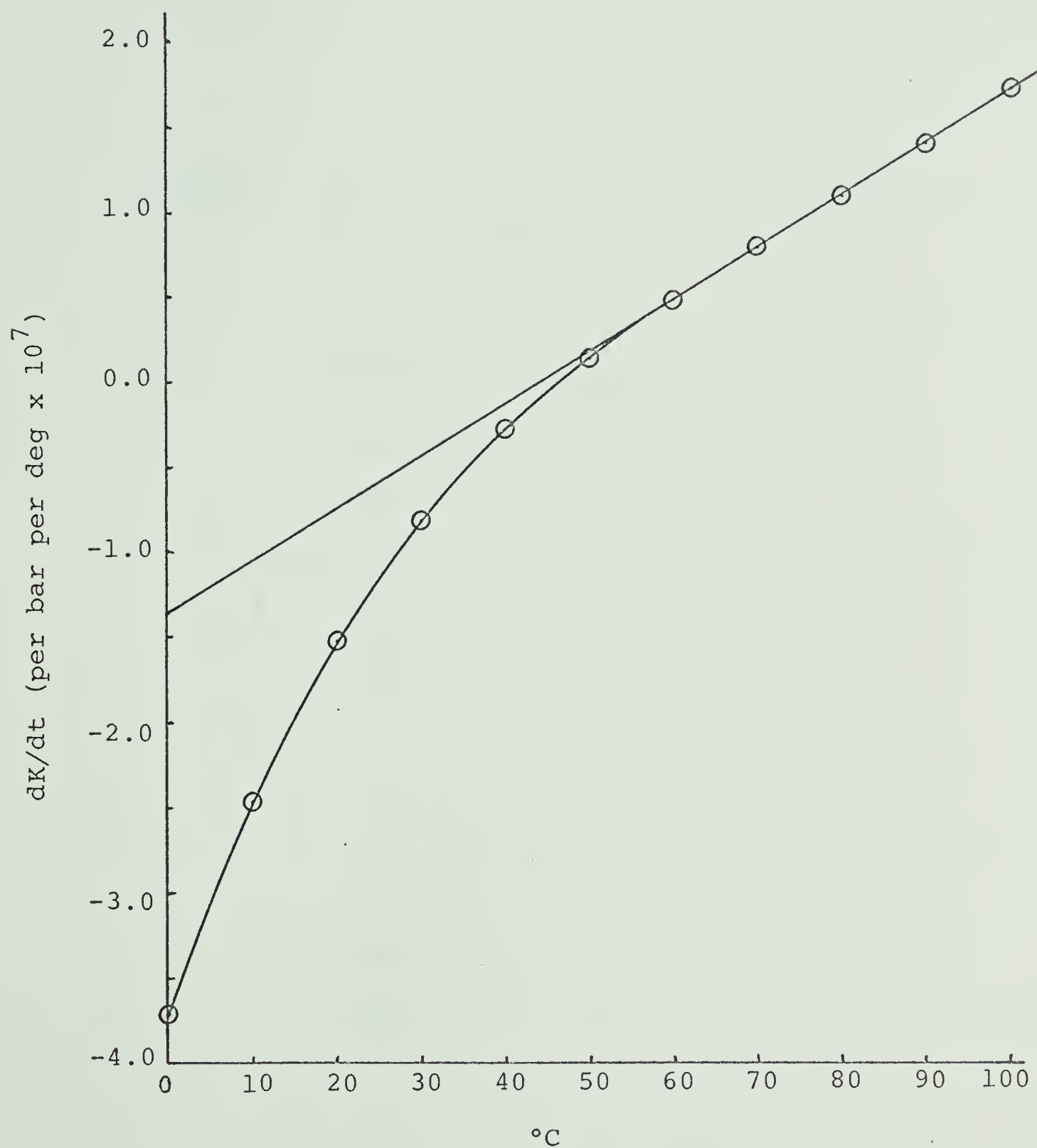


Fig. 3b. dK/dt , K' , vs Temperature, t .

Table I. Temperature of Minimum Compressibility,
 t_{\min} vs pressure.

<u>Pressure</u>	<u>$t_{\min.}$</u>
0 Bar	46.5°C
100	47.2
200	47.9
300	48.6
400	49.2
500	49.8
600	50.4
700	50.6
800	50.7
900	50.8
1000	50.8

The experimental specific heat data for water, C_{obs} , as a function of temperature, ⁽²⁰⁾ is shown in Fig. (2a). The plot of the derivative of specific heat with respect to temperature, Fig. (2b), obtained from the data in Fig. (2a) is a straight line for the temperature range 60°-100° and is a curve of some complexity below 60°.

A plot of isothermal compressibility, K , ⁽¹⁹⁾ vs t at atmospheric pressure is shown in Fig. (3a). Fig. 3(b) shows a plot of the derivative of isothermal compressibility, K' , vs t . Again it can be noticed that the change of K' with t is quite different below 60° to that above 60°.

The isothermal compressibility of water was measured at a large number of pressures by Kell and Whalley. From their data the temperature of the minimum, t_{min} , in the K vs t data, i.e., where $K' = 0$, was found for each pressure and the results are shown in Table I.

A plot of the log of specific viscosity of water, $\log \eta$, vs $1/T$, Fig. (4) is a straight line between 2.68×10^{-3} (100°) and 3.003×10^{-3} (60°) but departs from linearity at temperatures below 60°. A simple expression for the activation energy for viscous flow, ΔE_{vis} , is

$$\eta = A e^{\frac{\Delta E_{vis}}{RT}}$$

where A is a constant. For two points on the curve,

$$\Delta E_{\text{vis}} = R \frac{\ln \eta_1 - \ln \eta_2}{1/T_1 - 1/T_2}$$

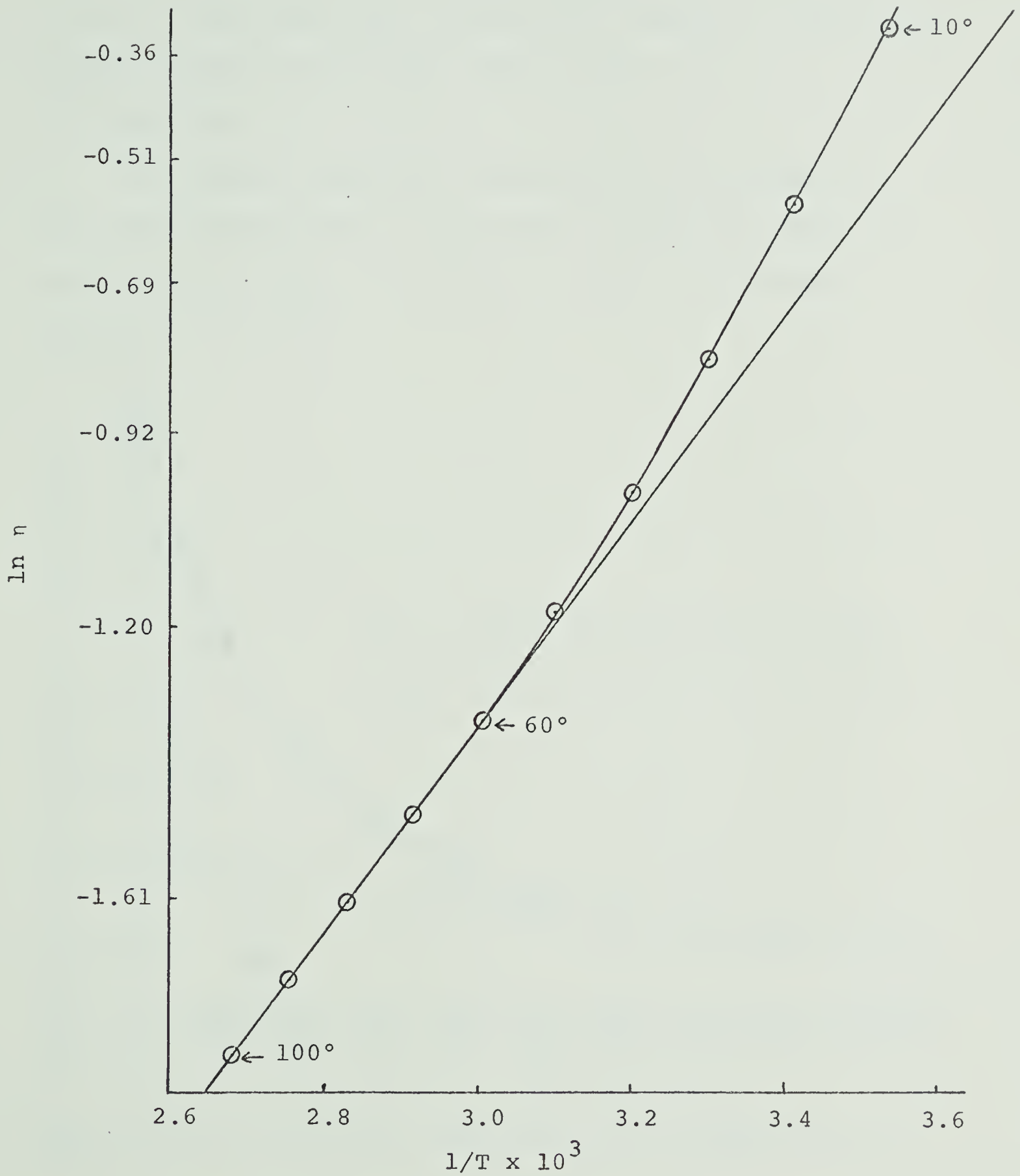


Fig. 4. $\log \eta$, (η = Specific viscosity) vs $1/T$, ($T = ^\circ K$).

For water between 60° and 100°C, $\Delta E_{\text{vis}} = 2.96$ kcal/mole. It can be seen from Fig. (4) that the tangent to the curve becomes steeper below 60°C, and at 0°C, $\Delta E_{\text{vis}} = 5.6$ kcal/mole.

The excess acoustical absorption of ultrasound is the sound energy which is absorbed in excess of that calculated due to shear viscosity by means of the Stokes equation. (17,24,25)

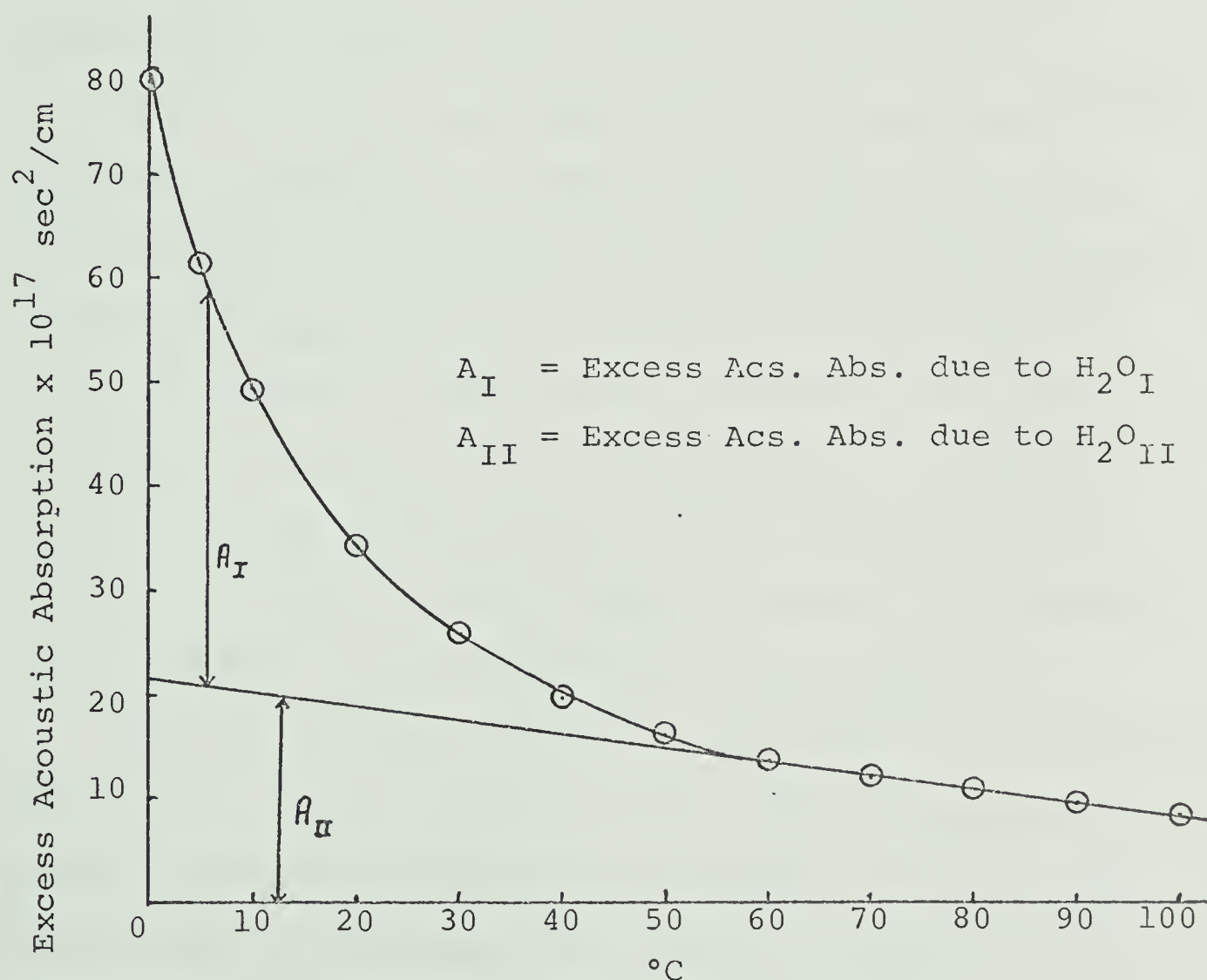


Fig. 5. Excess Acoustical Absorption, A vs Temperature, t

The plot of the excess acoustical absorption of water vs. temperature, Fig. (5) shows a straight line section between 60° and 100° with a large increase in absorption as the temperature decreases below 60° . Hall⁽²¹⁾ quotes experimental values for excess acoustical absorbance from 0° to 80° and also derives an equation which fits the data accurately over this temperature range. The values for 90° and 100° (Fig. (5)) were calculated by extrapolation of Hall's expression.

Hall's theory has been seriously questioned^(24,26) as to the correctness of some of his basic assumptions, but whatever are the faults of his theory, the expression given by Hall may well be regarded as correct from the empirical standpoint and as such, useful for the extrapolation of empirical data. As pointed out by Markham et al⁽²⁶⁾, any theory which predicts a constant ratio of bulk to shear viscosity might be regarded as adequate at the present state of knowledge of the subject.

The data in Figs. (6) and (7) are taken from Walrafen's paper.⁽²³⁾ It would appear that the curve fitted to these points would have two different sections. We have drawn two straight lines through the points to emphasize the two sections. It can be seen that the slope of the

curve changes markedly in the region of 60°.

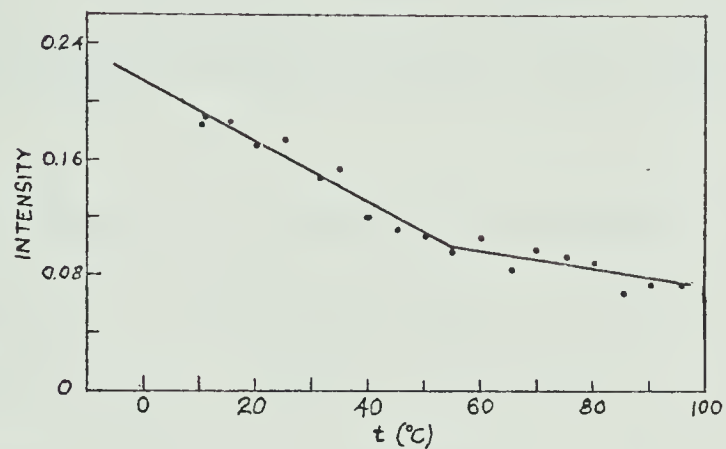


Fig. 6. Integrated Raman intensities of the total intermolecular librational contour of water obtained without filter.

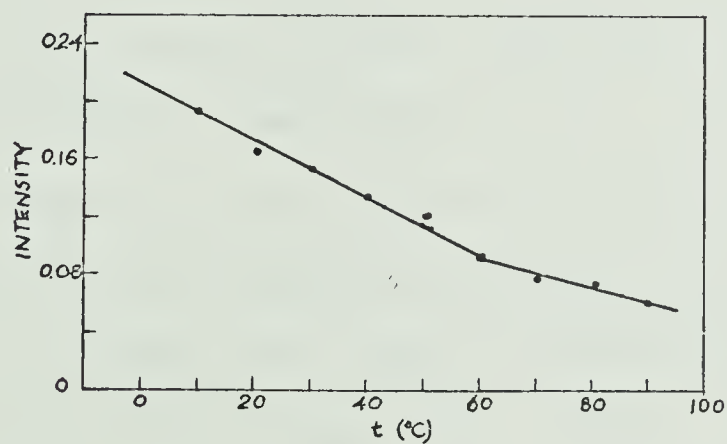


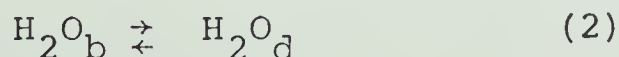
Fig. 7. Integrated Raman intensities of the total intermolecular librational contour of water obtained with NaNO₂ filter.

3 - Discussion

It is possible in principle to explain the phenomena of liquid water in terms of a model comprising an infinite number of species. However, such a model does not lead to manageable calculations which predict the observed behaviour of water.

An attempt has been made here to explain the behaviour of water in terms of a minimum number of species. It is not possible to explain the complex behaviour of water, for example the minimum in specific volume at 4°C and isothermal compressibility at 46.5°C, in terms of a single species model. Thus a two-species model will be used to attempt to explain the observed phenomena of water.

Specific volume, specific heat, and isothermal compressibility, when plotted against temperature have minima at the quite different temperatures of 4°, 35°, and 50°, respectively. However, our plots of the first derivatives of these properties with respect to temperature, indicated by primes, V' , C' , and K' all show a curved section below 60° and a straight section above 60°. (Figs. 1(a),(b); 2(a),(b); 3(a),(b)). These phenomena can be explained by postulating that water consists of two distinct species H_2O_b and H_2O_d in equilibrium with each other according to the process,



where H_2O_b represents bulky, ice-like water and H_2O_d represents a denser type of water. A volume decrease and an enthalpy increase are associated with the process represented by eqn. (2); that is $V_b > V_d$ and $H_b^\circ < H_d^\circ$. The decreased V'_{obs} of water between 0° and 60° is caused by the disappearance of H_2O_b with increasing temperature; the loss of volume thus incurred offsets the normal expansion, resulting in a very low V'_{obs} . If x_b represents the mole fraction of bulky water, H_2O_b , and x_d that of the dense water, H_2O_d , then the process can be represented by the following set of equations:

$$\begin{aligned} V_{obs} &= x_b V_b + x_d V_d \\ V'_{obs} &= x_b V'_b + x_d V'_d + V_b x'_b + V_d x'_d \\ x_b &= 1 - x_d \\ V'_{obs} &= (V_d - V_b) x'_d + x_d V'_d + (1 - x_d) V'_b \end{aligned} \quad (3)$$

At the lower temperatures, where there is rapid conversion of H_2O_b to H_2O_d with increasing temperature, x'_d is large and thus the first term in eqn. (3) is strongly negative, since $V_d < V_b$.

It is postulated that the species H_2O_b has completely disappeared by 60° and thus eqn. (3) reduces to

$$V'_{obs} = V'_d, \quad t > 60^\circ \quad (4)$$

Equation (1) accurately represents the volume of H_2O_d

above 60° and by substituting values for t from 0° to 60°, the volume of the dense species, V_d , below 60° can be calculated, permitting the calculation of the volume occupied by the bulky species below 60°. It would appear plausible to assign the volume of Ice I to the bulky species. Other open structures are possible but these probably will not differ markedly in specific volume from that of Ice I. A direct assignment of the Ice I structure to H_2O_b has been made in at least four models proposed recently for the structure of water.^(10,12,31,32)

Thus if H_2O_b has the same volume and coefficient of expansion as Ice I then

$$V_b = 1.0911 (1 + 0.000153t) \quad (5)$$

an assumption made by Grjotheim and Krogh-Moe.⁽¹⁰⁾ It follows that

$$V_{obs} = x_b V_b + (1-x_b) V_d \quad (6)$$

where V_d and V_b were obtained from equations (1) and (5) respectively. Values of x_b obtained from eqn. (6) are shown in Table II.

The mole percent of bulky structure ranges from 4.2% at 0° to 0.0% at 58°. These values for the mole percent of bulky species can of course be only regarded as approximate. However, they are lower than those suggested by other proponents of a bulky structure model

for water. The difference between the values presented here and those of other authors (10,12,31,32) are not easily explainable when only considering a two species model.

Table II. Mole % Bulky Species, ($X_b \times 100$),
in Water at Various Temperatures.

<u>Temperature</u> <u>in °C</u>	<u>Mole% Bulky</u> <u>Species</u>
0	4.21
5	3.15
10	2.34
20	1.24
30	0.60
40	0.26
50	0.07

The specific heat of ice is 0.52 cal/deg and of steam 0.48 cal/deg. (29a,b) The high specific heat of water is due to the breaking or bending of hydrogen bonds, (13) but the actual specific heat of a species of water whose temperature is raised but which undergoes very little change in bonding such as in the case of ice or steam, is probably very similar to that of

ice or steam. On this basis the important assumption is made that the different species of water have equal specific heats. A schematic energy level diagram is shown in Fig. (8) where H_b° and H_d° are the enthalpies of the bulky and dense species respectively at 0° .

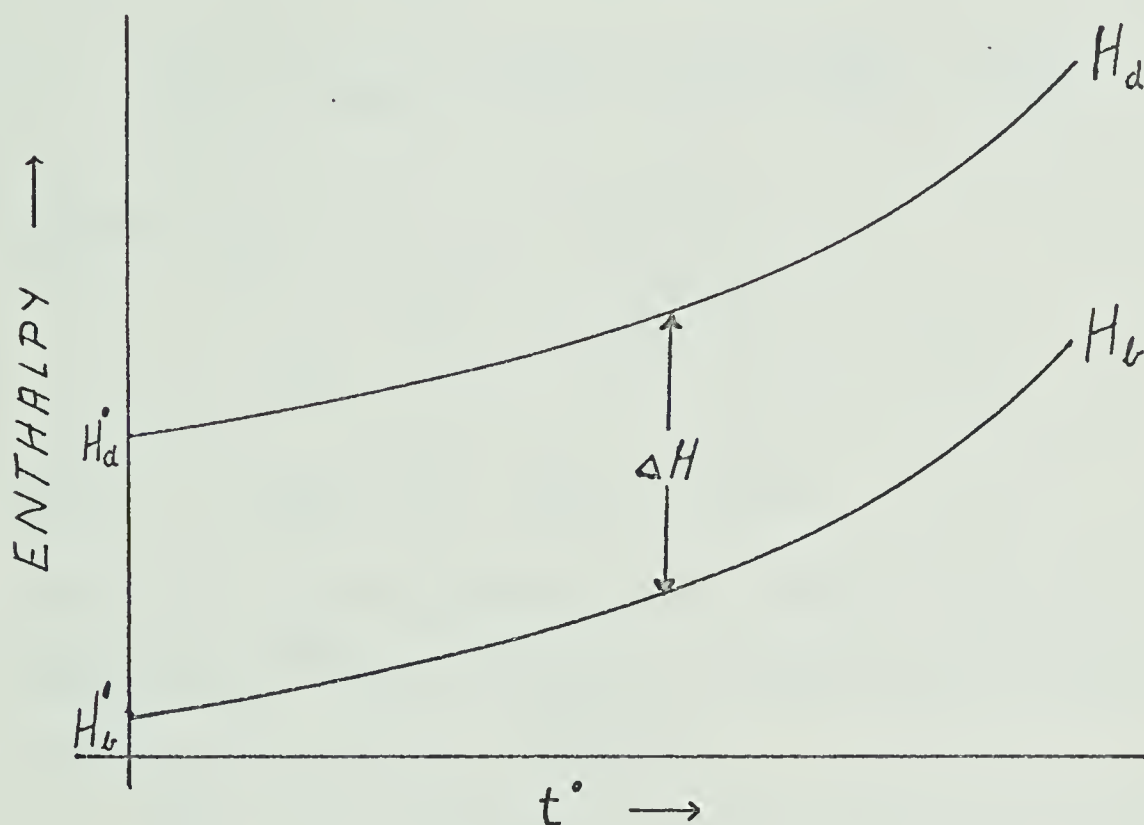


Fig. 8. Variation of Enthalpies of Bulky, H_b and Dense Species, H_d , with Temperature.

We have $C = H_b' = H_d'$. Also if H_b^t , H_d^t are the enthalpies of the bulky and dense species at temperature, t° we

have

$$\begin{aligned} (H_b^t - H_d^t) &= (H_b^\circ + \int_0^t C dt) - (H_d^\circ + \int_0^t C dt) \\ &= (H_b^\circ - H_d^\circ) \end{aligned} \quad (6a)$$

Also
$$\frac{d (H_b^t - H_d^t)}{dt} = 0 \quad (6b)$$

Thus, using the same symbols as previously,

$$H_{obs} = X_b H_b + X_d H_d$$

$$H'_{obs} = C_{obs} = X_b H'_b + X_d H'_d + H_b X'_b + H_d X'_d$$

However, $X_b = 1 - X_d$, therefore

$$C_{obs} = (X_b + X_d)C + (H_d - H_b)X'_d$$

and
$$C'_{obs} = C' + (H_d - H_b)X''_d \quad (7)$$

Below 60° , X'_d is positive, but becomes smaller as the temperature rises as there is less H_2O_b to convert to H_2O_d ; thus X''_d is negative.

Eqn. (7) therefore explains why C'_{obs} is lowered by the disappearance of a bulky species at low temperatures. Above 60° where $X_d = 1$

$$C'_{obs} = C' \quad (8)$$

Eqn. (8) shows that above 60° C'_{obs} follows a simple relationship. However, eqn. (7) does not explain the fact that C'_{obs} is slightly greater than C' in the region between 30° and 55° .

The variation of the isothermal compressibility of water at 1 bar pressure with temperature can be explained in terms of the two species model in which H_2O_b is absent above 60° .

$$\begin{aligned} \text{Since} \quad V_{\text{obs}} &= X_b V_b + X_d V_d \\ \text{and} \quad K_{\text{obs}} &= - \frac{1}{V_{\text{obs}}} \frac{d V_{\text{obs}}}{dp} \\ \text{then} \quad K'_{\text{obs}} &= \frac{d \left(\frac{1}{V_{\text{obs}}} \frac{d V_{\text{obs}}}{dp} \right)}{dt} \end{aligned} \quad (9)$$

The differentiation of the right side of eqn. (9) is very complex and leads to a large number of terms, many of which are cross terms in dp and dt . For this reason a simplified approach is used in the treatment of isothermal compressibility.

The compressibility of a liquid can be expressed by,

$$K = K_r + K_\infty \quad (10)$$

where K_r is the relaxational compressibility due to the volume decrease as a bulky species transforms into a denser species with increased pressure; in accord with the Le Chatelier principle. In the case of water, K_r decreases with increasing temperature as a result of the decreasing concentration of bulky species, that is K'_r

is negative. K_{∞} is the instantaneous compressibility and is a measure only of the decrease in the average distance between molecules with pressure and is independent of molecular rearrangement. K_{∞} increases with increasing temperature as the average distance between molecules increases due to expansion; that is K'_{∞} is positive.

Water is the only liquid, whose compressibility has been extensively measured, which shows a minimum in the compressibility vs. temperature curve. The minimum is at 46.7° at 1 atmosphere pressure. Three values of K for water are, 51.0×10^{-6} /Bar at 0°; 44.1×10^{-6} /Bar at 50° and 48.9×10^{-6} /Bar at 100°. It can be seen that K_r makes a large contribution to K in the region 0° to 50°. Since the concentration of H_2O_b is comparatively low this would mean that H_2O_b is easily transformed into another species by pressure.

Differentiating eqn. (10) leads to

$$K' = K'_r + K'_{\infty} \quad (11)$$

The low values of K' below 60°, (Fig. 3(b)), are explained by the negative term K'_r in eqn. (11).

At 46.7° eqn. (11) will become

$$-K'_r = K'_{\infty}$$

since $K' = 0$. Above 60° , where there is no more H_2O_b present eqn. (11) will become,

$$K' = K'_\infty$$

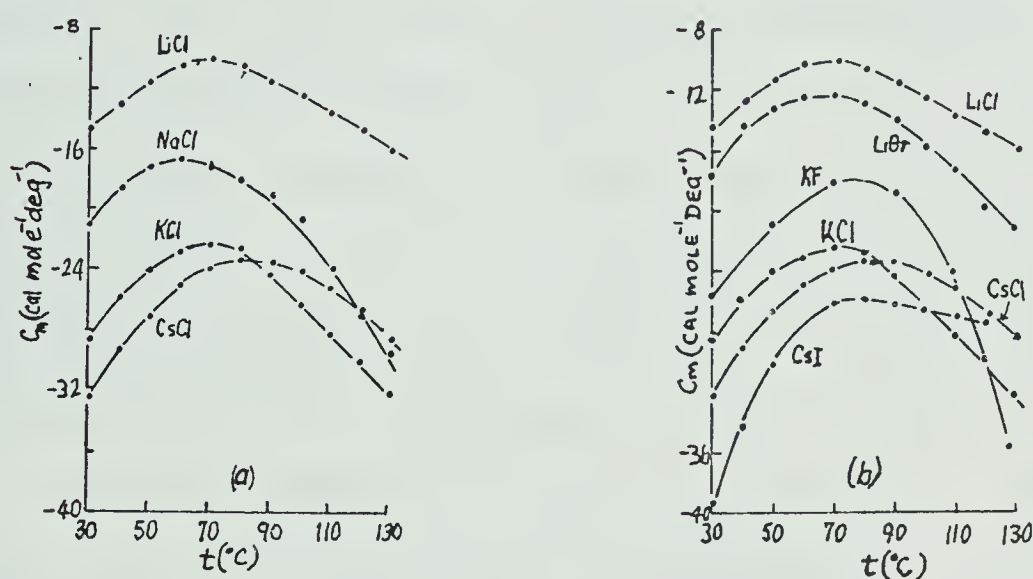
which makes the simple relationship between K' and t easily understandable in the temperature range 55° to 120° , (Fig. 3(b)).

The plot of $\log \eta$ vs $1/T$, Fig. (4), shows a constant activation energy, ΔE_{vis} for viscous flow from 100° to 60° , but below 60° , ΔE_{vis} increases with decreasing temperature. This behaviour is consistent with the model of water that predicts the appearance of a highly structured species at 60° which increases in concentration as the temperature is lowered.

At this point we examine the results of heat capacity measurements (30,31,32) of dilute solutions of alkali salts as summarized by Wicke, (13) to see whether these findings are consistent with a two species model.

Briefly the findings are, 1) the partial molar heat capacities of alkali halides are negative in the temperature range $0^\circ - 130^\circ$; 2) the partial molar heat capacities increase with increasing temperature, pass through maxima in the range $60^\circ - 80^\circ$, depending on the

salt, and then decrease again with increasing temperature; 3) below 60° the partial molar heat capacities generally become more negative as the radius of the cation or anion increases whereas at temperatures above the maxima in the curves, the smaller ions, with the exception of Li^+ , appear to cause the greatest decrease in the partial molal heat capacities with increasing temperature, Figs. 9 (a), (b).



Figs. 9. Partial molar heat capacities of alkali halides, C_m at infinite dilution.

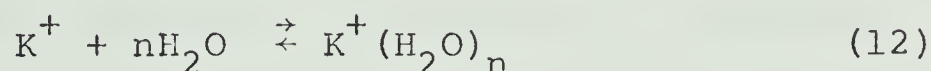
The heat capacity measurements (30,31) which Wicke (13) has made are in good agreement with the present findings between 0° and 60°. The strongly negative partial molar heat capacities of alkali halides at infinite dilution increase until a maximum is reached in the region of 60° - 80°. This evidence points to the presence of a strongly hydrogen bonded structure which disappears with increasing temperature and is no longer

present in the region between 60° and 80° . The fact that the effect is greatest with ions of the largest radii, correlates with the findings of Bingham, (33) which were that at 25° the ions of largest radius caused the greatest increase in the fluidity of water.

However, Wicke's findings in the temperature region, 60° - 130° are in strong disagreement with the behaviour predicted by a two species model, which predicts that the partial molar heat capacities would become less negative with increased temperature. Wicke's suggestions should be considered with great care because they could play a large part in the further development of knowledge about the structure of water. Briefly again, the findings were that between 60° - 80° and 130° the partial molar heat capacities of salts at infinite dilution were increasingly negative with increasing temperature and decreasing ion size.

Could the effect be caused by ion hydration? As an ion becomes hydrated it effectively removes some water molecules from the liquid, and since the abnormally high heat capacity of water is due to the thermal decay of hydrogen bonds, this would mean that fewer hydrogen bonds in the liquid were available for breaking and thus the heat capacity of the solution would be lowered.

At this point it is pertinent to study the temperature dependence of ion hydration. The enthalpies of ion hydration, ⁽³⁴⁾ ΔH_h° range from -62.0 kcal/mole for Cs^+ to -122.6 kcal/mole for F^- ; therefore, the hydration reactions are all strongly exothermic. If we consider the reaction for the hydration of potassium ion,



and if $[\text{H}_2\text{O}]$ represents the mole fraction of water present before hydration occurs, then the equilibrium constant for reaction (12) becomes

$$\begin{aligned} K &= \frac{[\text{K}^+(\text{H}_2\text{O})_n][[\text{H}_2\text{O}] - n[\text{K}^+]]}{[\text{K}^+][\text{H}_2\text{O}]^n} \\ &= \frac{[\text{H}_2\text{O} - n[\text{K}^+]]}{[\text{H}_2\text{O}]^n} \end{aligned} \quad (13)$$

Since $\Delta H_h^\circ (\text{K}^+) = -75.8$ kcal/mole, ⁽³⁴⁾ we get

$$\frac{d(\ln K)}{d(1/T)} = - \frac{\Delta H}{R} = \frac{75.8}{R} \text{ kcal/mole}$$

Thus the plot of $\ln K$ vs $1/T$ would have a positive slope and $\ln K$ would decrease with increasing temperature. This is only possible if the hydration number, n ,

becomes smaller with increasing temperature, because in the denominator of expression (13), n determines the power to which a number smaller than 1.0 is raised. Thus if the ion hydration is causing the observed decreased heat capacity, the partial molar heat capacities would become less negative with increasing temperature since fewer water molecules are removed from the body of the liquid by hydration. The opposite temperature dependence is observed--that is, the partial molar heat capacities become more negative, not less negative at the higher temperatures. Therefore these effects are not caused primarily by ion hydration.

The only other means by which a salt can cause a decrease in the number of hydrogen bonds in a solution is by breaking a bonded structure therein. Is then, the structure which is disrupted above 60° the same bulky, straight-hydrogen-bonded structure, which is believed to exist only below 60°?

There are two reasons why this is not believed to be the case. The first is that it is very unlikely the bulky structure would break down readily at low and high temperatures, but be resistant to breakdown at 60°. The second reason, according to Wicke, is that different ions are more effective at breaking structure

above 60°, which must mean that different structures are being acted on.

Are there two or three species of water? If there were only two, it would mean that as the structure existing above 60° is broken down, it would have to transform into the other species which exists at low temperatures, which leads to a conflict in logic.

Thus a study of the partial molar heat capacities of salts at infinite dilution lead us to the requirement of a different model for the structure of water to that proposed here previously. Three species are required.

The studies so far suggest that a model very similar to that proposed by Wicke would be the most acceptable. The model proposed here is that between 0° and 60°, 3 species of water exist; the first species is a straight-hydrogen-bonded species of high specific volume and low enthalpy, very similar to ice. This corresponds to H_2O_b in the foregoing discussion but will now be designated as H_2O_I . The second species is of lower specific volume and higher enthalpy than H_2O_I and could be similar to the flexible lattice water proposed by Leonard-Jones and Pople, ⁽⁵⁾ the bent-hydrogen-bonded structure of Davis and Litovitz, ⁽¹²⁾ or the bent-

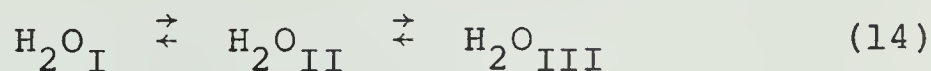
hydrogen-bonded structures of Pimentel. (14,15) This second species will be designated as H_2O_{II} . The third species, having a lower specific volume and higher enthalpy than H_2O_{II} , will be designated as H_2O_{III} . This third species may be an unbonded species similar to that existing in unassociated liquids, subject to van der Waals' forces and weak dipole-dipole interaction but with no hydrogen bonds to other molecules.

Briefly then,

$$V_I > V_{II} > V_{III} \quad \text{and}$$

$$H_I^\circ < H_{II}^\circ < H_{III}^\circ$$

The mole fractions for the species H_2O_I ; H_2O_{II} ; H_2O_{III} will be represented by X_I ; X_{II} ; X_{III} . It is proposed that the equilibria between the three species can be described by



What relation exists between this model and the two-species model discussed previously? The effects which were attributed to H_2O_b are easily explained by attributing them to H_2O_I . Those effects attributed to H_2O_d are now seen to be the averaged effects of the two species H_2O_{II} and H_2O_{III} . The concentrations calculated for X_b are still valid and will now be the

values for X_I .

To study the heat capacity of water in terms of a three species model, the same assumption which was made in the case of the two species model is made again, namely that the actual specific heats of all the species are the same. With the use of the symbols H_{obs} and C_{obs} for the experimental enthalpies and heat capacities of water, and primes and double primes to indicate first and second derivatives with respect to temperature, we get

$$H_{\text{obs}} = X_I H_I + X_{II} H_{II} + X_{III} H_{III} \quad (15)$$

$$\begin{aligned} H'_{\text{obs}} = C_{\text{obs}} &= X_I H'_I + X_{II} H'_{II} + X_{III} H'_{III} \\ &+ H_I X'_I + H_{II} X'_{II} + H_{III} X'_{III} \end{aligned}$$

but $C = H'_I = H'_{II} = H'_{III}$

$$X_I = 1 - X_{II} - X_{III}$$

$$\therefore C_{\text{obs}} = C + (H_{II} - H_I) X'_{II} + (H_{III} - H_I) X'_{III} \quad (16)$$

Above 60° eqn. (15) simplifies to

$$H_{\text{obs}} = X_{II} H_{II} + X_{III} H_{III}$$

$$C_{\text{obs}} = C + (H_{\text{III}} - H_{\text{II}}) X_{\text{III}}' \quad (17)$$

and since enthalpy differences are temperature-independent, (eqns. (6a,b)), we get

$$C_{\text{obs}}' = C' + (H_{\text{III}} - H_{\text{II}}) X_{\text{III}}'' \quad (18)$$

We have seen that ice at 0° has a heat capacity, $C = 0.52$ cal/gm.deg. and that steam has a very similar heat capacity, $C = 0.49$ cal/gm.deg. (29a,b)

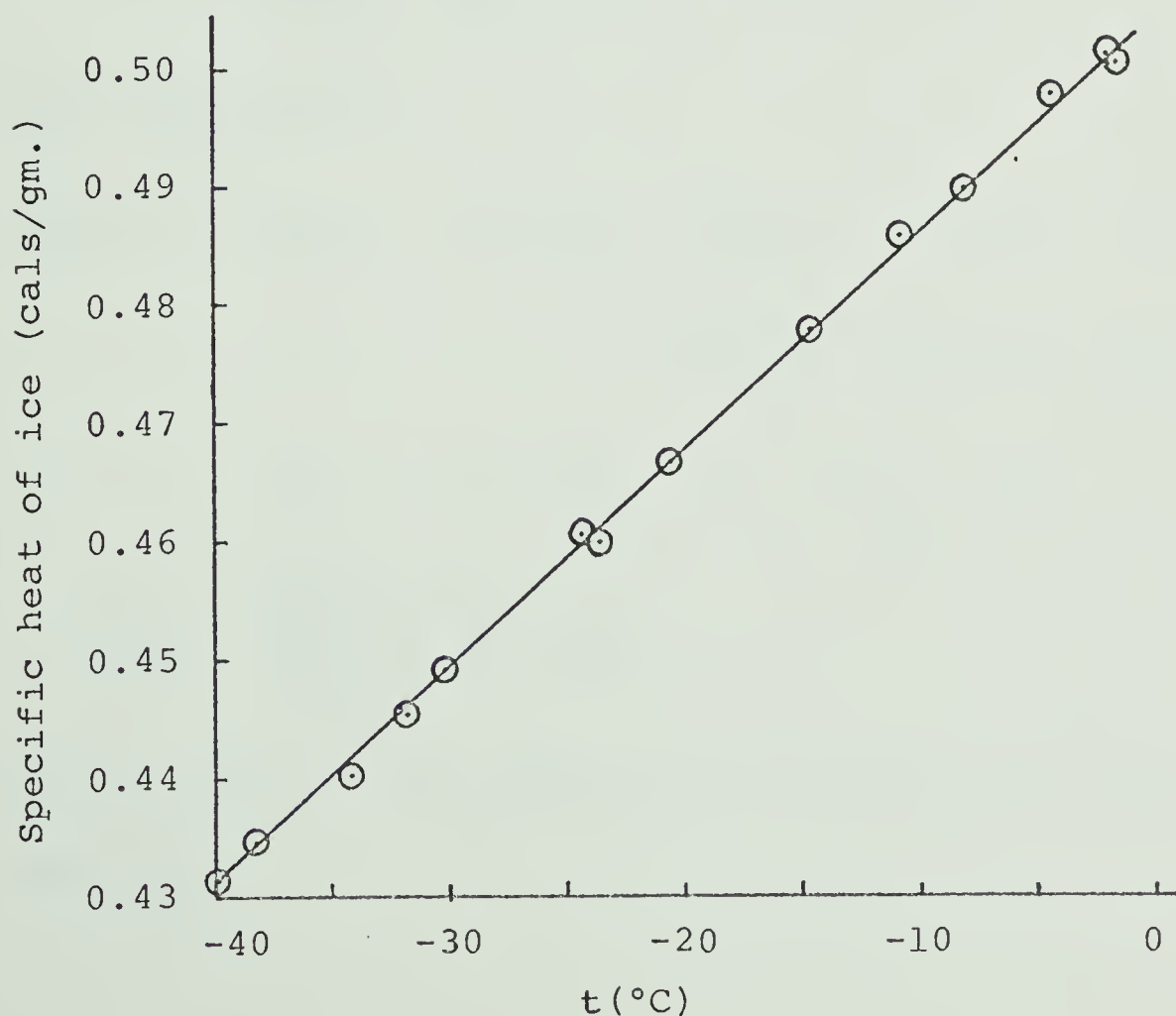


Fig. 10. Specific heat of ice vs. temperature.

If we now further assume that the different species of water at 0° have the same heat capacity as that of ice, 0.52 cal/gm.deg (Fig. 10) and that these species have the same C' as ice, which is 0.0018 cal/gm.deg it is then possible to solve partially equations (17) and (18) and to obtain a value for $(H_{III} - H_{II})$, which is temperature independent in view of the assumptions made that the heat capacity of all the species is the same. Since,

$$(H_{III} - H_{II}) X'_{III} = (C_{obs} - C) \quad (20)$$

$$(H_{III} - H_{II}) X''_{III} = (C'_{obs} - C') \quad (21)$$

cross multiplying,

$$\begin{aligned} (C'_{obs} - C') (H_{III} - H_{II}) X'_{III} &= (C_{obs} - C) (C'_{obs} - C') \\ &= (H_{III} - H_{II}) X''_{III} (C_{obs} - C) \end{aligned}$$

$$(C'_{obs} - C') X'_{III} = X''_{III} (C_{obs} - C) \quad (22)$$

$$X''_{III} - \frac{(C'_{obs} - C')}{(C_{obs} - C)} X'_{III} = 0 \quad (23)$$

The solution of the differential equation (23) takes the form

$$X_{III} = e^{\frac{(C_{obs} - C')}{(C_{obs} - C)} t} + C_{int} \quad (24)$$

where C_{int} is the integration constant.

$$X'_{III} = \frac{(C'_{obs} - C')}{(C_{obs} - C)} e^{\frac{(C'_{obs} - C')}{(C_{obs} - C)} t} \quad (25)$$

Substituting the value for X'_{III} obtained from eqn. (25) into eqn. (20) a value for $(H_{III} - H_{II})$ can be obtained. If one of the coefficients in eqn. (22) is negative then eqn. (23) takes the form

$$X''_{III} + \frac{(C'_{obs} - C')}{(C_{obs} - C)} X' = 0 \quad (26)$$

The solution of eqn. (26) takes the form

$$X_{III} = C_{int} - e^{-\frac{(C'_{obs} - C')}{(C_{obs} - C)} t} \quad (27)$$

and X'_{III} has the same value as in eqn. (25).

The values used in eqns. (25) and (20), together with the results obtained are shown in Table III.

The values shown in the last column of Table III show that $(H_{III} - H_{II})$ is indeed independent of temperature. Therefore the assumption is made that the heat

Table III. Observed and calculated heat capacities of water;
enthalpy difference between $\text{H}_2\text{O}_{\text{III}}$ and $\text{H}_2\text{O}_{\text{II}}$
calculated from eqn. (20).

t	$C_{\text{Obs.}}$ $\frac{\text{cal}}{\text{gm.deg.}}$	$C'_{\text{Obs.}}$ $10^{-3} \frac{\text{cal}}{\text{gm.deg.}^2}$	C $\frac{\text{cal}}{\text{gm.deg.}}$	C' $10^{-3} \frac{\text{cal}}{\text{gm.deg.}^2}$	$H_{\text{III}} - H_{\text{II}}$ $\frac{\text{cal}}{\text{gm.}}$
60°C	0.99943	0.10	0.628	1.80	105.6
70°	1.00067	0.15	0.646	1.80	105.5
80°	1.00229	0.19	0.664	1.80	104.5
90°	1.00437	0.23	0.682	1.80	105.5
100°	1.00697	0.26	0.700	1.80	103.0
					105.0 Av.

capacity of all species is given by

$$C_t = C^\circ + 1.8 \times 10^{-3} \text{ Cals/gm.deg}$$

where C_t is the heat capacity at temperature t . The value $C^\circ = 0.52 \text{ cal/gm.deg}$ appears plausible. It was found during the calculations that values for $(H_{III} - H_{II})$ were very sensitive to both the values of C° and C' , especially C' , and a change in either of these quantities caused $(H_{III} - H_{II})$ to vary with temperature.

By use of the above equation, eqn. (27) is converted to

$$X_{III} = C_{int} - e^{-(5 \times 10^{-6}t + 0.0043)t} \quad (28)$$

Two factors were considered in the evaluation of the integration constant, C_{int} . Grjotheim and Krogh-Moe⁽¹⁰⁾ give an expression in their paper for the specific volume of H_2O_{III} , V_{III} . The value of V_{III} obtained from their expression equals the observed specific volume of water at approximately 175° . Secondly we have found that a plot of V'_{obs} vs t , Fig. (11) showed a straight line section for the range 180° to 250° . On this basis the mole fraction of X_{III} is taken to be unity at 180° and thus eqn. (28) becomes

$$X_{III} = 1.386 - e^{-(5 \times 10^{-6}t + 0.0043)t} \quad (29)$$

It is now possible to calculate the mole fractions of each species at each temperature using eqn. (29) and the values for X_I from Table II.

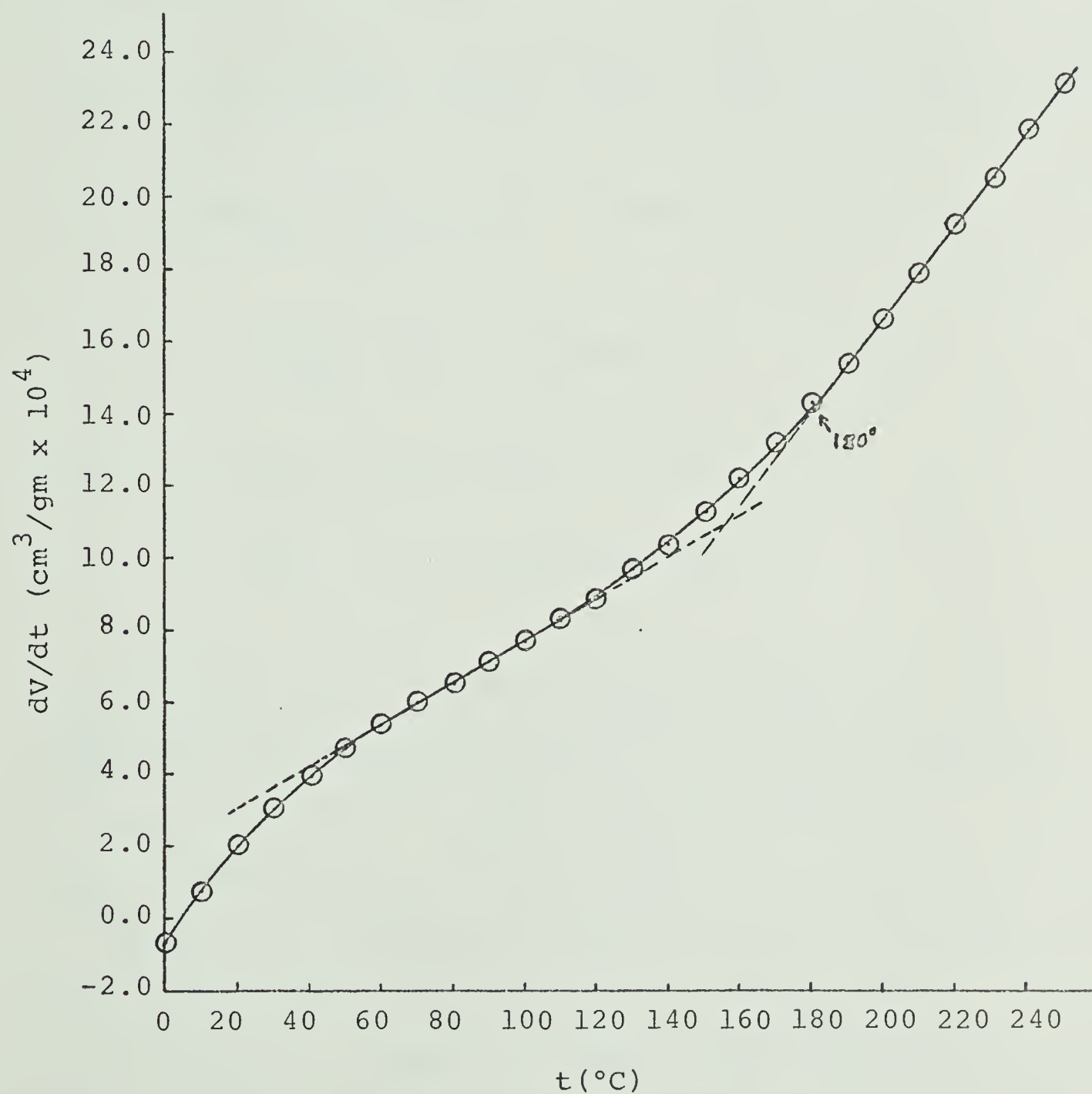


Fig. 11. $DV/dT, V'$ vs Temperature, t .

According to our three-species model, since $X_I = 0.042$ at 0° , then the mole fraction of ice changed to either H_2O_{II} or H_2O_{III} upon melting is 0.958 and 79.7 cal/gm of heat are absorbed in the process. From eqn. (29) it can be seen that $X_{III} = 0.386$ when $t = 0^\circ C$, thus we have

$$79.7 = 0.386((H_{III}^\circ - H_{II}^\circ) + (H_{II}^\circ - H_I^\circ)) + 0.572(H_{II}^\circ - H_I^\circ)$$

$$0.958(H_{II} - H_I) = 79.7 - 0.386 \times 105.0$$

$$H_{II}^\circ - H_I^\circ = 40.8 \text{ cal/gm}$$

Since $H_{III} - H_{II} = 105.0 \text{ cal/gm}$

$$H_{III} - H_I = 145.8 \text{ cal/gm}$$

The concentrations of species H_2O_{II} and H_2O_{III} at each temperature are dependent essentially on the assumption of $X_{III} = 1.0$ at 180° . This gives the values of $X_{III} = 0.766$ and $X_{II} = 0.233$ at 100° .

Thus in the temperature range 0° to 100° the value of X_I has changed from 0.0421 to 0.0 and X_{II} from 0.572 to 0.23. Since the change in the actual heat capacity of water approximates a linear relationship with temperature the average heat capacity of all the species

between 0° ($C_0 = 0.52$) and 100° ($C_{100} = 0.70$) is given by $(0.52 + 0.70)/2 = 0.61$ cal/gm deg. Thus the heat which would be absorbed by 1 gm of water being heated from 0° to 100° according to the model given here is given by

$$\begin{array}{rcl} \Delta X_I & = & 0.042; \text{ heat absorbed } = 0.042 \times 145.8 = 6.09 \text{ cal} \\ \Delta X_{II} & = & 0.338; \text{ heat absorbed } = 0.338 \times 105.0 = 35.4 \\ \text{heat absorbed due to heat} & & = 0.61 \times 100.0 = \underline{61.0} \\ & \text{capacity} & \\ & & \text{Total } 102.49 \text{ cal} \end{array}$$

The observed value is that 100.0 cal of heat are absorbed in heating 1.0 gm of water through 100° . Thus the observed and theoretical values agree reasonably well and the assumption that $X_{III} = 1$ in the region of 180° receives support.

One further test of the change of concentration of species with temperature was carried out in order to determine whether the model could predict the correct values for the heat capacity of water over the temperature range 0° to 100° . A rearranged form of eqn. (16) was used,

$$C_{\text{pre}} = C + (H_I - H_{II}) X_I' + (H_{III} - H_{II}) X_{III}'$$

The predicted heat capacity, C_{pre} should equal the

observed heat capacity, C_{obs} . The results are shown in Table IV.

The comparison between the observed heat capacity and predicted heat capacity is good except in the range $0^\circ - 30^\circ$ where the quantity X_I' , from the specific volume data contributes significantly. These results are shown on an expanded scale in Fig. (12).

The volume data can be reanalysed in terms of a three species model as follows,

$$V_{\text{obs}} = X_I V_I + X_{II} V_{II} + X_{III} V_{III} \quad (30)$$

which upon differentiation becomes

$$\begin{aligned} V_{\text{obs}}' &= X_I' V_I + X_{II}' V_{II}' + X_{III}' V_{III}' \\ &\quad + V_I X_I' + V_{II} X_{II}' + V_{III} X_{III}' \\ X_I &= 1 - X_{II} - X_{III} \\ V_{\text{obs}}' &= V_I' + X_{II}' (V_{II}' - V_I') + X_{III}' (V_{III}' - V_{II}') \\ &\quad + (V_{II} - V_I) X_{II}' + (V_{III} - V_I) X_{III}' \quad (31) \end{aligned}$$

It is probable that the less associated species of water have the greatest thermal expansion and thus the second and third terms on the right side of eqn. (31) are

Table IV. Concentration of each species with temperature; comparison

of observed and predicted heat capacities of water, (cal/gm.deg.)

<u>t</u>	<u>X_I</u>	<u>X_{II}</u>	<u>X_{III}</u>	<u>C</u>	<u>C_{Obs.}</u>	<u>C_{pre.}</u>	<u>C_{Obs.}-C_{pre.}</u>
0°C	0.043	0.572	0.386	0.520	1.0074	1.0628	-0.0554
10	0.023	0.551	0.424	0.538	1.0013	1.0328	-0.0315
20	0.011	0.517	0.472	0.556	0.9988	1.0120	-0.0140
30	0.005	0.484	0.511	0.574	0.9980	0.9993	-0.0013
40	0.002	0.447	0.441	0.592	0.9980	0.9930	+0.0050
50	0.0007	0.404	0.589	0.610	0.9985	0.9917	+0.0068
60	0.0	0.377	0.623	0.628	0.9994	0.9940	+0.0054
70	0.0	0.334	0.666	0.646	1.0007	0.9985	+0.0012
80	0.0	0.301	0.699	0.664	1.0023	1.0036	-0.0013
90	0.0	0.264	0.736	0.682	1.0044	1.0081	-0.0037
100	0.0	0.234	0.766	0.700	1.0070	1.0103	-0.0033

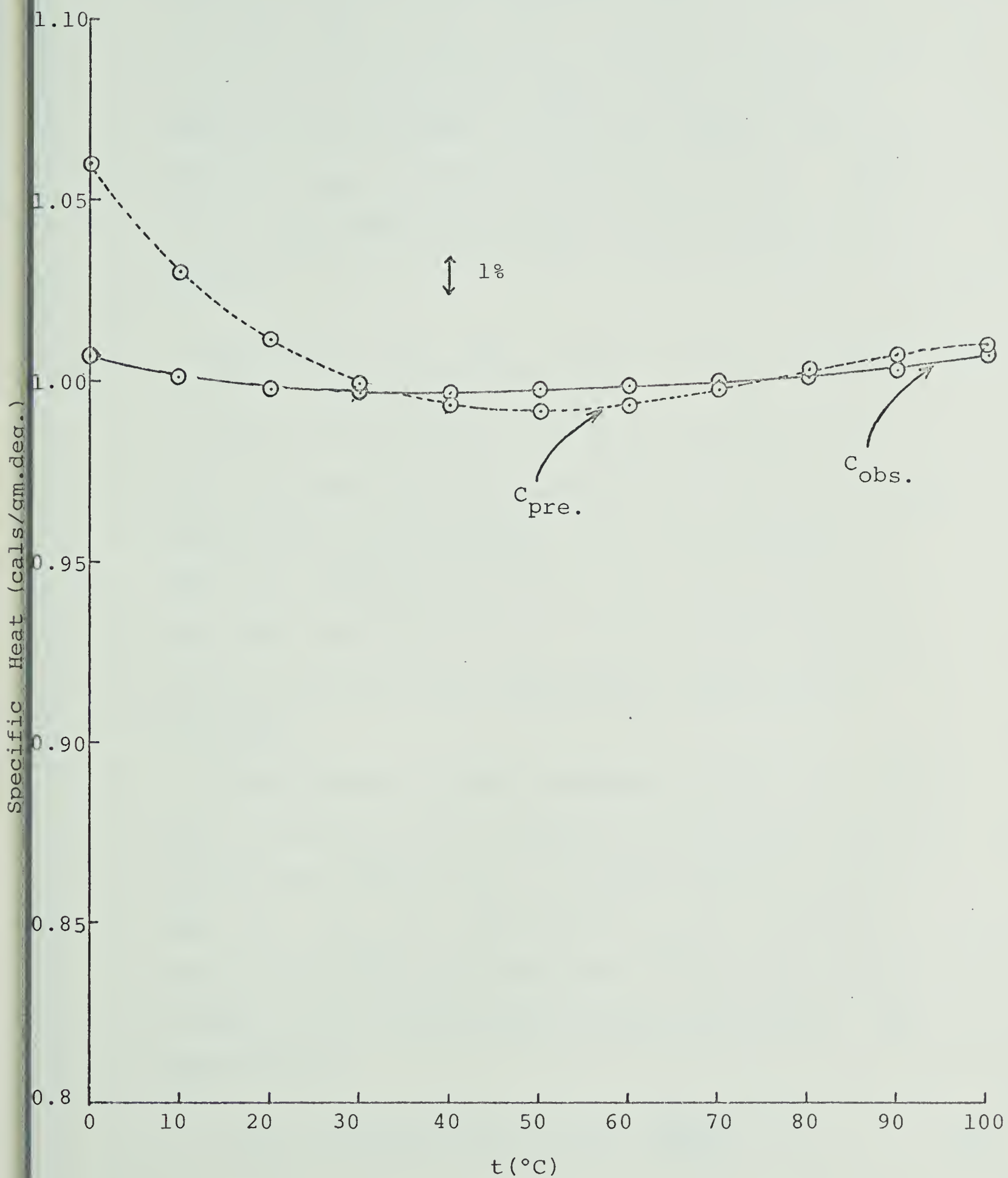


Fig. 12. Comparison of observed, C_{obs} , and calculated C_{pre} , heat capacities.

likely to be very small positive terms. However, the fifth term in eqn. (31) is negative because X'_{III} is positive and the term $(V'_{III} - V'_I)$ is large and negative in all ranges. This would explain the low value for V'_{obs} in the low temperature region. Above 60° the H_2O_I species no longer exists and eqn. (31) becomes

$$V'_{obs} = V'_{II} + X'_{III} (V'_{III} - V'_{II}) + (V'_{III} - V'_{II}) X'_{III} \quad (32)$$

It is not possible to solve the equations (31) and (32) numerically because there are too many unknown quantities in each equation. It is not feasible to make the assumptions that $V'_I = V'_{II} = V'_{III}$ and thus equations (31) and (32) are not able to be simplified to the extent that the differential equations can be solved.

Nevertheless, it was considered desirable to obtain some estimates of the volumes of the different species at different temperatures. V_I was obtained by use of eqn. (5). V_{III} was computed from the expression given by Grjotheim and Krogh-Moe ⁽¹⁰⁾ for the volume of water in the close-packed unassociated state. The expression is,

$$V_{III} = 0.7582 \left[1.546 - 0.546 \left(\frac{647-T}{647} \right)^{1/4} \right]^3 \quad (33)$$

Table V. Variation of volume and concentration of each

species of water with temperature, (x = mole fraction).

$\underline{X_I}$	$\underline{X_{II}}$	$\underline{X_{III}}$	\underline{t}	$\underline{V_{obs.}}$	$\underline{V_I}$	$\underline{V_{II}}$	$\underline{V_{III}}$
0.043	0.572	0.386	0°C	1.0002	1.0911	1.0420	0.9286 ml/gm
0.011	0.517	0.472	20°	1.0017	1.0944	1.0518	0.9465
0.002	0.447	0.551	40°	1.0078	1.0978	1.0646	0.9636
0.0	0.377	0.623	60°	1.0172	1.1011	1.0792	0.9826
	0.301	0.699	80°	1.0291	1.1045	1.0934	1.0029
	0.234	0.766	100°	1.0434		1.1047	1.0245
	0.179	0.821	120°	1.0600		1.1115	1.0476
	0.110	0.890	140°	1.0793		1.1128	1.0726
	0.056	0.944	160°	1.1085		1.1139	1.0996
	0.00	1.000	180°	1.1283		1.1150	1.1291

where T is the temperature in degrees Kelvin. Equation (33) is based on an empirical equation developed by Jacobson and Heedman ⁽³⁵⁾ who studied the volumes of non-hydrogen bonded liquids at different temperatures.

The values of V_{II} at different temperatures were found by using a rearrangement of eqn. (30), together with the mole fractions of each species from Table III.

$$V_{II} = \frac{X_I V_I + X_{III} V_{III}}{X_{II}}$$

The results are given in Table V.

The information on each species at 0° has been summarized in Table VI.

Table VI. Specific Volumes, V and mole fractions, x of all species at 0°.

	<u>H₂O_I</u>	<u>H₂O_{II}</u>	<u>H₂O_{III}</u>
x	0.042	0.572	0.386
V	1.0911	1.0420	0.9286

A widely accepted value of the strength of the hydrogen bond is 3.4 kcals/mole. (36,37)

We have

$$(H_{II} - H_I) = 40.8 \text{ cal/gm} = 0.73 \text{ kcal/mole} = 0.2 \text{ H-bond}$$

$$(H_{III} - H_{II}) = 105 \text{ cal/gm} = 2.0 \text{ kcal/mole} = 0.6 \text{ H-bond}$$

Thus an energy level diagram can be drawn for the different species, Fig. (11).

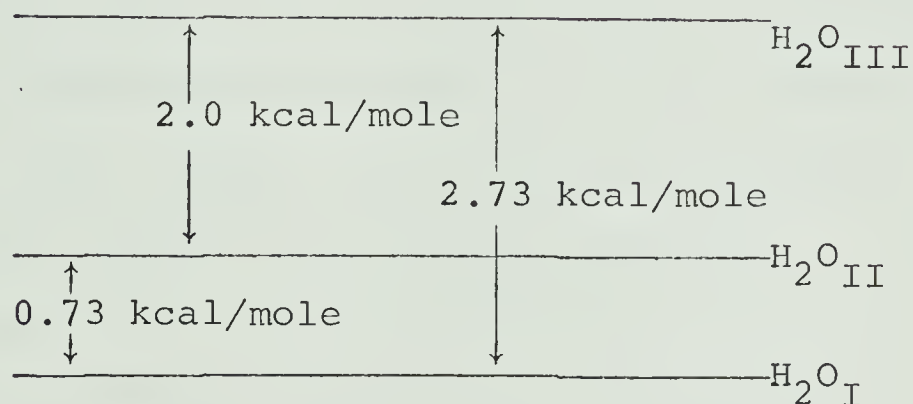


Fig. 11. Energy level for the 3 species of water.

H_2O_{II} , having a high specific volume and 1.8 hydrogen bonds per molecule, as compared with ice having 2.0 hydrogen bonds per molecule, suggests that H_2O_{II} would be very similar to the bent-hydrogen bonded species suggested by Pople ⁽⁵⁾ or Davis and Litovitz. ⁽¹²⁾ This agrees with the model for H_2O_{II} suggested earlier.

However, it is not so easy to correlate the H_2O_{III} species as proposed earlier with the present findings.

It might be more feasible to consider the $\text{H}_2\text{O}_{\text{III}}$ species to be similar to the aggregates suggested by Wicke⁽¹³⁾ and Pimentel^(14,15) since the $\text{H}_2\text{O}_{\text{III}}$ species still contains approximately the energy of 1 hydrogen bond per molecule.

Many models of water,^(9,10,11,12,21,24) have postulated a much greater concentration of ice-like species than is proposed here for $\text{H}_2\text{O}_{\text{I}}$, but if $\text{H}_2\text{O}_{\text{II}}$, with its large volume and high percentage of hydrogen bonds, were considered to be similar to the structures proposed by other authors, the discrepancy between this model and other models would largely disappear. The unique feature of our model is that $\text{H}_2\text{O}_{\text{I}}$ is the only species which is truly ice-like and is postulated to be present in very small amounts at low temperatures.

Table V shows that a reasonably high concentration of $\text{H}_2\text{O}_{\text{II}}$ exists at temperatures above 130°C. The continued structure-breaking effect of the ions would explain why the partial molar heat capacities of the salts could be so negative at such comparatively high temperatures.

From Table I it may be seen that the temperature of minimum compressibility increases with increasing pressure up to 900 Bar, remaining the same at 1000 Bar. From eqn. (11) we have

$$\frac{d(K')}{dp} = \frac{d(K_r')}{dp} + \frac{d(K_\infty')}{dp}$$

At 1000 Bar and 51.6° we get,

$$\frac{d(K')}{dp} = 0.$$

thus

$$\frac{d(K_r')}{dp} = \frac{d(K_\infty')}{dp} \quad (34)$$

Since there are no constants in eqn. (11), we get upon integrating eqn. (34),

$$K_r' = K_\infty' \quad \text{at 1000 Bar and } 51.6^\circ.$$

This illustrates the fact that in water there is still considerable structure remaining at 51.7° and 1000 Bar. This would not have been explainable in terms of a low concentration, (0.1 mole %) of the highly compressible species H_2O_I , but can be understood in terms of a high concentration, (40.0 mole %, 50°) of the structured species, H_2O_{II} .

Hall ⁽²¹⁾ and Litovitz and Carnevale ⁽²⁴⁾ have both related the excess acoustical absorbance of water to the structural rearrangement of a bulky species into a denser species.

The relaxational compressibility is given by

$$K_r = - \frac{V_I}{V} \left(\frac{\partial X_I}{\partial P} \right)_T - \frac{V_{II}}{V} \left(\frac{\partial X_{II}}{\partial P} \right)_T - \frac{V_{III}}{V} \left(\frac{\partial X_{III}}{\partial P} \right)_T \quad (35)$$

where $V = X_I V_I + X_{II} V_{II} + X_{III} V_{III}$

$$X_{III} = 1 - X_I - X_{II}$$

$$\text{thus } K_r = - \frac{(V_I - V_{II})}{V} \left(\frac{\partial X_I}{\partial P} \right)_T - \frac{(V_{III} - V_{II})}{V} \left(\frac{\partial X_{III}}{\partial P} \right)_T \quad (36)$$

As pointed out by Lieberman, ⁽²⁵⁾ the sign for relaxational compressibility, or excess acoustic absorbance, could be either positive or negative. It is assumed to be negative in the form of Stokes' original equation, widely accepted to be applicable to liquids. Experimentally, it is positive at all temperatures, which is in accord with eqn. (36) in which both terms on the right side of the equation are positive. The excess acoustic absorbance above 60° is attributed to the second term in eqn. (36) and the absorbance below 60° to both terms.

It follows that for the first term in eqn. (36) to be large either or both of the factors, $(V_I - V_{II})$ or $\left(\frac{\partial X_I}{\partial P} \right)_T$ must be large. Since the enthalpy change for the conversion of H_2O_I to H_2O_{II} is much smaller than for the change of H_2O_{II} to H_2O_{III} , it is likely that although there is little H_2O_I present below 60° it could be a predominant factor in determining the excess acoustic absorbance,

since $\text{H}_2\text{O}_\text{I}$ is far more easily transformed than $\text{H}_2\text{O}_\text{II}$. The large increase in excess absorbance below 60° is not easily explained in terms of the same two species existing above 60° ; but is much more understandable in terms of a model in which a third species exists only at temperatures below 60° .

The excess acoustical absorbance of $\text{H}_2\text{O}_\text{II}$, A_II at all temperatures is obtained by extrapolation of the straight line section, (Fig. (5)) to 0° . The excess acoustical absorbance due to $\text{H}_2\text{O}_\text{I}$, A_I , is obtained by subtracting the absorbance due to $\text{H}_2\text{O}_\text{II}$ from the total excess absorbance. These values are shown in Table VI.

Since in first order processes the reaction of a substance is proportional to its concentration, and since relaxational compressibility is a first order process, a plot of A_I (Table II) against X_I (calculated from eqn. (1)) was made, Fig. (14). A plot of the excess absorbance due to $\text{H}_2\text{O}_\text{II}$, A_II vs X_II was also made, Fig. (15). A linear correlation was found between A_I and X_I , and between A_II and X_II . The structural absorbance of $\text{H}_2\text{O}_\text{I}$ is $12.6 \times 10^{-15} \frac{\text{sec}^2}{\text{cm.mole}}$ and $\text{H}_2\text{O}_\text{II}$ is $0.37 \times 10^{-5} \frac{\text{sec}^2}{\text{cm.mole}}$.

These two correlations are particularly interesting since the mole fractions of X_I and X_II were determined independently from two different properties, namely

volume and heat capacity, and then found to be in good agreement in the explanation of the behaviour of a third property of water, namely excess sound absorption.

Table VI. Variation of Excess Acoustic Absorbance by $\text{H}_2\text{O}_\text{I}$ (A_I) and by $\text{H}_2\text{O}_{\text{II}}$ (A_{II}) with Temperature.

Temperature	A_I	A_{II}
0°C	58.0 $\text{sec}^2/\text{cm} \times 10^{17}$	21.6 $\text{sec}^2/\text{cm} \times 10^{17}$
5	40.4	21.0
10	29.1	20.4
20	15.3	19.0
30	7.4	17.5
40	3.3	16.2
50	1.0	15.0
60		13.5
70		12.1
80		10.9
90		9.5
100		8.2

Since energy is required for the transformation of species, it is likely that the transformation requiring the least

energy will occur the most easily and frequently, thus the enthalpy difference between species could be the determining factor of the extent to which a species undergoes compressional relaxation. If this assumption is correct, then the fact that A_I and A_{II} are found to be proportional to X_I and X_{II} only, irrespective of temperature, lends further credence to the hypothesis that $(H_{II} - H_I)$ and $(H_{III} - H_{II})$ are independent of temperature.

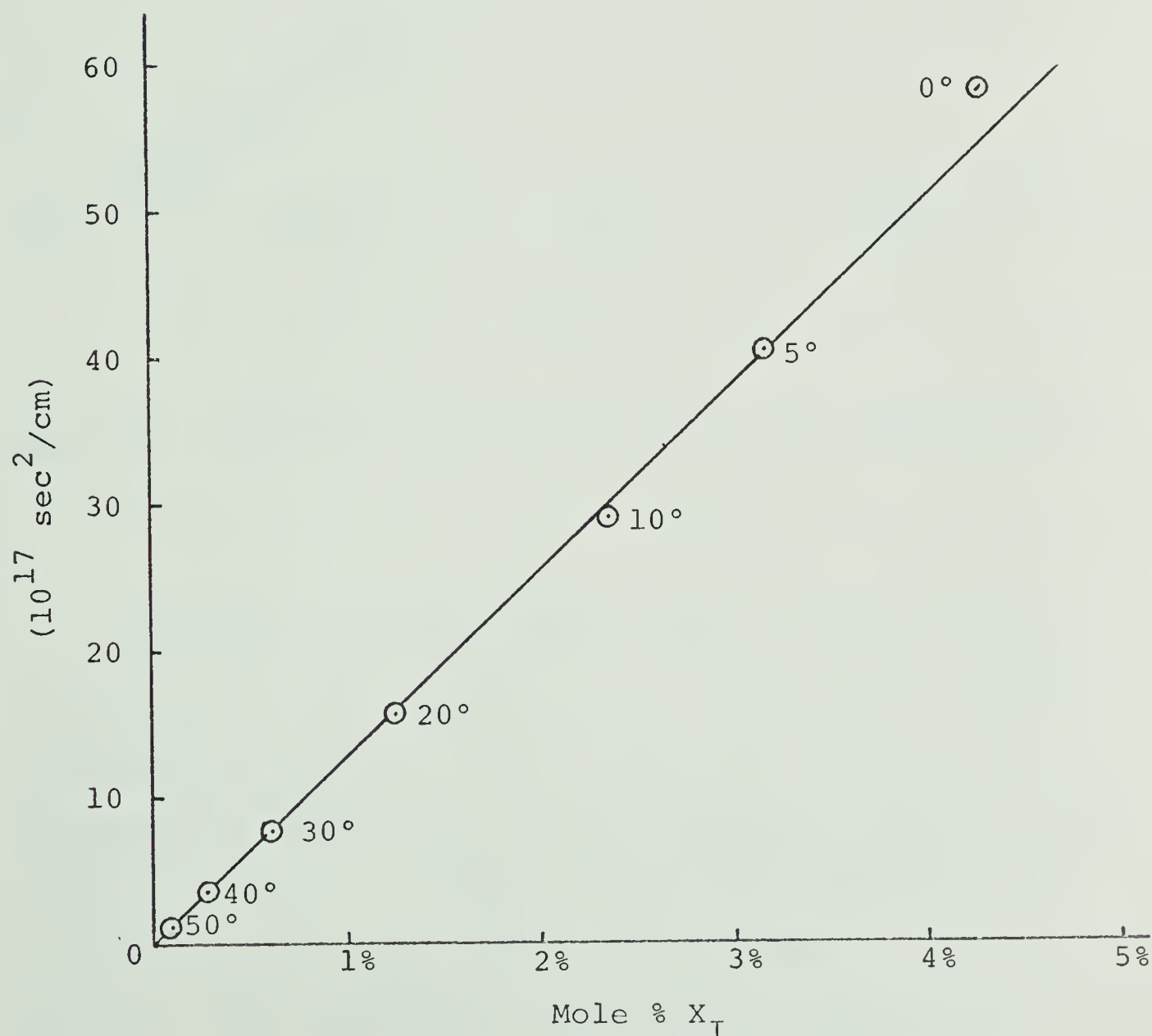


Fig. 14. Excess acoustic absorbance due to H_2O_I , A_I vs concentration.

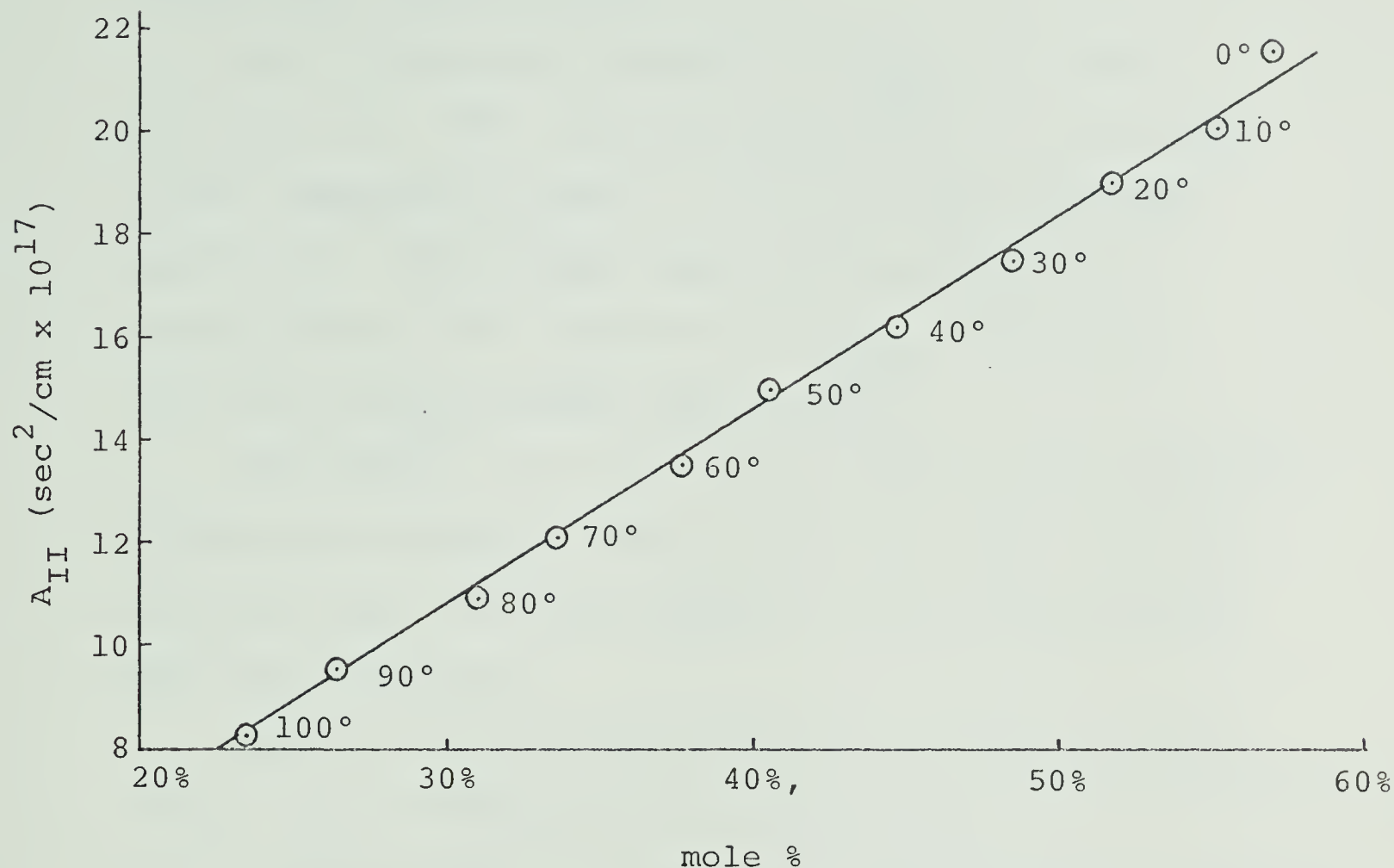


Fig. 15. Absorbance due to H_2O_{II} , A_{II} vs. concentration.

Walrafen's spectral values (Figs. 6 and 7) could be fitted to a curve similar to the curve of the excess acoustic absorbance of water, (Fig. 13), and can be explained by suggesting that the strongly negative slope in the region of 0° to 60° is due to the disappearance of both H_2O_I and H_2O_{II} and the less negative slope in the $60^\circ - 100^\circ$ range due to the slower disappearance

of the $\text{H}_2\text{O}_{\text{II}}$ species only.

Fig. 11 shows the variation of V'_{obs} vs t , over the range $0^\circ - 250^\circ$. The characteristics of this curve in the temperature range $0^\circ - 180^\circ$ has been discussed previously. The straight line section above 180° is probably due to the expansion of $\text{H}_2\text{O}_{\text{III}}$. Therefore above 180° , V'_{obs} becomes equal to V'_{III} .

The findings of a few recent studies on the structure of water are presented here to ascertain that the model of water which has been proposed is not in disagreement with these findings.

There is considerable disagreement between workers in the field of Raman and I.R. spectroscopy (16,17,23,37a,37b,39) as to whether water is a mixture of distinguishable species or is a continuous medium. Walrafen (37a), in his recent paper has shown that the arguments of the authors who claim that water is a continuous medium are not conclusive. He also explains his Raman and I.R. spectra of a 6.2 m solution of HDO in H_2O from 16° to 97° , in terms of a hydrogen-bonded species decreasing linearly in concentration with increasing temperature and a non-hydrogen bonded species increasing linearly in concentration with increasing temperature over the range $16^\circ - 97^\circ$, together with a small concentration of a third species which is present only at low temperatures. The Raman spectra yield a

a value of $\Delta H^\circ = 2.8$ kcal/mole for the conversion of the hydrogen-bonded species into the non-hydrogen bonded species while the near infrared spectra show $\Delta H^\circ = 2.4$ kcal/mole for the same conversion. An I.R. study by Bonner and Woolsey (37b) has yielded results very similar to Walrafen (37a).

The model presented here shows the concentration of H_2O_{II} decreasing linearly with increasing temperature and H_2O_{III} increasing linearly with increasing temperature over the range $0^\circ - 100^\circ$, together with a small concentration of H_2O_I at low temperatures. Also the conversion of H_2O_{II} to H_2O_{III} has an enthalpy value $\Delta H^\circ = 2.0$ kcal/mole associated with the process.

Narten, Danford and Levy (37c) have recently carried out an extensive X-ray diffraction pattern study of the surface of liquid water over the temperature range $4^\circ - 200^\circ$. They proposed a two state model of water consisting of an expanded ice structure in which a fraction of the large holes in the lattice are filled with interstitial molecules. This model fits the X-ray data well in all temperature ranges but 5 parameters were adjusted to obtain the fit. The enthalpy of evaporation predicted by this model is close to the experimental value, but has too small a temperature dependence. The consideration of a small amount of a third species may improve the

temperature dependence. There is no real qualitative disagreement between the model of water presented in this study and that of Narten, Danford and Levy in that both models have considered a highly structured form together with a less associated form of water.

Collie, Hasted and Ritson^(37d) have studied the dielectric constant of water and have found water to have a single dielectric relaxation time which decreases with increasing temperature. Thus it would seem that all water molecules have a similar environment, which favors the model regarding water as a continuous medium. Frank,^(37e) however, interprets this single relaxation time as being the average lifetime of a 'flickering' cluster before it disintegrates. If this idea is correct then the structured parts of water as discussed in the model presented in this study, may be disintegrating and reforming again having an average lifetime equal to the dielectric relaxation time.

5 - Conclusions

This study shows that a two state theory of water satisfactorily explains the behaviour of the specific viscosity of water and partly explains the behaviour of the specific volume, specific heat and isothermal compressibility of water. However, a model postulating

the existence of 3 species, H_2O_I , H_2O_{II} , H_2O_{III} , with H_2O_I disappearing in the region up to 60° and H_2O_{II} in the region up to 180° , satisfactorily explains the variation of the following properties of water with temperature: specific volume, specific heat, isothermal compressibility, excess acoustic absorption of sound, Raman spectra, and the partial molar heat capacities of salts at infinite dilution. All of these properties with surprising consistency are in accord with the postulate that a straight-hydrogen-bonded structure disappears as the temperature is raised above 60° .

CHAPTER III

The Effect of Potassium Iodide and Potassium Fluoride on the Specific Volume of Water

1 - Introduction

It is a well recognized fact that salts affect the structure of water with the fluoride and hydroxide ions being regarded as structure makers and the potassium and iodide ions being regarded as structure breakers. (38,39,40)

Frank and Evans (38) have calculated the structure breaking entropy, ΔS^{st} , of a number of ions using thermodynamic data at 25°. Some of their values for ΔS^{st} are: $F^- = -3.5$ e.u., $I^- = +10.2$ e.u., $K^+ = +12.0$ e.u. If we add the appropriate values to obtain an idea of the behaviour of a salt we get; $\Delta S^{st}(KF) = +8.5$ e.u.; $\Delta S^{st}(KI) = +22.2$ e.u. This indicates that both KF and KI are net structure breakers with KI being a stronger structure breaker than KF. The partial molal heat capacity data of Eigen and Wicke, (30) as discussed in Chapter II are in agreement with this conclusion.

By measuring the specific volumes of various concentrations of KI and KF solutions as a function of temperature, it was thought that it might be possible to determine from the results whether there is structural action by the salts, and perhaps determine with some precision the magnitude of the effect. This could shed further light

on the nature of the structure of water and possibly confirm or disprove the model as outlined in the previous chapter.

2 - Experimental

Eleven solutions each of KI and of KF were made up having concentrations of 0.1 molal; 0.2 m, and thereafter with increments of 0.2 m up to 2.0 m. Shawinigan analytical grade KI was dried for two days at 180° and then used to make up the iodide solutions with distilled, deionzed water, which had been filtered to remove any particles from the ion exchange column. It was found that prolonged heating of the KF caused some of the salt to become insoluble, thus Allied Chemical analytical grade, anhydrous KF was placed in a vacuum dessicator for two weeks before the fluoride solutions were made up.



Fig. 16. Fisher Density Bottle

The densities of these different solutions were measured using 25 ml Fisher density bottles with fitted ground glass stoppers and caps. The measurements were made in triplicate on each solution at temperatures at 5° intervals from 0° to 95° by the following procedure. The bottles were placed in a water bath for 20 minutes. The bath had previously been thermostated to within 0.005° by means of a Sargent Thermistor control unit. The absolute temperature of the bath was set to within 0.02° of the required temperature by means of an N.B.S. calibrated thermometer. When the bottles had equilibrated, the droplet on the top of the stopper was removed with a piece of Kimwipe tissue to ensure that the column of liquid in the stopper was always of uniform height. The bottle was then removed from the bath and dried, special care being given to drying the groove between the stopper and bottleneck. The bottle was then capped, allowed to equilibrate to room temperature, and weighed to within 0.0001 gm.

This method worked very well for temperatures in the vicinity of room temperature but at other temperatures there were a number of experimental difficulties. When the bottles which were full of solution at room temperature were equilibrated in the water bath which had been set at a lower temperature, further additions of solution were required

because of contraction of the solution. These additions were made with a syringe, with care being taken that no air bubbles were introduced. As the bottles were equilibrating to room temperature, after removal from the bath, the solution would expand and flow out of the hole in the stopper. If sufficient liquid was pushed out of the bottle it would touch the ground glass section between the bottle and cap, flow down it and come into contact with the air, with subsequent loss of water by evaporation. On the other hand if a few bottles were weighed before equilibrating to room temperature the balance pan would cool, resulting in incorrect weighings due to convection currents. These difficulties were overcome by weighing a bottle quickly, before it had equilibrated to room temperature. Quick weighings were possible because the weight of the bottle and solution could be guessed closely from previous weighings and the weights adjusted before the bottle was set on the pan. The pan was then allowed to return to room temperature before a further weighing was done. This technique appeared to eliminate errors in weighing due to convection currents. Results were as reproducible as in the experiments near room temperature.

At high temperatures the difficulties were more severe. When the lid of the water bath was lifted off at temperatures above 70°; cold, relatively dry air

entered immediately, which cooled the tops of the bottles which projected above the water and also caused evaporation of some of the water in the bath, resulting in a slight drop in the temperature of the water bath. These effects were minimized by cutting the lid of the water bath into sections and only lifting off that section directly above the density bottles to be removed.

The effect which caused the greatest error in the high temperature measurements and which was the most difficult to eliminate was caused by air in the solutions. As the temperature of the solutions was raised, the dissolved air came out of solution, forming air bubbles which were then trapped in the bottles. To prevent this the solutions were deaerated as much as possible before filling the density bottles. The deaeration was done by stoppering the flask containing the solution with a rubber bung in which was inserted a long, thin glass rod (to prevent evaporation but allow for expansion) and then placing the flask in boiling water for a few hours. As soon as the density bottles were filled with this solution and the stopper fitted into the bottles, they were placed in the temperature bath for the 95° readings. Even with these precautions air bubbles still tended to form in the bottles. If this happened the bottle was removed from the bath and cooled. The air bubble formed in the bottle by contraction of the solution would join with that formed by deaeration

and when the bottle was placed in the bath, the one large bubble was pushed out of the bottle by the expanding liquid. On occasion this process had to be repeated a number of times until finally no air bubbles would form in the density bottle.

After the bottles were filled with deaerated solution, the densities were measured at 95° and then at lower temperatures to 80°. The densities were then measured at 0° and at increasing temperatures to 75°. This gave the minimum trouble with air bubbles and the maximum convenience by not having to top up the bottles, as occurred when measuring densities at decreasing temperatures.

The volumes of the density bottles were determined by carrying out the same experimental procedure with pure water as was done with the solutions and then using the values given in the literature ⁽¹⁸⁾ for the specific volume of water for the necessary calculations.

The weights of each bottle plus solution at the twenty different temperatures were entered on computer cards and subjected to a general least squares analysis, the adjusted weights were then used to calculate the densities and specific volumes, and the average of the three values for the specific volume at each temperature was then obtained. Coefficients of a polynomial expression of the form:

$v = a + bt + ct^2 + dt^3$ were then found by means of the general least squares program for each solution, which fitted the specific volumes at each temperature. The values of V' for each solution and temperature were then obtained by differentiating the appropriate expressions.

Ideally, density bottles should not be used to determine densities of solutions at temperatures which are more than 15° different from room temperature. The magnetic densitometer ⁽⁴¹⁾ giving values to six significant figures is an instrument which is well suited to the determination of densities over the temperature range discussed here. However, with this instrument between only 5 or 10 values per day can be obtained since considerable time is required to check the calibration of the instrument.

I have not yet seen in the literature a study of the density of salt solutions over the temperature and concentration range discussed here, which was carried out by a single investigator. The results presented below are essentially those of a preliminary survey which nevertheless took more than one year to complete. They will show, I believe, that although it would be worthwhile to perform a similar study with instruments capable of giving densities to six decimal places, the general trend in results is nevertheless clearly

apparent in the present study.

3 - Results

The average standard deviation calculated from the three values for each specific volume are as follows:

$$\text{KF (0.1 to 1.0 m)} = 0.00003 \text{ ml/gm}$$

$$\text{KF (1.2 to 2.0 m)} = 0.00010 \text{ ml/gm}$$

$$\text{KI (0.1 to 1.0 m)} = 0.00005 \text{ ml/gm}$$

$$\text{KI (1.2 to 2.0 m)} = 0.00009 \text{ ml/gm}$$

These errors are sufficiently large to throw much doubt on the fifth decimal figure in the values reported below. However, the average change in the specific volume with a 5° temperature rise is 0.00220 gm/ml; it is 0.00800 gm/ml with a change of 0.2 m in KF concentration at constant temperature; and it is 0.01900 gm/ml with a change of 0.2 in KI concentration at constant temperature. Thus the observed changes are large in comparison with the errors.

The specific volumes obtained from the densities determined as outlined above are shown in Tables VII and VIII. The expansibilities, E ($E = \frac{1}{V} dv/dt$), for each temperature and concentration for all the solutions were also calculated. The expansibilities, E , and not V' were plotted against t because E measures the rate of

Table VII. Specific Volumes of KI solutions at Various Temperatures

	<u>0.0m</u>	<u>0.1005 m</u>	<u>0.2002 m</u>	<u>0.4010 m</u>	<u>0.5877 m</u>	<u>0.79954 m</u>
0.0°C	1.00010	0.98766	0.97594	0.95348	0.93573	0.91320
5.0	1.00003	0.98766	0.97606	0.95379	0.93617	0.91376
10.0	1.00030	0.98800	0.97651	0.95439	0.93689	0.91458
15.0	1.00089	0.98867	0.97726	0.95525	0.93786	0.91563
20.0	1.00177	0.98963	0.97828	0.95636	0.93905	0.91688
25.0	1.00293	0.99084	0.97954	0.95769	0.94044	0.91832
30.0	1.00433	0.99229	0.98102	0.95922	0.94201	0.91992
35.0	1.00596	0.99395	0.98270	0.96093	0.94374	0.92167
40.0	1.00781	0.99580	0.98457	0.96281	0.94562	0.92356
45.0	1.00985	0.99784	0.98660	0.96485	0.94764	0.92558
50.0	1.01210	1.00004	0.98880	0.96703	0.94979	0.92772
55.0	1.01449	1.00240	0.99116	0.96936	0.95207	0.92998
60.0	1.01706	1.00492	0.99366	0.97182	0.95447	0.93236
65.0	1.01980	1.00759	0.99631	0.97443	0.95700	0.93486
70.0	1.02270	1.01042	0.99910	0.97717	0.95967	0.93747
75.0	1.02576	1.01341	1.00206	0.98006	0.96247	0.94022
80.0	1.02897	1.01657	1.00517	0.98310	0.96542	0.94311
85.0	1.03235	1.01992	1.00845	0.98631	0.96854	0.94614
90.0	1.03589	1.02347	1.01191	0.98969	0.97185	0.94934
95.0	1.03961	1.02724	1.01557	0.99326	0.97536	0.95272

Table VII (continued)

	<u>0.9985 m</u>	<u>1.2123 m</u>	<u>1.4025 m</u>	<u>1.5995 m</u>	<u>1.8015 m</u>	<u>1.9935 m</u>
0.0°C	0.89479	0.87769	0.86068	0.84528	0.83069	0.81728
5.0	0.89546	0.87855	0.86161	0.84630	0.83168	0.81843
10.0	0.89636	0.87957	0.86270	0.84745	0.83283	0.81969
15.0	0.89749	0.88076	0.86394	0.84873	0.83414	0.82107
20.0	0.89881	0.88211	0.86532	0.85013	0.83558	0.82254
25.0	0.90029	0.88360	0.86684	0.85166	0.83716	0.82413
30.0	0.90193	0.88524	0.86848	0.85332	0.83886	0.82581
35.0	0.90371	0.88701	0.87025	0.85509	0.84067	0.82760
40.0	0.90561	0.88891	0.87215	0.85699	0.84258	0.82948
45.0	0.90763	0.89093	0.87416	0.85900	0.84459	0.83146
50.0	0.90975	0.89308	0.87629	0.86113	0.84670	0.83354
55.0	0.91198	0.89534	0.87854	0.86336	0.84890	0.83571
60.0	0.91431	0.89772	0.88089	0.86570	0.85119	0.83798
65.0	0.91675	0.90020	0.88335	0.86814	0.85356	0.84034
70.0	0.91930	0.90279	0.88591	0.87068	0.85602	0.84279
75.0	0.92198	0.90548	0.88858	0.87332	0.85858	0.84534
80.0	0.92478	0.90827	0.89135	0.87604	0.86122	0.84799
85.0	0.92774	0.91117	0.89422	0.87885	0.86936	0.85074
90.0	0.93086	0.91416	0.89720	0.88173	0.86680	0.85358
95.0	0.93417	0.91725	0.90028	0.88469	0.86975	0.85652

Table VIII. Specific Volumes of KF solutions at various temperatures.

	<u>0.0 m</u>	<u>0.1021 m</u>	<u>0.1922 m</u>	<u>0.3980 m</u>	<u>0.4965 m</u>	<u>0.8066 m</u>
0.0°C	1.00010	0.99470	0.99006	0.98053	0.97525	0.96086
5.0	1.00003	0.99473	0.99015	0.98075	0.97556	0.96135
10.0	1.00030	0.99509	0.99057	0.98126	0.97615	0.96206
15.0	1.00089	0.99573	0.99127	0.98205	0.97699	0.96300
20.0	1.00177	0.99666	0.99224	0.98309	0.97805	0.96415
25.0	1.00293	0.99784	0.99346	0.98435	0.97934	0.96548
30.0	1.00433	0.99925	0.99490	0.98583	0.98083	0.96700
35.0	1.00596	1.00090	0.99656	0.98750	0.98250	0.96869
40.0	1.00781	1.00275	0.99841	0.98936	0.98435	0.97054
45.0	1.00985	1.00497	1.00044	0.99138	0.98637	0.97254
50.0	1.01210	1.00720	1.00270	0.99357	0.98855	0.97468
55.0	1.01449	1.00941	1.00502	0.99590	0.99087	0.97697
60.0	1.01706	1.01197	1.00755	0.99839	0.99334	0.97938
65.0	1.01980	1.01467	1.01023	1.00102	0.99595	0.98193
70.0	1.02270	1.01753	1.01307	1.00380	0.99869	0.98461
75.0	1.02576	1.02051	1.01605	1.00673	1.00156	0.98741
80.0	1.02897	1.02363	1.01919	1.00981	1.00456	0.99034
85.0	1.03235	1.02668	1.02249	1.01304	1.00770	0.99339
90.0	1.03589	1.03025	1.02595	1.01645	1.01096	0.99658
95.0	1.03961	1.03375	1.02958	1.02004	1.01437	0.99989

Table VIII. (continued)

	<u>1.0031 m</u>	<u>1.2633 m</u>	<u>1.3894 m</u>	<u>1.6030 m</u>	<u>1.8019 m</u>	<u>1.9980 m</u>
0.0°C	0.95209	0.94127	0.93598	0.92749	0.91989	0.91256
5.0	0.95270	0.94197	0.93674	0.92832	0.92077	0.91347
10.0	0.95351	0.94286	0.93767	0.92930	0.92181	0.91454
15.0	0.95452	0.94393	0.93875	0.93045	0.92298	0.91574
20.0	0.95572	0.94517	0.93999	0.93173	0.92429	0.91707
25.0	0.95710	0.94657	0.94138	0.93316	0.92574	0.91853
30.0	0.95864	0.94812	0.94292	0.93472	0.92731	0.92011
35.0	0.96034	0.94982	0.94460	0.93642	0.92900	0.92180
40.0	0.96218	0.95166	0.94642	0.93823	0.93081	0.92360
45.0	0.96417	0.95362	0.94838	0.94017	0.93273	0.92551
50.0	0.96629	0.95572	0.95046	0.94223	0.93476	0.92752
55.0	0.96854	0.95794	0.95267	0.94440	0.93690	0.92963
60.0	0.97092	0.96028	0.95501	0.94668	0.93915	0.93184
65.0	0.97341	0.96273	0.95748	0.94907	0.94151	0.93415
70.0	0.97603	0.96529	0.96002	0.95156	0.94397	0.93657
75.0	0.97877	0.96797	0.96270	0.95416	0.94653	0.93908
80.0	0.98162	0.97075	0.96548	0.95687	0.94920	0.94170
85.0	0.98459	0.97365	0.96837	0.95968	0.95197	0.94442
90.0	0.98769	0.97666	0.97135	0.96259	0.95485	0.94725
95.0	0.99090	0.97978	0.97443	0.96561	0.95784	0.95020

change of unit volume with temperature and thus permits the comparison of the rate of expansion of solutions having different densities. This is not possible with V' which measures the change in volume with temperature of 1 gm of the material under consideration.

The plots of the E vs t data of all the solutions are shown in Figs. (17 - 24). Fig. (25) shows a comparison of the expansivities of the KI and KF solutions at 0° and 95° .

4 - Discussion

It was seen in Chapter I that the plot of V' vs t for water (Fig. (1b)) consisted of both straight line and curved sections. A plot of E vs t is very similar to that of V' vs t . The curved section in the E vs t data occurs from $0^\circ - 54^\circ$ and, as in the case of the V' vs t data, is presumed to denote the presence of H_2O_I . Also it was assumed that a rise in temperature causes the disappearance of some H_2O_I , causing a loss of volume, which causes the expansivity to be lower than that which would have occurred with no H_2O_I present. This in turn causes the points for the curved section to fall below the extrapolated straight line in the E vs t data, Figs. (1, 17-24). It was also assumed that the straight line represents the expansivity of water if no H_2O_I were present. In Figs. (17-24), the

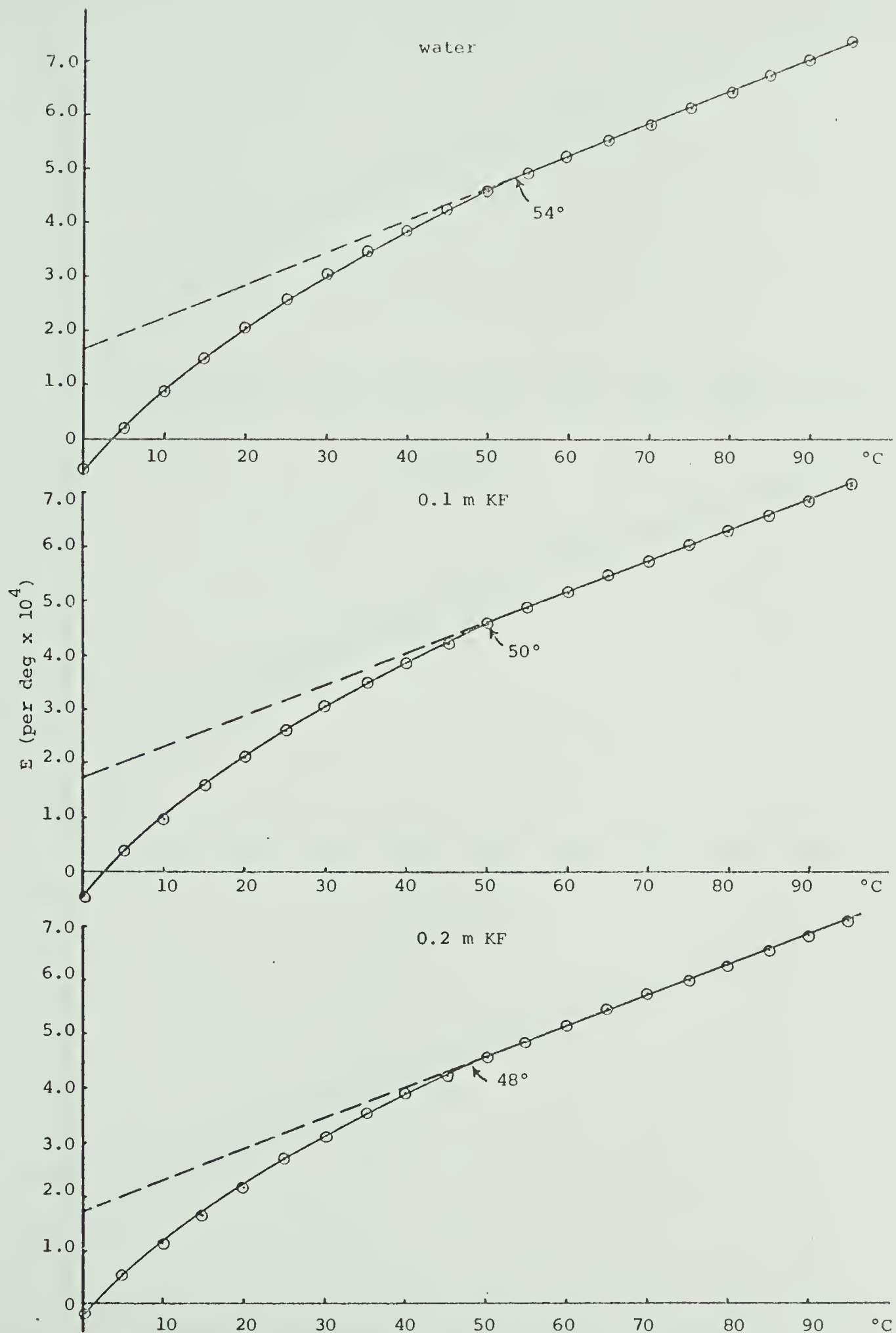


Fig. 17: Expansivity of KF solutions vs temperature.

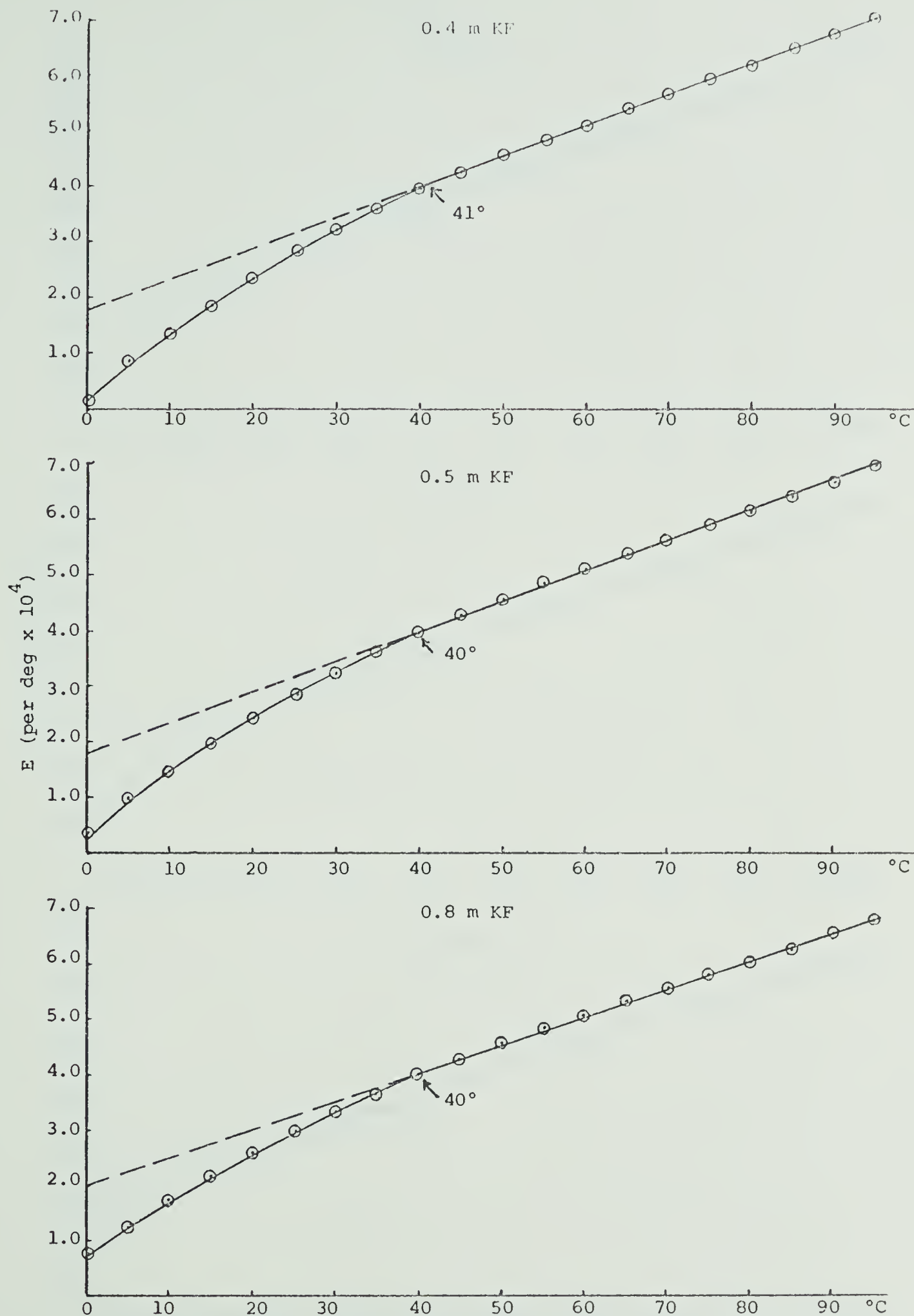


Fig. 18: Expansivity of KF solutions vs temperature.

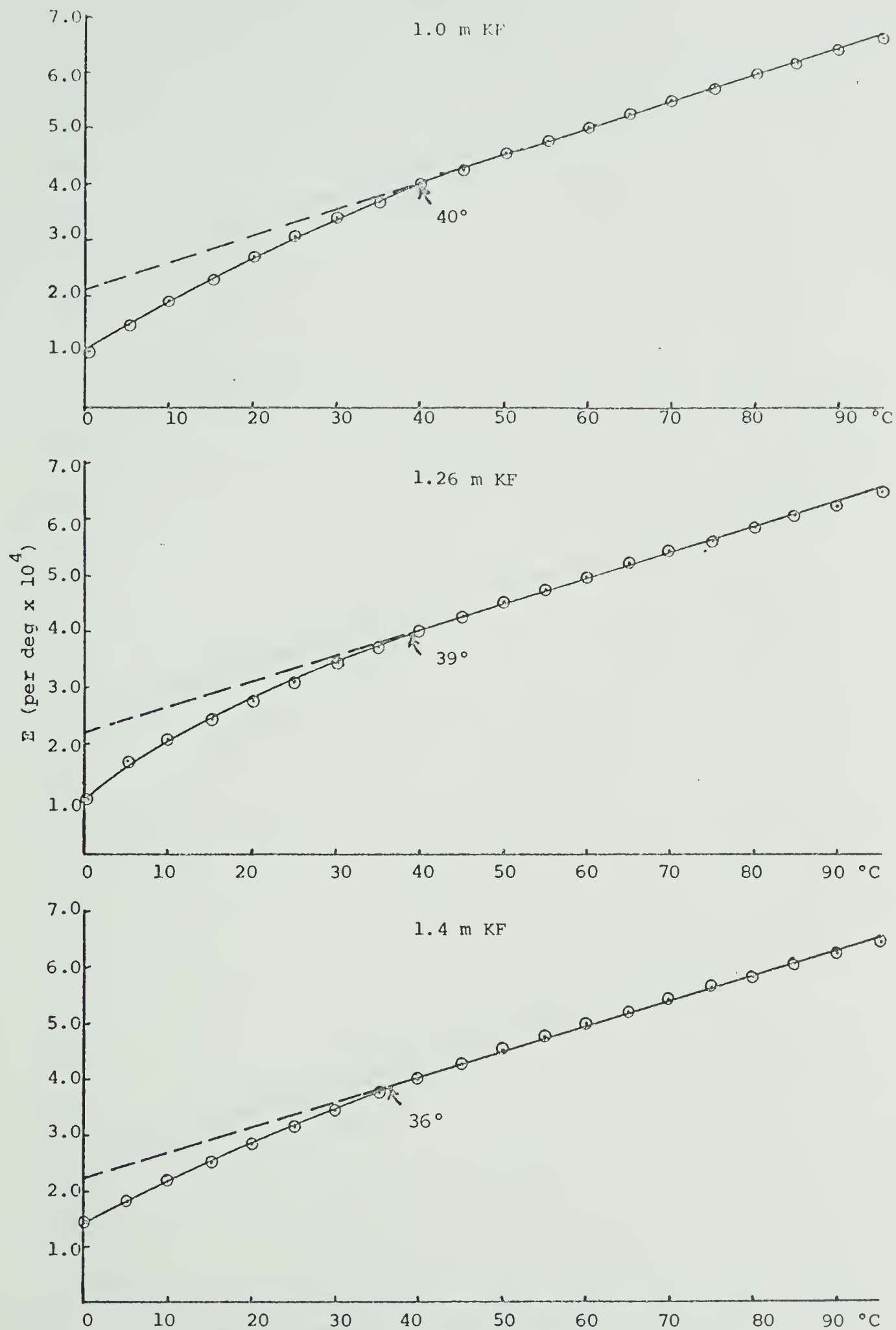
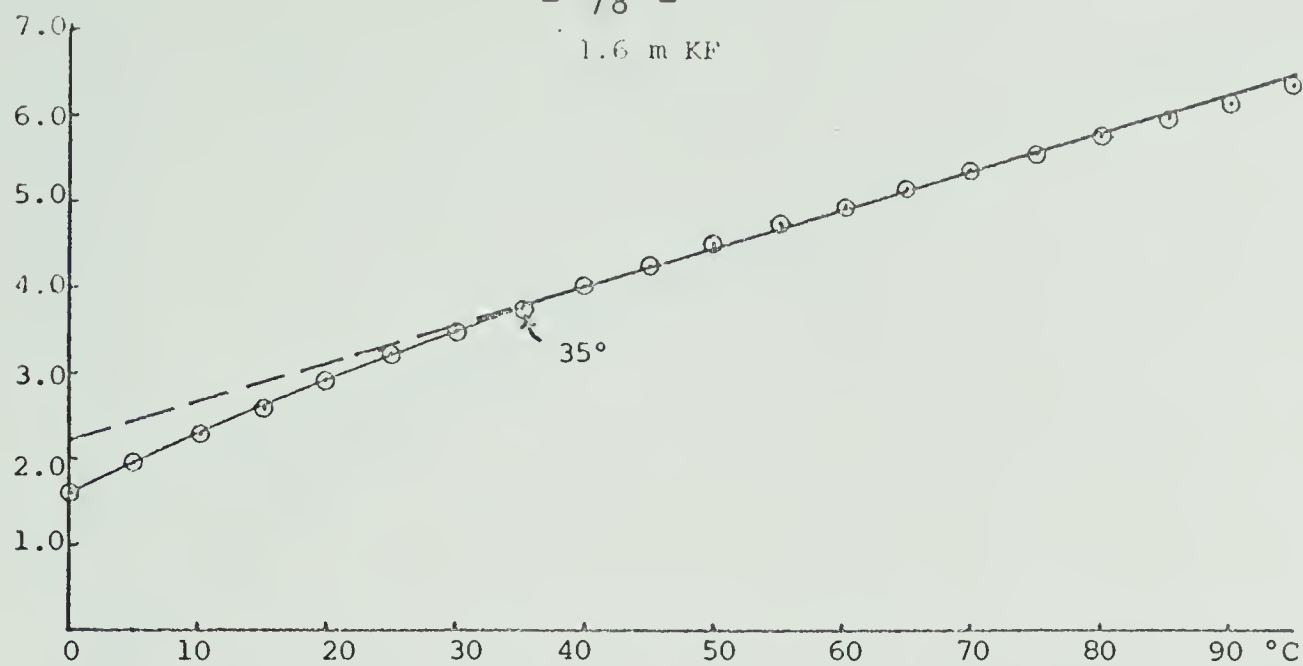


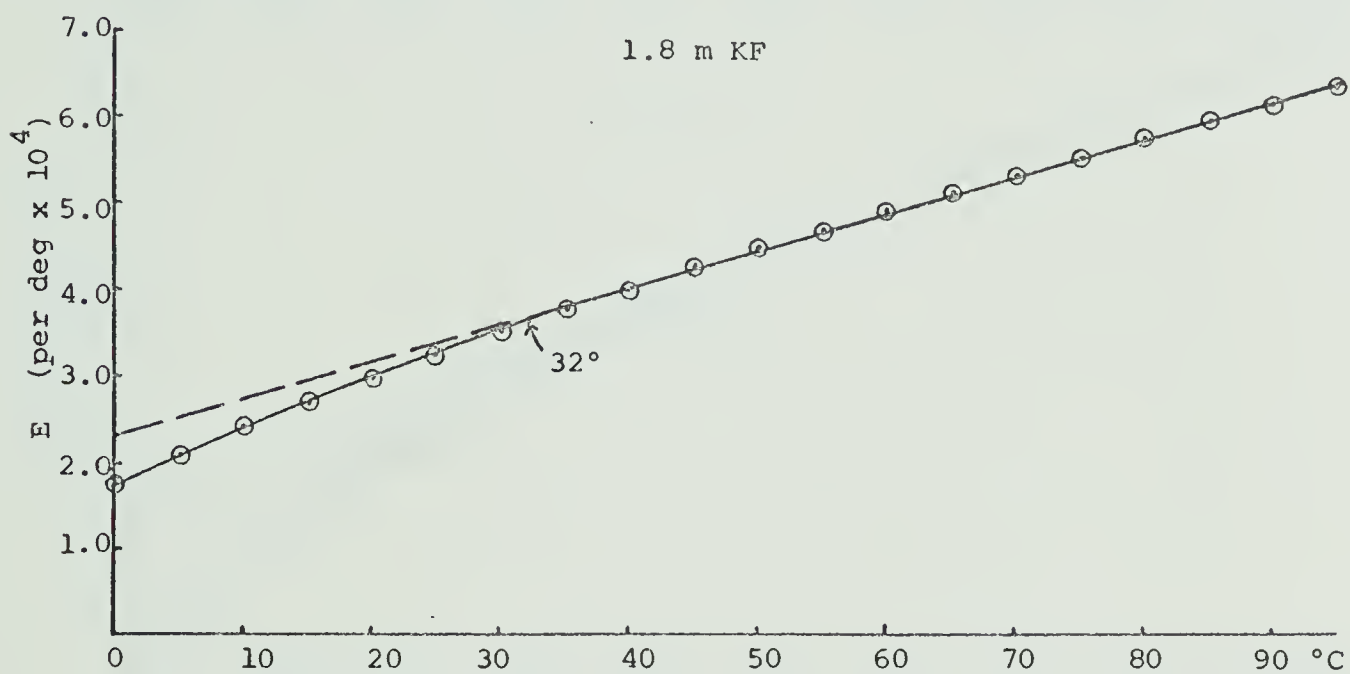
Fig. 19: Expansivity of KF solutions vs temperature.

- 78 -

1.6 m KF



1.8 m KF



2.0 m KF

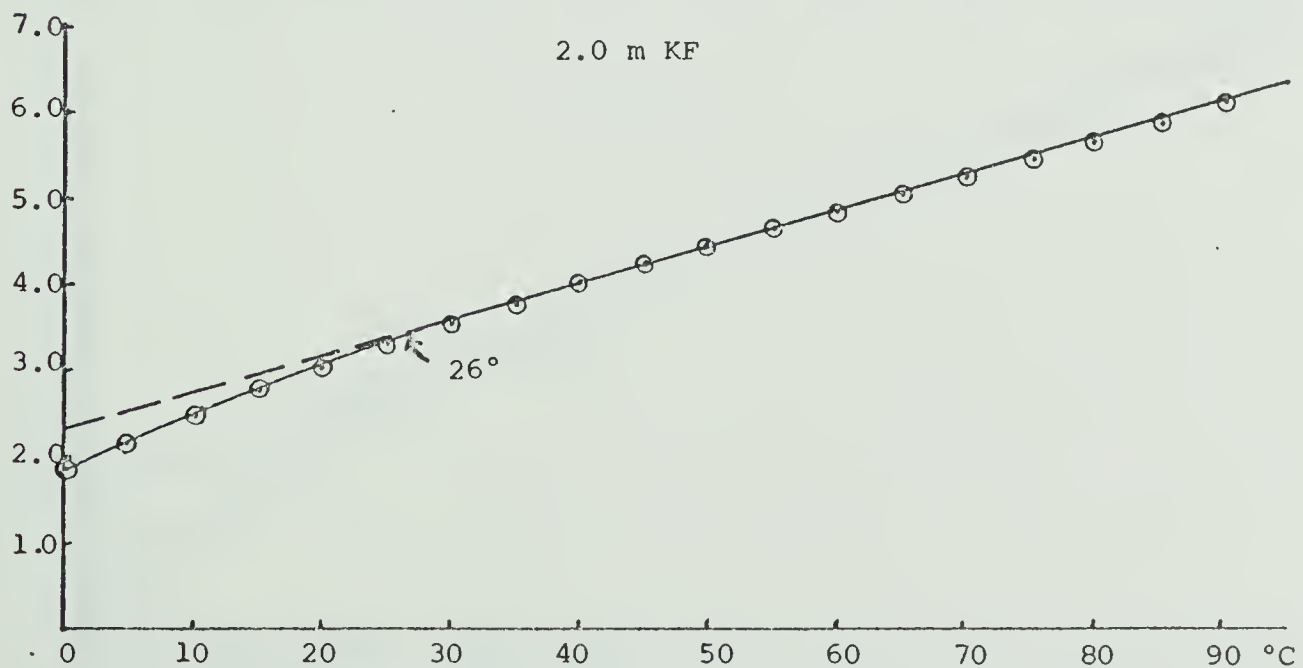


Fig. 20: Expansivity of KF solutions vs temperature.

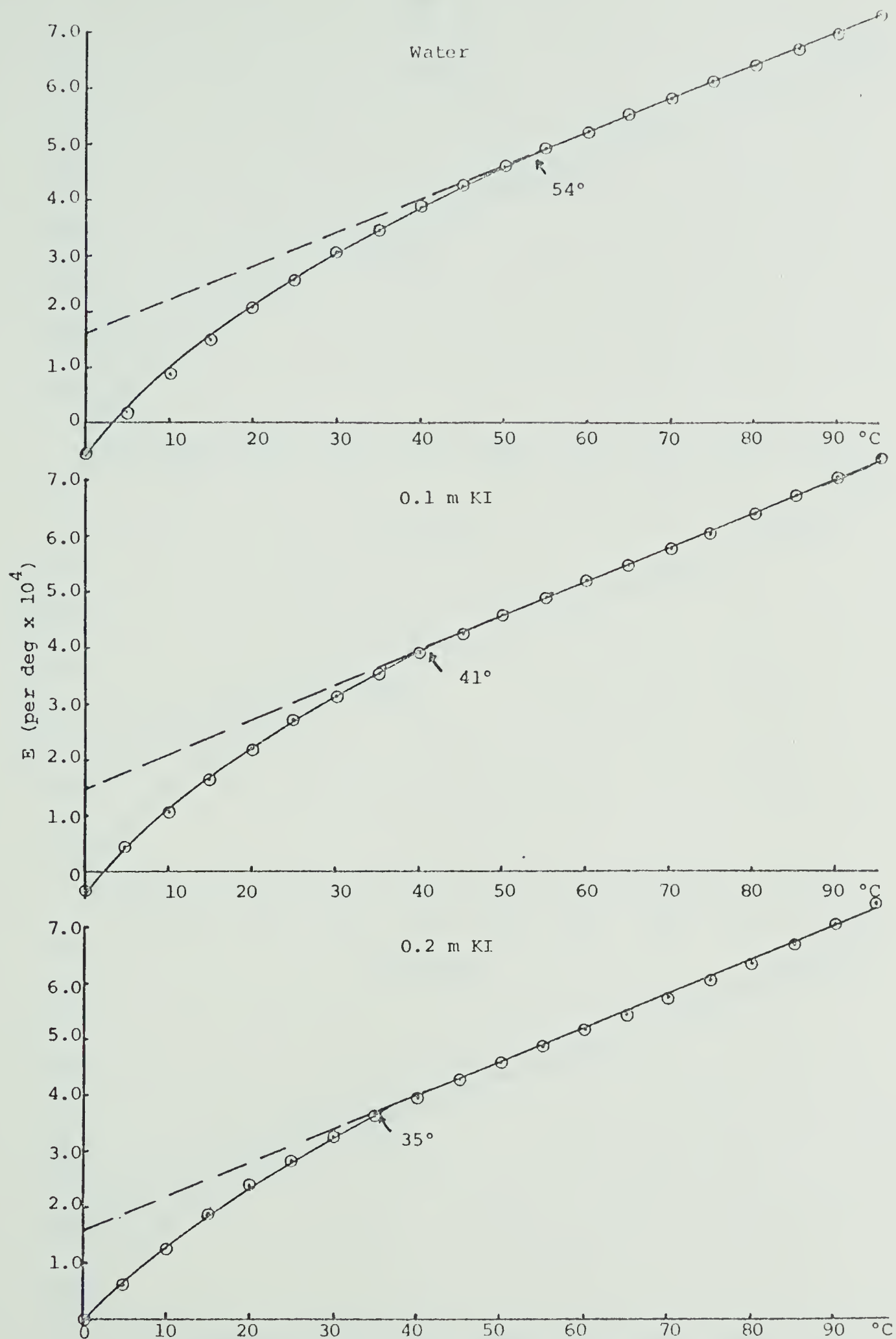


Fig. 21: Expansivity of KI solutions vs temperature.

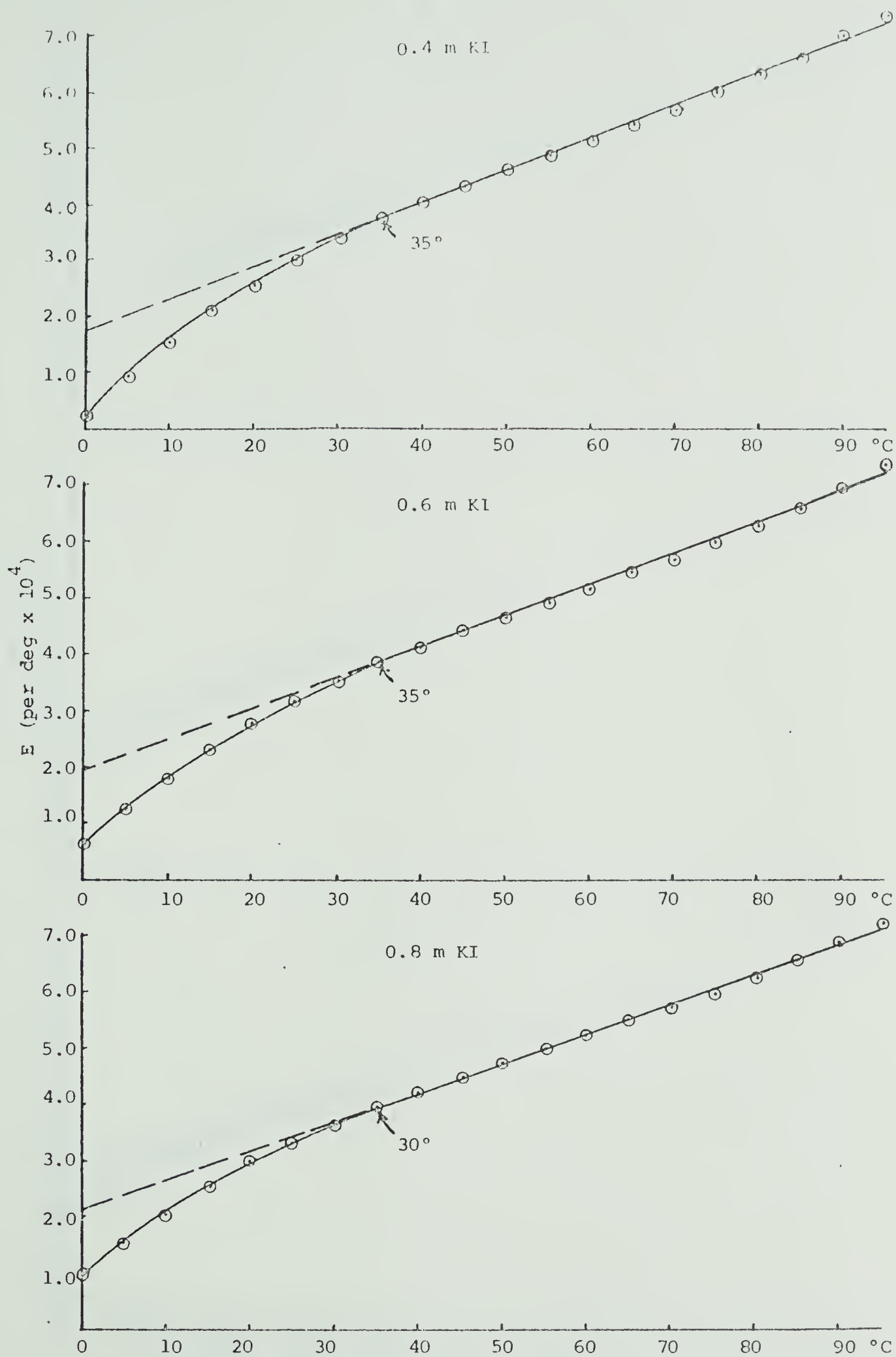


Fig. 22: Expansivity of KI solutions vs temperature.

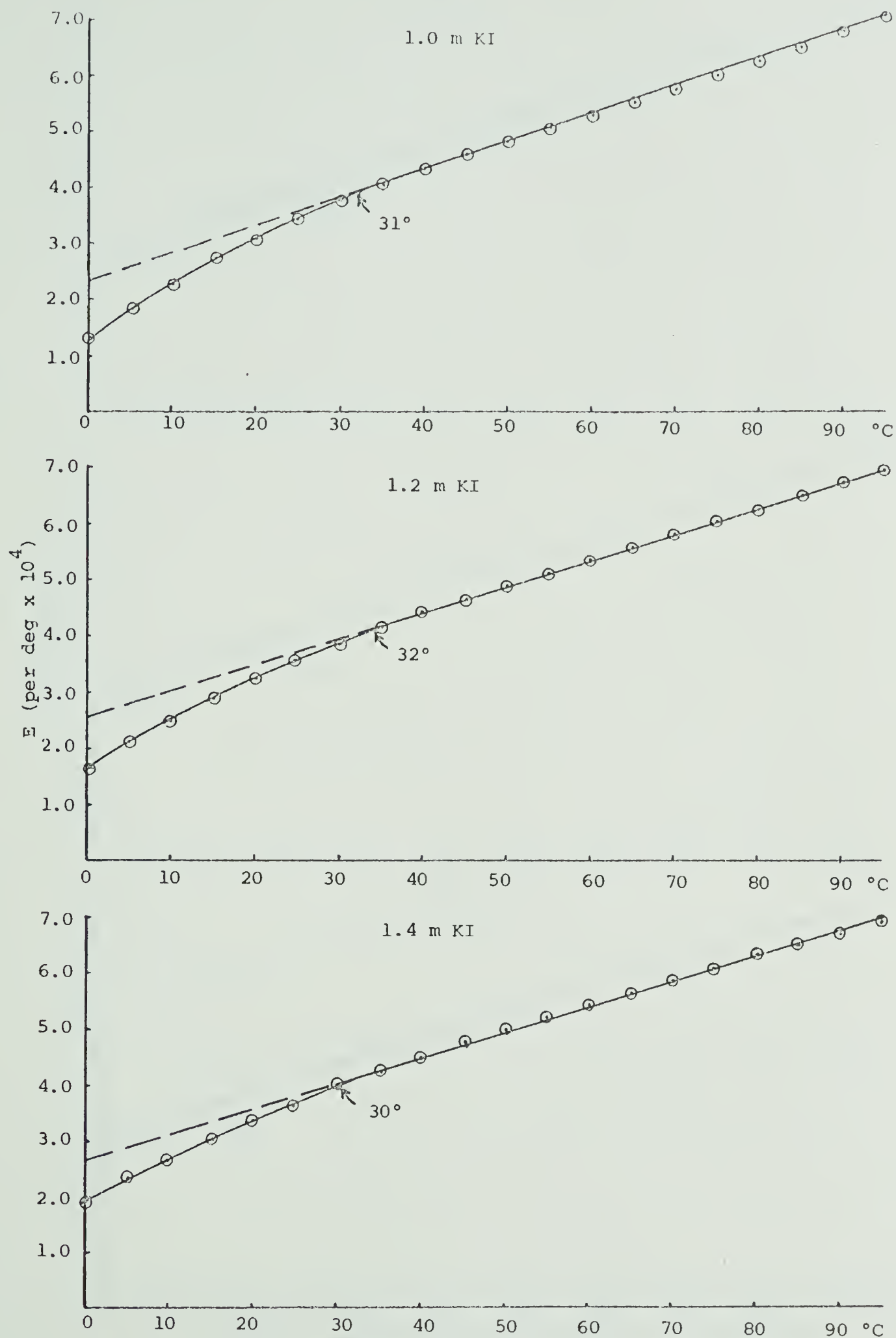


Fig. 23: Expansivity of KI solutions vs temperature.

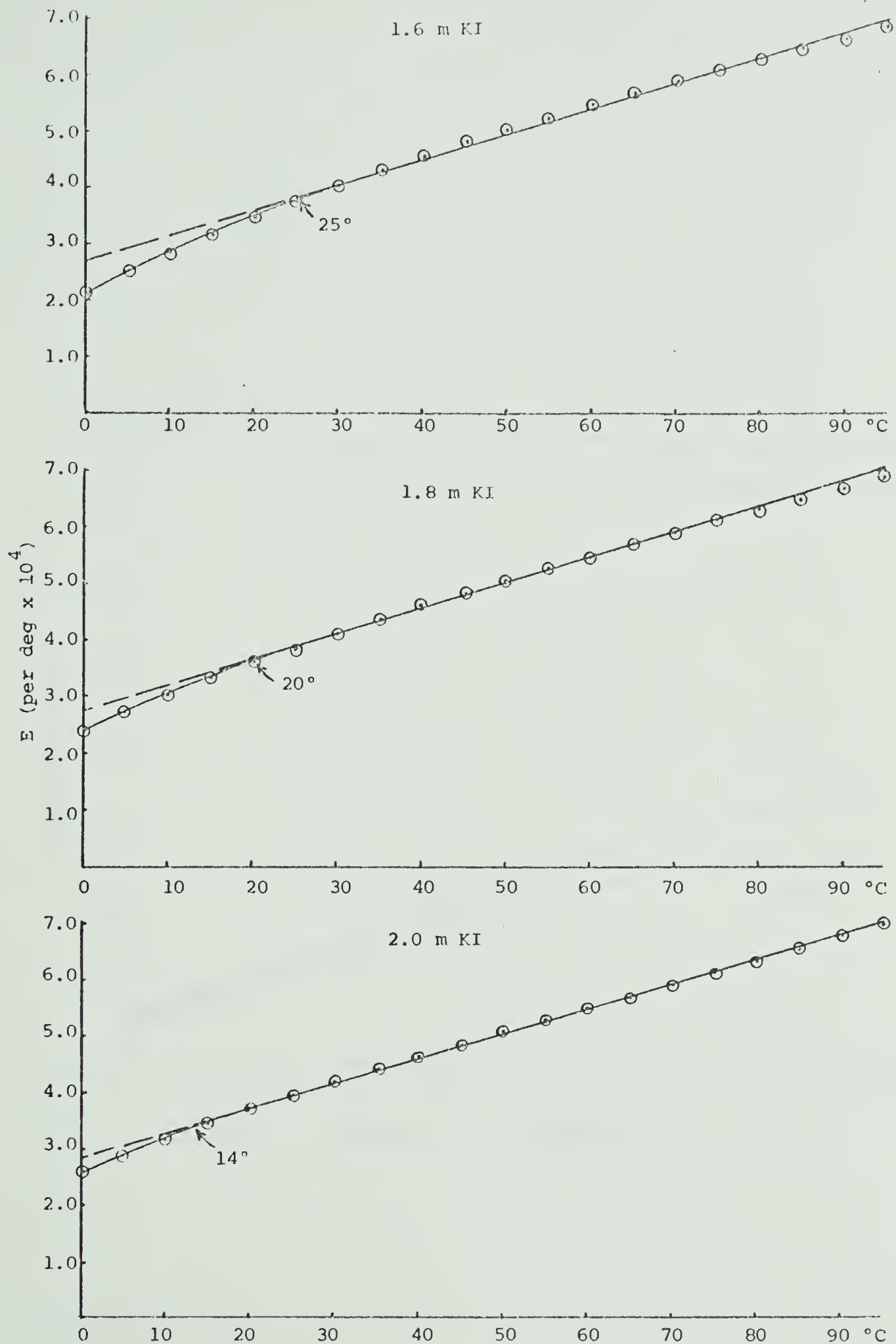


Fig. 24: Expansivity of KI solutions vs temperature.

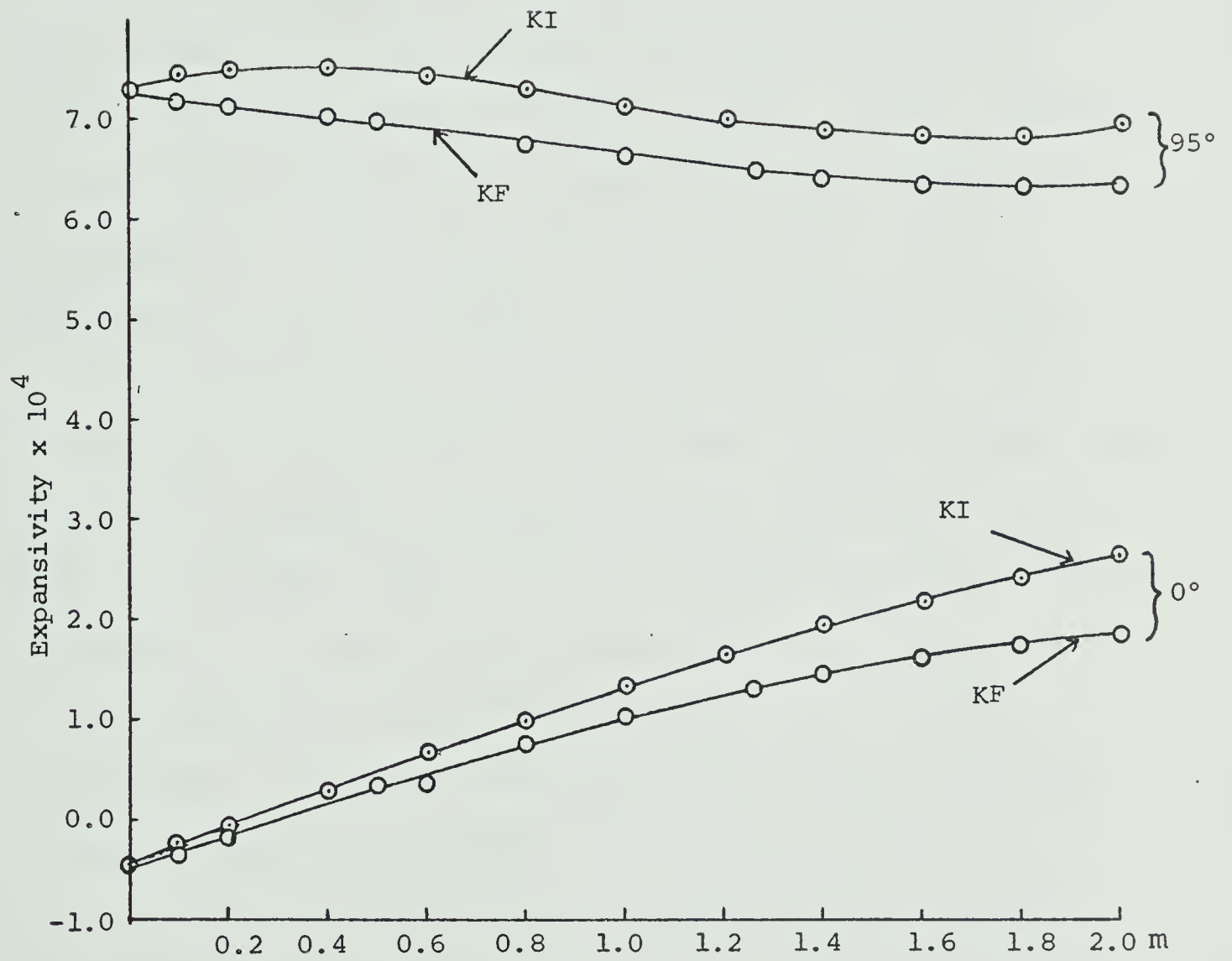


Fig. 25: Expansivity vs concentration.

straight line portions of the E vs t plots are extended to lower temperatures with increasing salt concentrations, which is in accord with the supposition that salts break down water structure. In Fig. (26) the minimum temperature for each solution at which the E vs t data fall on a straight line is plotted against temperature. The points shown in Fig. (26) were obtained by visual inspection of the E vs t data shown in Figs. (17-24). Thus, according to our interpretation, we see that KI always causes H_2O_I to disappear at lower temperatures than does KF. In other words, KI is a stronger structure breaker of H_2O_I than is KF, especially in the region 0.0 to 0.4 m. By extrapolation of the data in Fig. (26) it would appear that H_2O_I would no longer be present at 0° in solutions of KI which are stronger than 2.2-2.4 m. Higher concentrations of KF would be necessary to remove all of the H_2O_I at 0° .

The expansivities of the solutions at 0° without H_2O_I present, (obtained from the values of the intercept of the extrapolated straight line portion of the E vs t plots with the E axis,) show an increase with increased salt concentration, Figs. (17-24,29). These data, suggest that at 0° H_2O_{II} is also being broken down by the salts. This will be discussed later in greater detail.

Fig. (25) shows that the expansivities of KI solutions are greater than those of KF at 0° and 95° . At 0° the

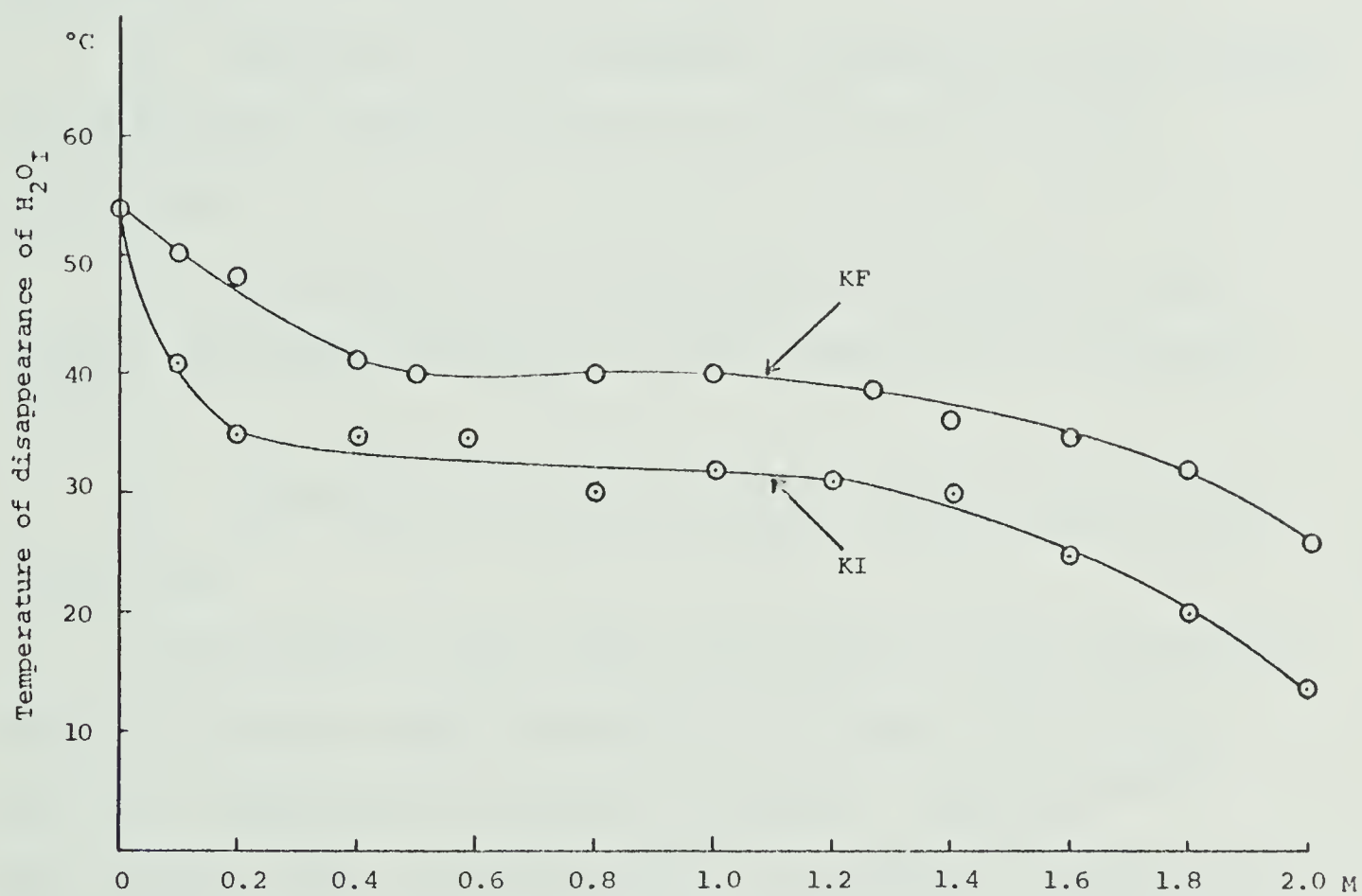


Fig. 26: Temperature of disappearance of H_2O_2 vs concentration.

difference between the KI and KF expansivities increases with increasing salt concentration. At 95°, the difference between the KI and KF expansivities remains virtually the same with increasing concentration (the difference at 0.4 m is the same as that at 1.8 m). To explain these results, the widely accepted Frank-Wen model ⁽⁶⁾ for the structure of electrolyte solutions is adopted. It states that three regions surround an ion in water;

a) the first is an innermost structure-forming region of polarized, immobilized and electrostricted water molecules;

b) the second is an intermediate structure-broken region in which the water is more random than in ordinary water;

c) the third is an outer region having normal water structure.

In the first region the phenomenon of electrostriction occurs in which water molecules are firmly bound to an ion and compressed by electric forces. Mukerjee ⁽⁴²⁾ has assumed that electrostriction is inversely proportional to the radius of the ion for the alkali metals and halides (excluding Li^+). Benson and Copeland ⁽⁴³⁾ have presented evidence that this hypothesis is correct.

In the discussion of expansivity of water, the reasonable assumption is made that water which is relatively

unstructured will undergo the greatest expansion with increasing temperature, whereas highly structured water or electrostricted water will have a smaller expansivity. Since the electrostrictive effect of the fluoride ion is greater than that of the iodide ion, electrostriction by the fluoride ion should decrease the expansivity of water more than the iodide ion. On the other hand, since the iodide ion is thought to be a stronger structure breaker of $\text{H}_2\text{O}_\text{I}$, its structure breaking effect should be greater than that of the fluoride ion at 0° . Therefore, from the standpoint of structure breaking effects, the iodide ion should increase the expansivity of water at 0° more than the fluoride ion.

To summarize, the electrostrictive effect of iodide is small whereas the structure-breaking effect of iodide on $\text{H}_2\text{O}_\text{I}$ is large with a resultant increase in expansivity of water at 0° . For the fluoride ion, its structure-breaking effect on $\text{H}_2\text{O}_\text{I}$ is smaller and its electrostrictive effect is larger. Both of these factors combine to cause a smaller increase in expansivity of water at 0° by the addition of fluoride than by the addition of iodide, as shown in Fig. (25).

The situation at 95° is different since no $\text{H}_2\text{O}_\text{I}$ is present and the F^- ion is supposed to be the bigger structure-breaker of $\text{H}_2\text{O}_{\text{II}}$. Thus from the standpoint of

structure breaking, the KF solution should have the higher expansivity. However, the large electrostrictive effect of the F^- ion overpowers the structure-breaking effect. On the other hand, the net effect of KI addition at 95° is enhanced expansivity, since, as at 0° , the small electrostrictive effect is overpowered by a larger structure-breaking effect. The results at 95° are that the expansivities of the KI solutions are still greater than those of KF but increased salt concentration makes very little difference in the expansivities of KF and KI solutions. If only the structure breaking effect were operating at higher temperatures there would be a definite trend in the difference between the expansivities of the KF and KI solutions with increased concentration. It would appear that at 0° the structure breaking effect predominates over the electrostrictive effect since the expansivities of both salt solutions increases with increasing concentration. In contrast, at 95° it would appear that electrostriction predominates slightly over structure breaking since there is a small general decrease in expansivity with increasing salt concentration. This is also in accord with the idea that there is considerably less structure at high temperatures than at low temperatures.

Padova ⁽⁴⁴⁾ has considered the problem of the actual volume of an ion in solution and suggests the following

volumes for salts in solution; $V_{KF}^{\circ} = 23.1$ ml/mole
(compared to the volume in crystal form, $V_C = 23.4$ ml/mole);
 $V_{KI}^{\circ} = 52.4$ ml/mole ($V_C = 53.2$ ml/mole). The small
difference between the volume of the ions in solution
and in the crystal form is thought to be due to different
distortions of the electron orbitals of the ions in
water and in the crystal. (44,45)

As can be seen from Figs. (27(a),(b)) the partial
molal volume of KF, \bar{V}_{KF} varies from 6.4 ml/mole at
infinite dilution and 0° to 14.2 ml/mole for 2 m KF at
45°. Both values are considerably less than the 23.1
ml/mole value suggested by Padova. (44) These low values
in \bar{V}_{KF} are caused by two effects : a decrease in partial
molal volume due to structure breaking, \bar{V}^{st} and also
due to electrostriction, \bar{V}^{es} .

The partial molal volume of a salt in solution, \bar{V}
is defined by

$$\bar{V} = \left(\frac{\partial V}{\partial n} \right)_{P,T}$$

where the volume of the solution increases by the amount,
 ∂V when ∂n moles of salt are added. If there was ideal
mixing, $\bar{V}_{KF} = V_{KF}^{\circ}$; $\bar{V}_{KI} = V_{KI}^{\circ}$. Similarly, \bar{V}^{st} would be
defined as

$$\bar{V}^{st} = \left(\frac{\partial V^{st}}{\partial n} \right)_{P,T}$$

where the volume of the solution decreases by the amount v^{st} due to the breakdown of a certain quantity of structured water into unstructured water on the addition of dn moles of salt. Also \bar{V}^{es} would be defined as

$$\bar{V}^{es} = \left(\frac{\partial V^{es}}{\partial n} \right)_{P,T}$$

where the volume of the solution decreases by the amount v^{es} due to electrostriction of the hydration molecules when dn moles of salt are added to the solution. Thus we obtain

$$\bar{V}_{KF} = V_{KF}^{\circ} - \bar{V}_{KF}^{es} - \bar{V}_{KF}^{st} \quad (37)$$

The term \bar{V}^{es} is caused by the hydration of ions which has been shown in Chapter II to decrease with increasing temperature. Therefore \bar{V}_{KF}^{es} becomes smaller in magnitude with increasing temperature. The term \bar{V}_{KF}^{st} is more complex, being affected by the loss of volume as H_2O_I breaks down, $\bar{V}_{KF}^{st(I)}$, and the loss of volume as H_2O_{II} breaks down, $\bar{V}_{KF}^{st(II)}$. Thus eqn. (37) can be rewritten as

$$\bar{V}_{KF} = V_{KF}^{\circ} - \bar{V}_{KF}^{es} - \bar{V}_{KF}^{st(I)} - \bar{V}_{KF}^{st(II)} \quad (38)$$

It will be assumed that V_{KF}° is temperature independent. The simplest explanation for the results shown in Figs. (27(a),(b)) is that at low temperature \bar{V}_{KF}^{es} and

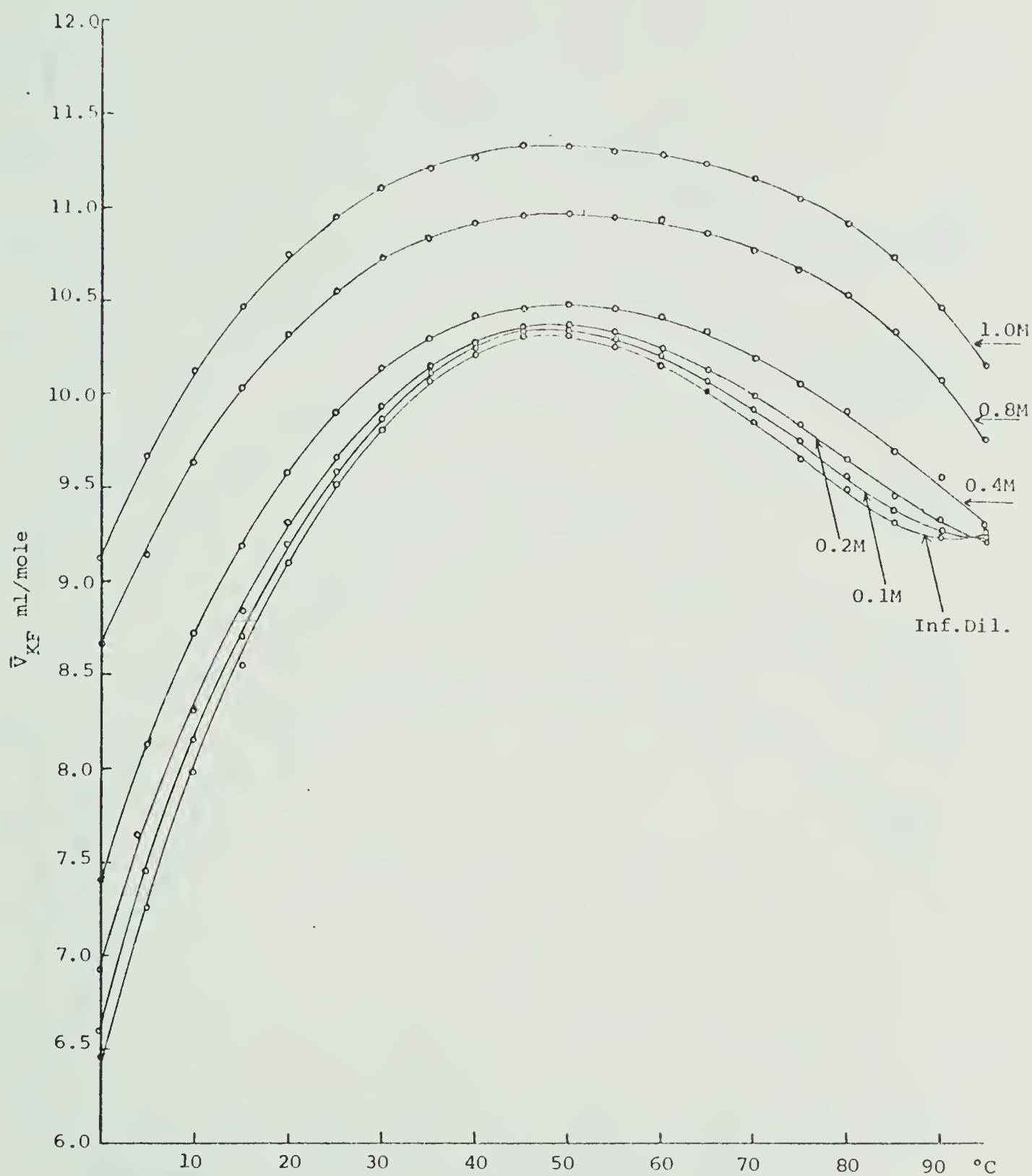


Fig. 27(a): Partial Molal Volumes of KF, \bar{V}_{KF} , vs Temperature.

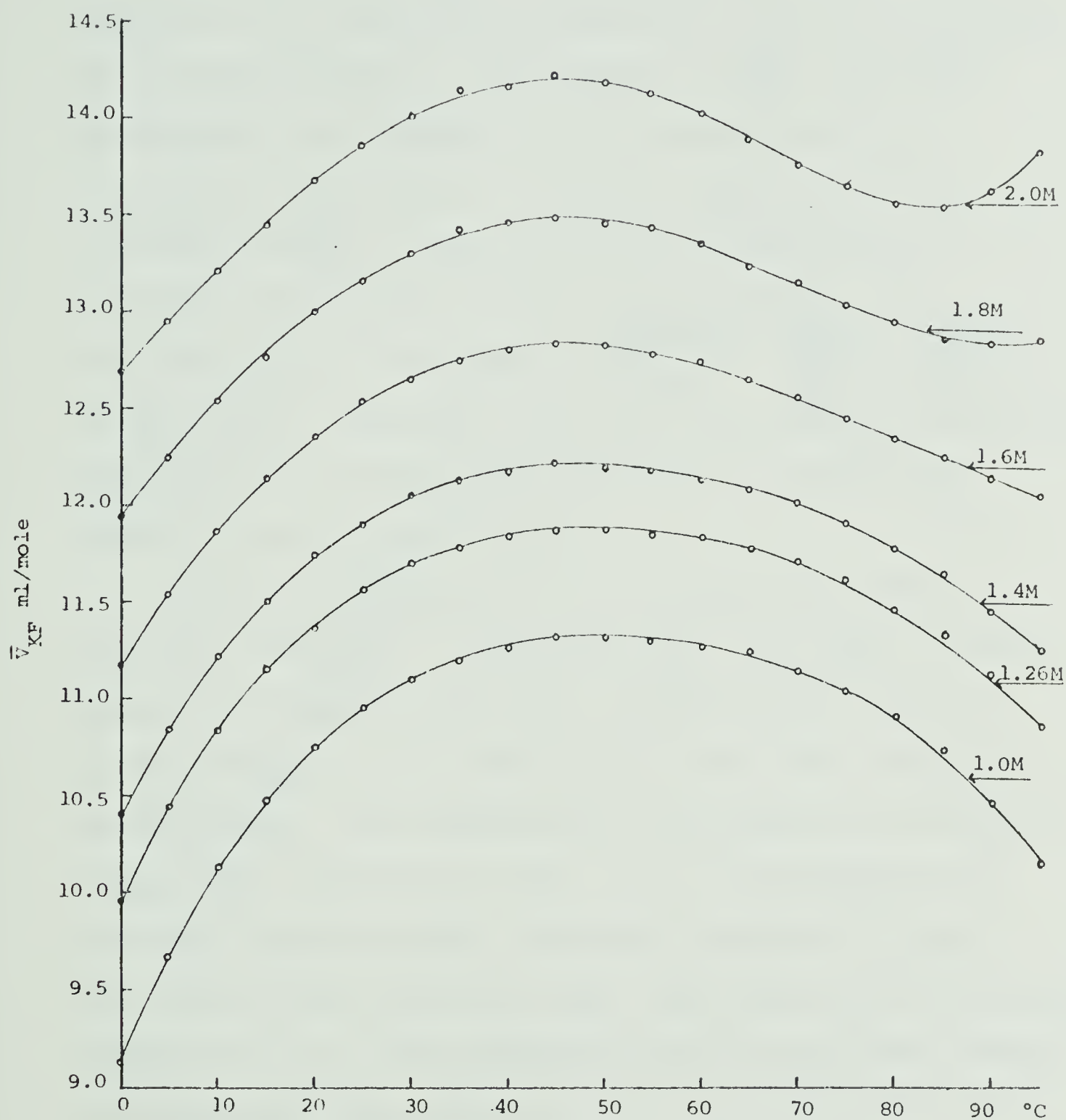


Fig. 27(b): Partial Molal Volumes of KF, \bar{V}_{KF} vs Temperature.

$\bar{V}_{KF}^{st(I)}$ are large but decreasing in magnitude with increasing temperature, whereas $\bar{V}_{KF}^{st(II)}$ is small but increasing in magnitude with increasing temperature. As the temperature is increased above 0° , the decrease in \bar{V}_{KF}^{es} and $\bar{V}_{KF}^{st(I)}$ is dominant and accounts for the increase in \bar{V}_{KF} according to eqn. (38). At higher temperatures, the increase in $\bar{V}_{KF}^{st(II)}$ with increasing temperature is dominant and accounts for the decrease in \bar{V}_{KF} . At the positions of the maxima,
$$\frac{d\bar{V}_{KF}^{st(II)}}{dt} = \frac{d\bar{V}_{KF}^{es}}{dt} + \frac{d\bar{V}_{KF}^{st(I)}}{dt}.$$
 If \bar{V}_{KF}^{es} , $\bar{V}_{KF}^{st(I)}$ and $\bar{V}_{KF}^{st(II)}$ did not have opposite temperature dependencies it would not be possible to explain the maxima in the \bar{V}_{KF} vs t curves.

As the concentrations of KF is increased there is less H_2O_I and H_2O_{II} . Therefore $\bar{V}_{KF}^{st(I)}$ and $\bar{V}_{KF}^{st(II)}$ become smaller so that \bar{V}_{KF} increases. This explains why the curves of \bar{V}_{KF} vs t lie above each other with increasing concentration. The explanation also agrees with Wicke's⁽¹³⁾ suggestions which state that; a) at low temperatures, straight hydrogen bonded structures (similar to H_2O_I) are broken down with this effect decreasing with increasing temperature; b) bent-hydrogen-bonded structures (similar to H_2O_{II}) are also broken down by ions, with this effect increasing with increasing temperature.

The partial molal volumes of the KI solutions at different temperatures are shown in Figs. 28(a), (b).

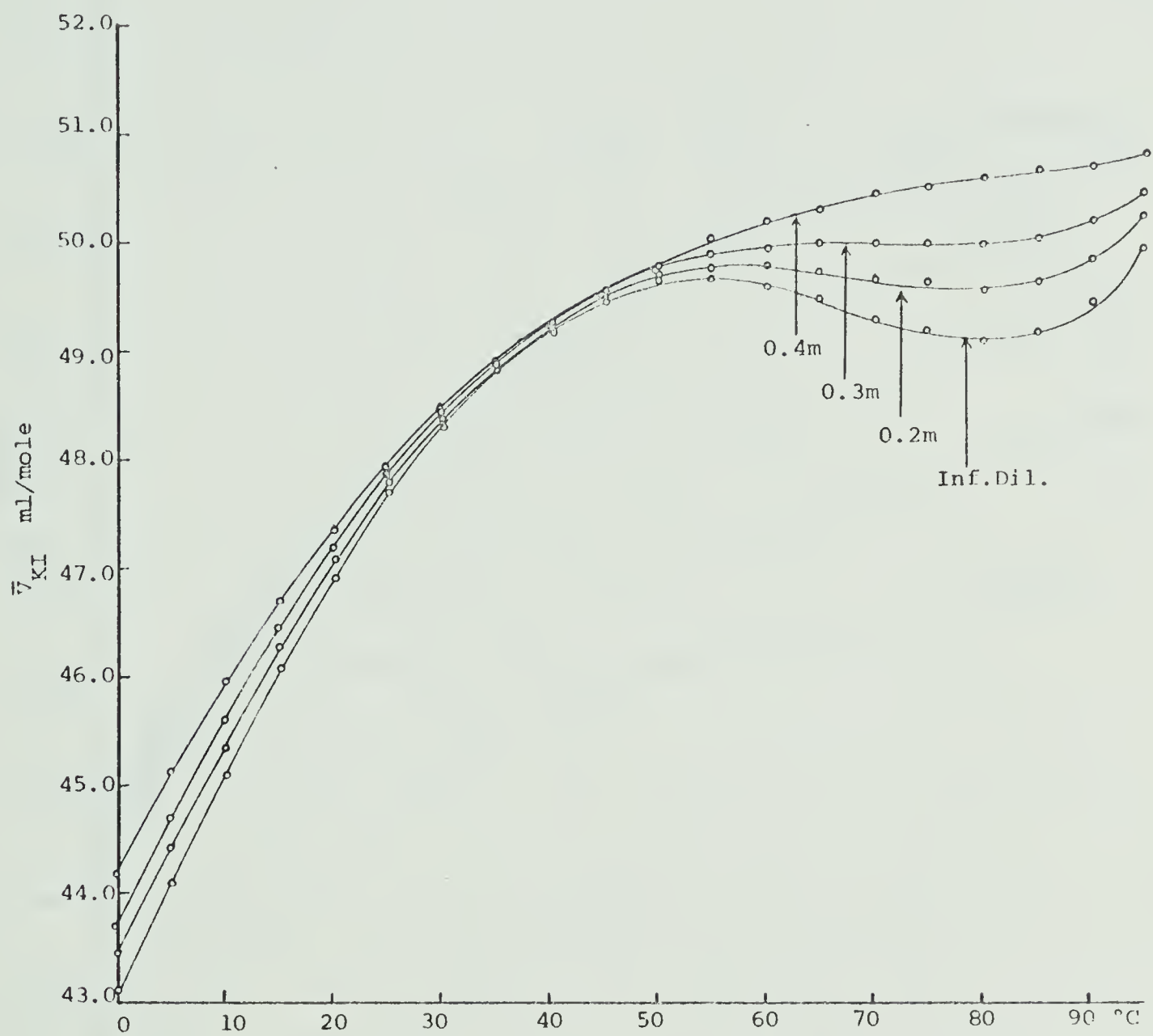


Fig. 28(a): Partial Molal Volumes of KI, \bar{V}_{KI} vs Temperature.

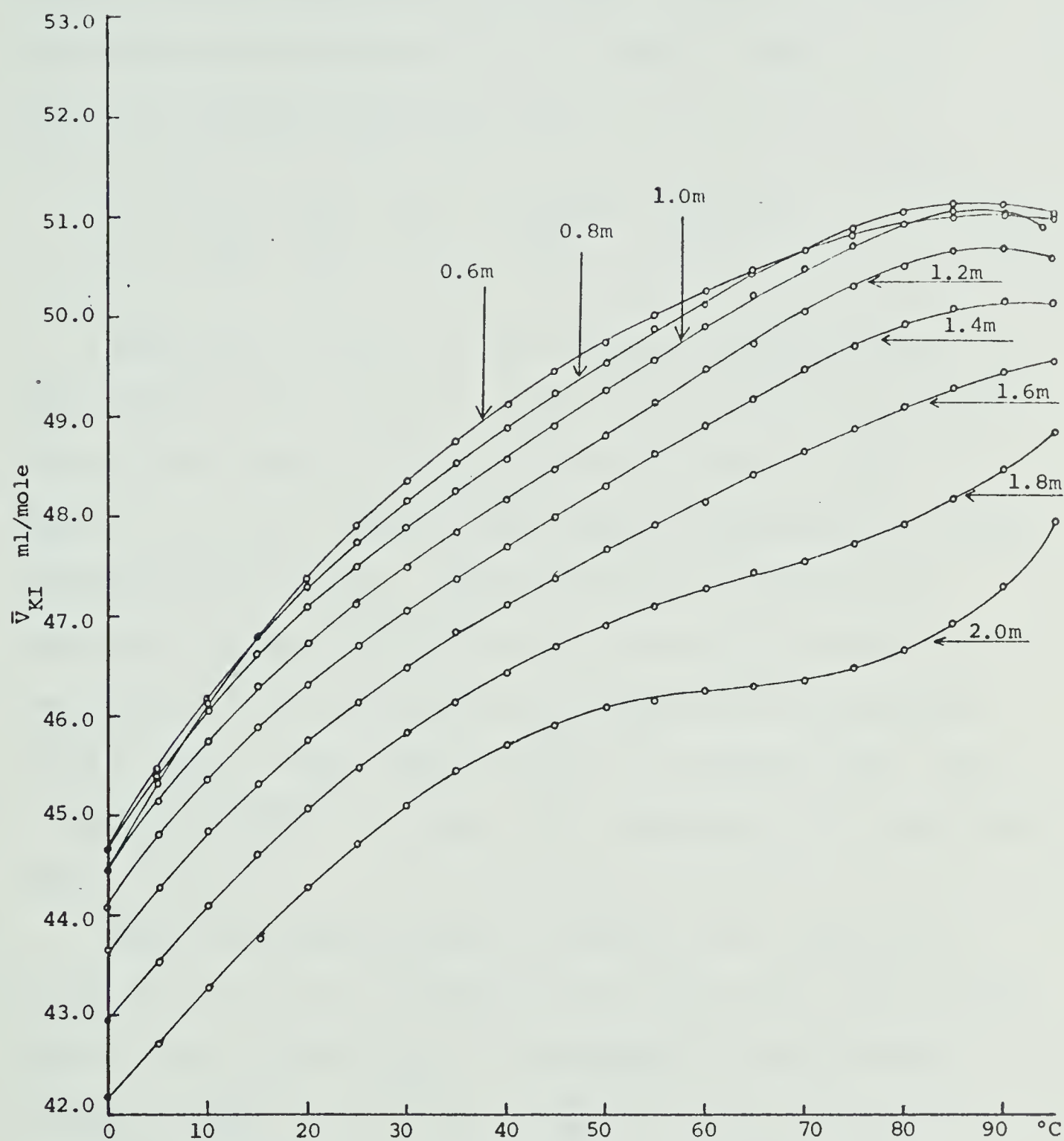


Fig. 28(b): Partial Molal Volumes of KI, \bar{V}_{KI} vs Temperature.

The same structural and electrostrictive effects will occur with KI as with KF but to different extents because of the difference in radius and hence in charge-to-radius ratio between F^- and I^- ions. Thus we can write, in analogy with Eq. (38),

$$\bar{V}_{KI} = V_{KI}^{\circ} - \bar{V}_{KI} - \bar{V}_{KI}^{st(I)} - \bar{V}_{KI}^{st(II)} \quad (39)$$

The plots of \bar{V}_{KI} vs t at infinite dilution and 0.1 m pass through small maxima at 55°. Presumably the explanation of the maxima is very similar to that for the \bar{V}_{KF} vs t curves. However, the maxima disappear for higher concentrations of KI. This fact does not necessarily mean that the term $\bar{V}_{KI}^{st(II)}$ is not finite for these concentrations, but merely that the temperature dependence of the combined term $(\bar{V}_{KI}^{es} + \bar{V}_{KI}^{st(I)})$ is greater than that of the term $\bar{V}_{KI}^{st(II)}$ in eqn. (39) throughout the temperature range 0° to 95°.

Thus the general shape of the \bar{V}_{KI} vs t curves for 0.4 m to 2.0 m can be explained by saying that the partial molal volume of KI, \bar{V}_{KI} , is decreased by the breakdown of H_2O_I , $(\bar{V}_{KI}^{st(I)})$, of H_2O_{II} , $(\bar{V}_{KI}^{st(II)})$, and by electrostriction, (\bar{V}_{KI}^{es}) , with the temperature dependence of \bar{V}_{KI}^{es} and $\bar{V}_{KI}^{st(I)}$ opposite to, but greater than the temperature dependence of $\bar{V}_{KI}^{st(II)}$.

An important difference between the \bar{V}_{KF} vs t and the \bar{V}_{KI} vs t curves is that all the KF curves lie above each other with increasing concentration, whereas, although this is true for the KI curves to 0.6 m, the opposite effect is observed for KI solutions with greater than 0.6 m concentration. A possible explanation of these differences between the behaviour of the partial molal volume curves of KF and KI as a function of temperature is that the breakdown of H_2O_{II} by KF, $\bar{V}_{KF}^{st(II)}$ depends only on the concentration of H_2O_{II} in the solution, whereas with KI the value for $\bar{V}_{KI}^{st(II)}$ depends more on the concentration of KI than on the concentration of H_2O_{II} . This would indicate that in dilute solutions the F^- ion breaks down H_2O_{II} more strongly than the I^- ion, but in solutions more concentrated than 0.6 m this position is reversed. This suggestion receives support from the evidence in Fig. (29) which compares the theoretical expansivities of KI and KF solutions of all concentrations at 0° if there were no H_2O_I present. The method used in obtaining these values was explained on pg 84. This evidence is most easily interpreted by postulating that from 0.0 m to 0.5 m the F^- ion is more effective at breaking down H_2O_{II} than I^- since the fluoride solutions have the highest expansivities in this concentration range.

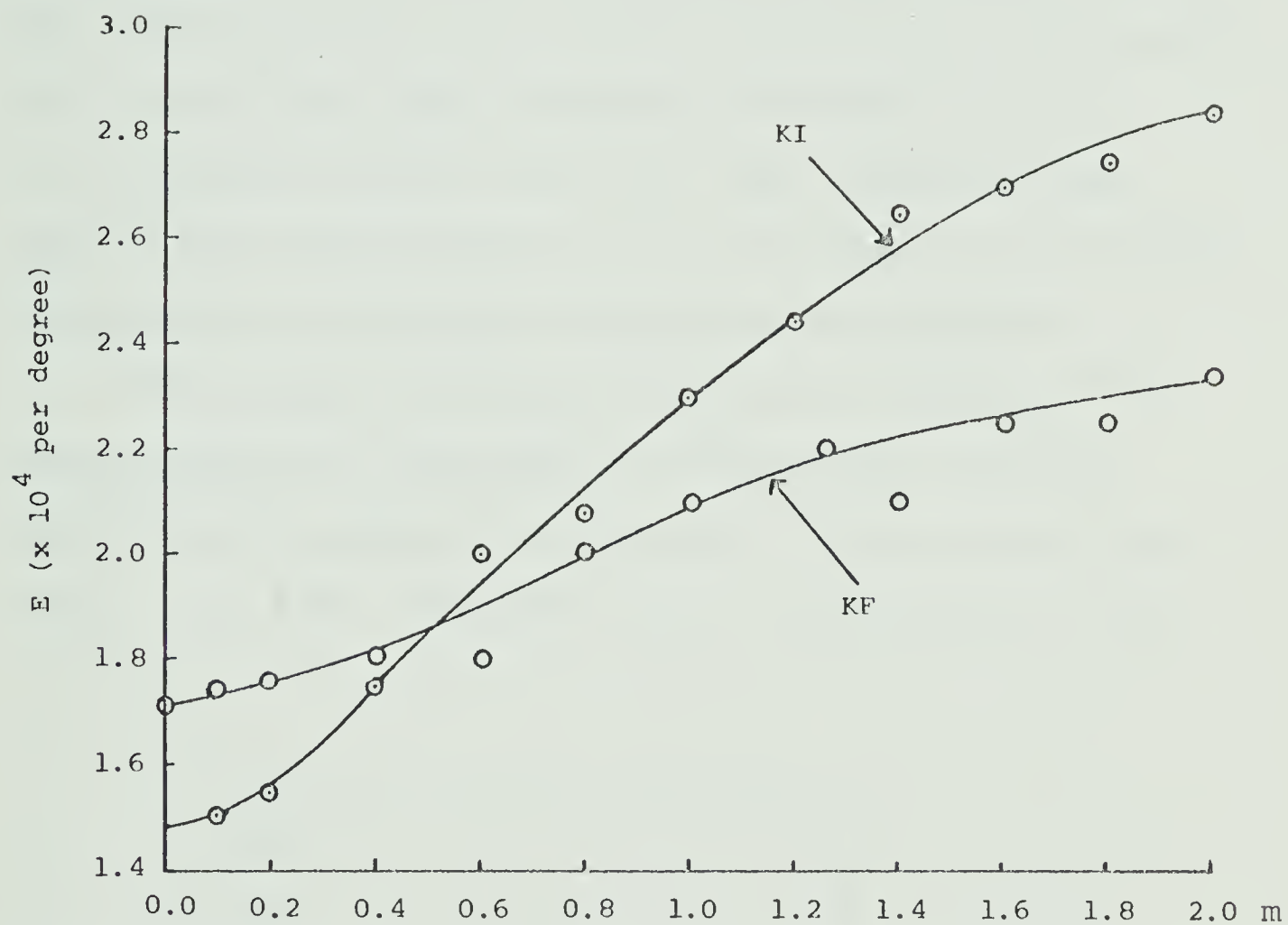


Fig. 29: Expansivity, E , at 0° if no H_2O_I were present vs concentration.

Above 0.5 m the KI solutions have the greater expansivities and thus the I^- ions are more effective at breaking down H_2O_{II} . This does not disagree with Wicke (13), whose data were obtained only for very dilute solutions.

Fig. (26) indicates the presence of H_2O_I at low temperatures in solutions more concentrated than 2.0 m. Fig. 28(b) indicates that water structure is still present in 2.0 m KI since the structural breakdown in 2.0 m KI is greater than in 1.8 m KI. This information may lead to some understanding of the strength of the electric field which is necessary for structural breakdown.

The microwave studies of Harris and O'Konski (46) on the dielectric constants of electrolyte solutions provide useful information relevant to the structure of water, Fig. (30). Solutions of 1:1 electrolytes at 25°C

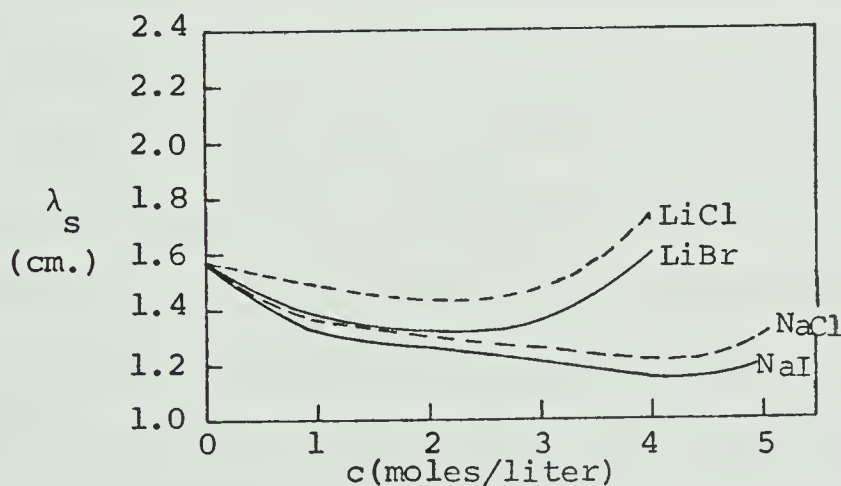


Fig. 30: Wave length of central relaxation vs concentration for various electrolytes at 25°.

in the concentration range of 0.0 m to 2.8 m - 4.3 m (depending on the particular salt) show a decreased relaxation time which decreases with increasing concentration. The decreased relaxation time is interpreted as being caused by structural breakdown of water by the salts. (46,47) Thus both the present specific volume study and the microwave study of Harris and O'Konski indicate the presence of water structure in fairly concentrated salt solutions. The increase in relaxation time above 2.8 m - 4.3 m is not interpreted as being due to structure forming by the salts but as due to the effect of a water molecule in the second zone of a central ion being also in the second zone of an adjacent ion (which in general will have the opposite charge to the central ion). The effect of the second ion would be to immobilize further the water molecule, thus lengthening the relaxation time. According to this interpretation, the original structure of the water will exist in very small amounts at the concentration where the dielectric relaxation time vs concentration passes through a minimum, since water molecules immobilized by electric fields do not form part of normal water structure. Thus beyond the concentration of minimum relaxation time there is very little structure breaking possible.

The average distance of separation of ions in a 1:1 electrolyte solution with a concentration of

$$2 \text{ m} = 8.7 \text{ \AA} \text{ (half av. sep. dist.} = 4.35 \text{ \AA)}$$

$$3 \text{ m} = 8.1 \text{ \AA} \text{ (half av. sep. dist.} = 4.05 \text{ \AA)}$$

$$4 \text{ m} = 7.5 \text{ \AA} \text{ (half av. sep. dist.} = 3.75 \text{ \AA)}$$

In a 2 m solution, a water molecule midway between two ions in the solution will be 4.35 \AA from both ions and can thus presumably take part in a more or less normal water structure. In a 4 m solution there is very little structure present. A water molecule midway between two ions will be 3.75 \AA from either ion at which distance the field strength is evidently great enough to immobilize most water molecules.

The concept of the formation of ion pairs in solution has been used to explain the decreased conductivity in more concentrated solutions. When a pair of oppositely charged ions come into close association in solution they become effectively neutral and do not contribute to the conductivity of the solution. For an ion pair to be stable e^2/aD must be large compared to kT ⁽⁴⁸⁾ where,

e = electronic charge

a = distance between ions

D = dielectric constant

k = Boltzman constant per molecule.

Even if we take into account the reduced effective

concentration of ions resulting from ion pair formation, the situation changes very little because of the fairly small change in half the average separation distance of ions with concentration. Thus it would appear that water molecules which are beyond 4\AA or 5\AA from a univalent ion are mobile and can presumably participate in normal water structure.

The analyses of Ritson and Hasted, ⁽⁴⁷⁾ and Grahame ⁽⁴⁹⁾ predict a region of complete dielectric saturation to about 2\AA from a point electronic charge; this is followed by a region of rapid rise in dielectric constant to the ordinary bulk value at about 4\AA . The analysis of Bolt ⁽⁵⁰⁾ suggests that the bulk value is attained at 5\AA from the center of a monovalent ion. Thus it is suggested here that the electric field strengths which disrupt water structure and hence change the dielectric constant of water are those which exist up to about 4\AA (dependent to some extent on the ion under consideration) from a hydrated monovalent ion. This is the same as saying that the third region of the Frank-Wen model exists at a distance greater than 4\AA or 5\AA from an ion. One-half the average separation distance of a monovalent ion in 3 m solution, without intimate ion association, is 4.05\AA . Thus it would appear that the third region does not exist around ions to any large extent at concentrations greater than 3.0 m.

5 - Conclusions

Fig. (26) shows the maximum temperature for each concentration of KI and KF at which $\text{H}_2\text{O}_{\text{I}}$ is present in the solution and shows that KI breaks down $\text{H}_2\text{O}_{\text{I}}$ more strongly than KF. The analysis of the partial molal volumes of the KF and KI solutions shows that two effects, electrostriction and breakdown of $\text{H}_2\text{O}_{\text{II}}$ are operating in all temperature ranges and have quite different temperature dependencies. It appears that in solutions 0.0 - 0.5 m, KF is a stronger structure breaker than KI of $\text{H}_2\text{O}_{\text{II}}$ but above ~ 0.5 m this position is reversed. It would appear that the dielectric and structural properties of water are similarly affected by the presence of salts and that the electric field 5\AA from an ion is too weak to affect substantially the basic structure of water. In general the findings of this chapter are most easily explained in terms of the model of water put forward in Chapter I.

CHAPTER IV

The Effect of Potassium Iodide and Potassium Fluoride on the Compressibility of Water

1 - Introduction

As outlined in Chapter II, part of the measured isothermal compressibility of water is due to structural rearrangement of the liquid when it is put under pressure. Since salts affect water structure and hence the compressibility of water, it was thought that the study of the compressibility of water containing various concentrations of salts might further knowledge of the structures present in liquid water.

The compressibility of water differs from that of other liquids in two ways. Firstly, water is the only liquid with an isothermal compressibility which passes through a minimum value as a function of temperature. Secondly, water has a low isothermal compressibility in comparison with other liquids, whose compressibilities are generally twice to four times larger. ^(29d) Ethylene glycol, however, has a compressibility lower than that of water. ^(29d) Presumably, the high degree of hydrogen bonding which is probably present in ethylene glycol is partly responsible for its low compressibility.

It is very difficult to make any general statements in regard to the compressibility of salt solutions

because there are very few studies in the literature on this topic and those studies which do exist have only covered a very limited concentration or temperature range. (51)

The findings of Chapters II and III indicated that an extensive study of the compressibilities of KI and KF solutions would be of potential value, so a study of the compressibilities of solutions of KF and KI over the concentration range of 0.0 m to 2.0 m and the temperature range of 0° to 95° was undertaken.

Pena and McGlashan (52) have compared the measurements of isothermal compressibility of water obtained by a number of experimentalists. They found the results of Tyrer, (53) one of the earliest experimentalists in this field, to be in good agreement with other generally accepted values. Tyrer (53) measured adiabatic, and not isothermal, compressibilities. He applied a conversion factor to obtain isothermal compressibilities from his adiabatic compressibilities.

Isothermal compressibilities are much more difficult to measure than adiabatic compressibilities, since temperature control of better than 0.001° is needed for isothermal measurements. A change of 0.02° in temperature of the fluid causes, on the average, the same change in volume as does a change of pressure of 1 atm. Because of adiabatic heating or cooling an isothermal measurement

requires a long waiting period after the pressure has been applied or released to allow the piezometer to equilibrate to the temperature of the bath. If during this equilibration period the temperature of the bath changes slightly an obvious error is introduced.

Kell and Whalley ⁽¹⁹⁾ have carried out the accurate, direct measurement of the isothermal compressibility of water over a wide range of temperatures and pressures but their investigation required very expensive apparatus.

Because of the difficulty and cost of direct isothermal measurements it was decided to use an experimental method similar to Tyrer's ⁽⁵³⁾ to measure the adiabatic compressibilities.

Adiabatic compressibility, K_s , is calculated from the expression:

$$K_s = -\frac{1}{V} \left(\frac{dV}{dp} \right)_s \quad (40)$$

where the subscript s means, 'under the condition of constant entropy', V is the volume of fluid and dV is a change in the volume of the fluid caused by a change in pressure of dp.

The isothermal compressibility, K , can be calculated from adiabatic compressibility by means of the thermodynamic expression, ^(52,53)

$$K = K_s + \frac{TE^2V}{C} \text{ per bar} \quad (41)$$

where T = absolute temperature (deg)

E = expansivity of the fluid (per deg)

V = specific volume of the fluid (cm^3/gm)

C = specific heat of the fluid (joules/gm-deg)

The adiabatic compressibilities of 11 solutions of KF and 11 solutions of KI, having the same concentrations as the solutions described in Chapter III, were measured at 5° intervals from 0° to 95° . To do this, two piezometers of 500 ml capacity having the design shown in Fig. (31), were built and set up in thermostated water baths. The piezometer consisted of the inner vessel, A which contained the solution under investigation. The sidearm, B consisted of the capillary along which the solution travelled as the pressure was released at stopcock D. The stopcock E was kept closed during a measurement but opened when the temperature of the piezometer was being raised. The piezometer was filled and emptied through stockcock, E. The water jacket was kept full of water to the mark 'm'. By means of interconnecting tubes, the pressures at C and D were kept equivalent. The temperature control and the accuracy of the absolute temperature of the water baths was the same as described in Chapter III.

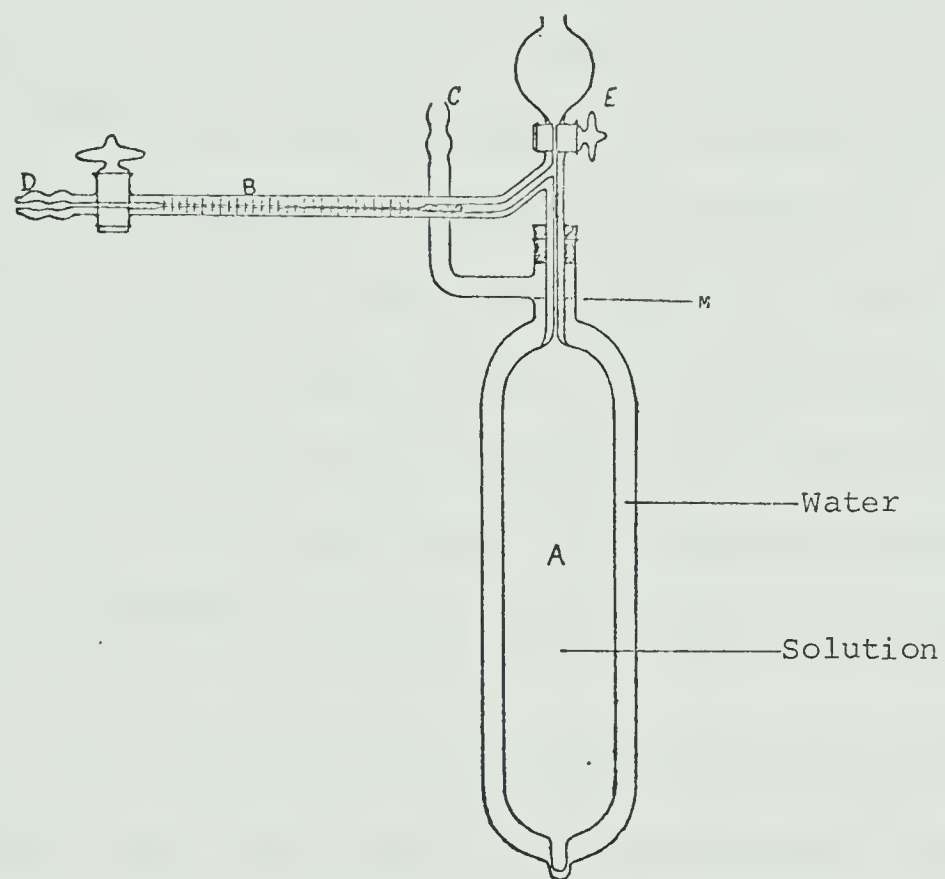


Fig. 31: Piezometer for measuring adiabatic compressibilities at low pressures.

Each apparatus was first weighed dry, then filled with filtered deionized water (with the outer jacket kept dry), placed in a water bath at 45°, allowed to equilibrate, and then taken out of the bath, dried and reweighed. The weight of the water contained in the piezometer was then obtained by difference. This procedure was repeated twice. From the specific volume of water (18) it was then possible to calculate the volume of the piezometer. This same process was repeated twice at 85°. From the results of the calibrations at the two temperatures, the coefficient of cubical expansion of the piezometers was found to be 1.0×10^{-5} , in close agreement with the coefficient of cubical expansion of Pyrex glass which is 0.99×10^{-5} (29e).

There were three major experimental difficulties to overcome. The first was that the stopcocks tended to leak under pressure as the higher temperatures were reached. This difficulty was overcome by using large, high-vacuum stopcocks which were greased carefully. The stopcocks were prevented from being heated by the surrounding equipment by using radiation shields of aluminum foil. Secondly, the outer jacket of the piezometer had to be kept as full of water as possible.

If it was not completely full there was a small amount of evaporation from the damp upper surfaces of the water jacket on decompression, which caused cooling of the inner vessel of the piezometer and cooled the solution so that insufficient expansion was obtained.

Thirdly, the capillary tube had to be kept scrupulously clean because it was of narrow diameter (0.5 mm) and thus any surface contaminant would cause a large deviation from the calibrated volume of the capillary. Since the chief contaminant was grease from the stopcocks, the stopcocks were greased only after the piezometer was filled with fresh solution. The solution was deaerated as outlined in Chapter III before filling the piezometer. Naturally, even the smallest air bubble in the piezometer would cause incorrect readings.

The experimental method followed was to fill the two piezometers with deaerated solution, place them in the same temperature bath and cool them to 0° . When they were equilibrated, five adiabatic compressibility measurements were taken, the temperature then was raised 5° and after equilibration the next five readings were taken. This process was repeated until the 95° readings were obtained. Equilibration of the piezometer to the temperature of the water bath took two hours so that it

1. The first part of the document discusses the importance of maintaining accurate records of all transactions and the role of the accounting department in ensuring the integrity of the financial statements. It also highlights the need for regular audits and the importance of transparency in financial reporting.

2. The second part of the document outlines the various methods used to collect and analyze financial data, including the use of statistical models and the application of advanced data analysis techniques. It also discusses the challenges associated with data collection and the importance of ensuring the accuracy and reliability of the data.

3. The third part of the document focuses on the development of financial models and the use of these models to predict future financial performance. It also discusses the importance of validating these models and the need for ongoing monitoring and evaluation of their performance.

4. The fourth part of the document discusses the role of the accounting department in managing the company's financial risk and the importance of implementing effective risk management strategies. It also highlights the need for regular communication and collaboration between the accounting department and other departments within the organization.

5. The fifth part of the document discusses the importance of maintaining accurate records of all transactions and the role of the accounting department in ensuring the integrity of the financial statements. It also highlights the need for regular audits and the importance of transparency in financial reporting.

6. The sixth part of the document outlines the various methods used to collect and analyze financial data, including the use of statistical models and the application of advanced data analysis techniques. It also discusses the challenges associated with data collection and the importance of ensuring the accuracy and reliability of the data.

7. The seventh part of the document focuses on the development of financial models and the use of these models to predict future financial performance. It also discusses the importance of validating these models and the need for ongoing monitoring and evaluation of their performance.

8. The eighth part of the document discusses the role of the accounting department in managing the company's financial risk and the importance of implementing effective risk management strategies. It also highlights the need for regular communication and collaboration between the accounting department and other departments within the organization.

9. The ninth part of the document discusses the importance of maintaining accurate records of all transactions and the role of the accounting department in ensuring the integrity of the financial statements. It also highlights the need for regular audits and the importance of transparency in financial reporting.

10. The tenth part of the document outlines the various methods used to collect and analyze financial data, including the use of statistical models and the application of advanced data analysis techniques. It also discusses the challenges associated with data collection and the importance of ensuring the accuracy and reliability of the data.

was generally possible to obtain only four or five values a day per piezometer. There was no equilibration period required between individual readings at the same temperature because the adiabatic heating as the pressure was put on and the cooling as the pressure was removed were equivalent and there was no net change of temperature.

Sudden compression of the fluid in the piezometer caused droplets to be left in the capillary as the fluid was pushed back. Thus the method adopted for taking the adiabatic compressibility measurements was to put the liquid under one atmosphere pressure, building up the pressure slowly, then to release the pressure suddenly and to observe the distance which the liquid travelled along the capillary on decompression. This procedure was repeated five times and the average of the readings was taken. The average deviation from the mean of these five readings was generally of the order of 0.2%.

A scale which was graduated in $1/60$ of an inch (~ 0.4 mm) was glued onto the capillary tube of the piezometer with an epoxy resin adhesive. This scale was read easily to 0.2 of a division (~ 0.1 mm) by means of a magnifier.

The calibration of the capillary was of great

importance. Water and not mercury was preferred for the calibration since experiments were performed on water or salt solutions and since water has different surface wetting properties to mercury. However, it was difficult to obtain consistent values when using water for calibration so a different approach was used. Tyrer's⁽⁵³⁾ values for the adiabatic compressibility of water from 10° to 90° were assumed to be correct. They were compared to our own measurements of the same quantities and a value for a calibration constant, x, was calculated from the comparison as shown below.

3 - Calculations

The adiabatic compressibility can be calculated from the equation

$$K_s = - \frac{1}{V} \left(\frac{x d + \Delta V_g}{\Delta p} \right) \quad (42)$$

where $(x d + \Delta V_g / \Delta p)$ is equivalent to the dV/dP term of eqn. (40)

K_s = adiabatic compressibility of water (per atm)

V = volume of piezometer

d = distance water travelled along capillary on
release of pressure

ΔP = 1 atm.

x = calibration constant

ΔV_g = correction for compressibility of glass

Eqn. (42) can be rearranged to yield

$$x = - \left(\frac{VK_s - \Delta V_g}{d \cdot \Delta P} \right) \quad (43)$$

The values for x obtained in this manner were constant and did not vary with temperature.

The correction for the compressibility of glass is important. A bottle which sinks to the bottom of the sea undergoes the same change in volume as would a solid block of glass with the same shape as the bottle. (54)

The magnitude of the correction, ΔV_g , is calculated from the expression, $\Delta V_g = - V_p \Delta P \cdot K_g$

where V_p = the volume of glass container

ΔP = change in pressure

K_g = compressibility of glass

= 3.0×10^{-6} per atm. (55)

Equation (41) was used to calculate the isothermal compressibilities from the adiabatic compressibilities. To obtain the isothermal compressibilities in the units of atm^{-1} the second term in eqn. (41) had to be multiplied by the factor 1.0132 since 1 atm. = 1.0132 bar. The values for V, the specific volumes of the salt were obtained from Tables VII and VIII and from these values the expansivities, E, were calculated. The values for C,

the specific heat of the KI solutions were calculated at all temperatures using the values for the apparent molal heat capacities of KI solutions measured at 25°. (56)

The values for the specific heat of the KF solutions were calculated from the equation

$$C = 4.176 - 54.7 \times 10^{-3} p + 380.9 \times 10^{-6} p^2$$

where p = weight percentage of KF in the solution. This equation was obtained by Jauch (57) on the basis of his measurements on the heat capacities of KF solutions at 18°.

4 - Results

On measuring K_s for water twice with each piezometer over the whole temperature range, the average difference in the values obtained for the adiabatic compressibility of water was 1.0×10^{-7} per atm which gives a percentage error of 0.2% on a compressibility of 50.0×10^{-6} per atm.

The results of the measurements of the adiabatic compressibilities of the 11 different concentrations of the KI and KF solutions at 20 temperatures ranging from 0° to 95° at 5° intervals are given in Tables IX and X. The isothermal compressibilities calculated from the adiabatic compressibilities are given in Tables XI and XII. The plots of isothermal compressibility,

Table IX. Adiabatic Compressibilities of KI solutions
vs Temperature and Concentration ($K_s \times 10^6 \text{ atm}^{-1}$)

<u>°C</u>	<u>Water</u>	<u>0.1005 m</u>	<u>0.2002 m</u>	<u>0.4010 m</u>	<u>0.5877 m</u>	<u>0.7995 m</u>
0.0	51.98	50.96	50.32	49.04	47.91	46.68
5.0	50.15	49.26	48.68	47.54	46.52	45.41
10.0	48.66	47.84	47.31	46.27	45.34	44.34
15.0	47.33	46.67	46.18	45.22	44.36	43.43
20.0	46.27	45.70	45.24	44.35	43.54	42.68
25.0	45.39	44.91	44.48	43.63	42.87	42.05
30.0	44.68	44.27	43.85	43.04	42.32	41.54
35.0	44.09	43.75	43.35	42.57	41.88	41.13
40.0	43.61	43.32	42.94	42.19	41.53	40.80
45.0	43.23	42.98	42.62	41.90	41.25	40.55
50.0	42.93	42.71	42.36	41.67	41.05	40.35
55.0	42.70	42.49	42.16	41.51	40.91	40.24
60.0	42.54	42.34	42.03	41.40	40.82	40.17
65.0	42.45	42.24	41.94	41.34	40.78	40.15
70.0	42.43	42.20	41.92	41.34	40.79	40.17
75.0	42.47	42.23	41.96	41.39	40.86	40.25
80.0	42.61	42.34	42.07	41.51	40.98	40.37
85.0	42.86	42.55	42.27	41.70	41.16	40.55
90.0	42.22	42.88	42.58	41.97	41.41	40.78
95.0	43.73	43.35	43.01	42.34	41.74	41.08

Table IX. (continued)

<u>°C</u>	<u>0.9985 m</u>	<u>1.2123 m</u>	<u>1.4025 m</u>	<u>1.5995 m</u>	<u>1.8015 m</u>	<u>1.9935 m</u>
0.0	45.61	44.55	43.69	42.90	42.21	41.68
5.0	44.44	43.46	42.65	41.89	41.20	40.62
10.0	43.44	42.53	41.78	41.05	40.36	39.76
15.0	42.60	41.75	41.04	40.35	39.68	39.09
20.0	41.90	41.10	40.43	39.77	39.13	38.55
25.0	41.32	40.56	39.93	39.30	38.69	38.14
30.0	40.84	40.13	39.52	38.93	38.35	37.83
35.0	40.46	39.77	39.19	38.63	38.08	37.59
40.0	40.15	39.49	38.94	38.40	37.88	37.42
45.0	39.92	39.28	38.75	38.22	37.73	37.29
50.0	39.76	39.13	38.61	38.10	37.62	37.21
55.0	39.64	39.03	38.52	38.02	37.56	37.17
60.0	39.58	38.98	38.47	37.99	37.53	37.15
65.0	39.57	38.97	38.47	37.99	37.54	37.17
70.0	39.60	39.01	38.51	38.03	37.59	37.22
75.0	39.68	39.09	38.60	38.12	37.68	37.31
80.0	39.81	39.22	38.73	38.25	37.82	37.46
85.0	39.98	39.40	38.91	38.44	38.02	37.67
90.0	40.21	39.63	39.15	38.70	38.29	37.96
95.0	40.50	39.92	39.45	39.02	38.65	38.35

Table X. Adiabatic Compressibilities of KF solutions
vs Temperature and Concentration ($K_s \times 10^6 \text{ atm}^{-1}$)

<u>°C</u>	<u>Water</u>	<u>0.1021 m</u>	<u>0.1922 m</u>	<u>0.3980 m</u>	<u>0.4965 m</u>	<u>0.8066 m</u>
0.0	51.98	51.13	50.13	48.06	47.16	44.64
5.0	50.15	49.37	48.47	46.59	45.77	43.45
10.0	48.66	47.87	47.06	45.35	44.59	42.43
15.0	47.33	46.61	45.87	44.30	43.59	41.57
20.0	46.27	45.56	44.88	43.41	42.76	40.85
25.0	45.39	44.68	44.05	42.68	42.06	40.24
30.0	44.68	43.95	43.36	42.07	41.48	39.74
35.0	44.09	43.36	42.80	41.57	41.00	39.34
40.0	43.61	42.88	42.34	41.16	40.62	39.01
45.0	43.23	42.50	41.98	40.84	40.32	38.76
50.0	42.93	42.21	41.70	40.59	40.08	38.57
55.0	42.70	42.00	41.50	40.41	39.92	38.44
60.0	42.54	41.86	41.37	40.30	39.81	38.37
65.0	42.45	41.79	41.31	40.25	39.77	38.35
70.0	42.43	41.80	41.32	40.27	39.79	38.38
75.0	42.47	41.89	41.41	40.36	39.88	38.48
80.0	42.61	42.06	41.58	40.53	40.05	38.63
85.0	42.86	42.33	41.85	40.79	40.30	38.85
90.0	43.22	42.70	42.22	41.15	40.65	39.14
95.0	43.73	43.21	42.72	41.62	41.11	39.52

Table X. (continued)

<u>°C</u>	<u>1.0031 m</u>	<u>1.2633 m</u>	<u>1.3894 m</u>	<u>1.6030 m</u>	<u>1.8019 m</u>	<u>1.9980 m</u>
0.0	43.24	41.53	40.74	39.41	38.15	36.84
5.0	42.15	40.56	39.83	38.62	37.48	36.83
10.0	41.21	39.73	39.04	37.92	36.88	35.85
15.0	40.42	39.01	38.36	37.31	36.35	35.41
20.0	39.75	38.40	37.78	36.78	35.88	35.01
25.0	39.19	37.89	37.30	36.33	35.48	34.66
30.0	38.73	37.47	36.90	35.96	35.14	34.36
35.0	38.35	37.13	36.58	35.67	34.87	34.12
40.0	38.06	36.87	36.33	35.45	34.67	33.94
45.0	37.83	36.68	36.15	35.29	34.53	33.81
50.0	37.67	36.55	36.03	35.19	34.44	33.74
55.0	37.56	36.47	35.97	35.15	34.42	33.72
60.0	37.51	36.45	35.96	35.16	34.44	33.76
65.0	37.51	36.47	35.99	35.21	34.51	33.85
70.0	37.56	36.54	36.07	35.31	34.63	33.98
75.0	37.66	36.64	36.18	35.43	34.77	34.15
80.0	37.80	36.79	36.32	35.59	34.95	34.36
85.0	38.00	36.96	36.50	35.76	35.14	34.59
90.0	38.25	37.17	36.69	35.95	35.34	34.84
95.0	38.57	37.42	36.91	36.14	35.55	35.09

Table XI. Isothermal Compressibilities of KF solutions
vs Temperature and Concentration ($K \times 10^6 \text{ atm}^{-1}$).

<u>°C</u>	<u>Water</u>	<u>0.1021 m</u>	<u>0.1922 m</u>	<u>0.3980 m</u>	<u>0.4965 m</u>	<u>0.8066 m</u>
0.0	51.89	51.13	50.13	48.06	47.16	44.68
5.0	50.15	49.38	48.49	46.63	45.82	43.56
10.0	48.66	47.94	47.15	45.47	44.74	42.64
15.0	47.48	46.79	46.07	44.54	43.86	41.91
20.0	46.56	45.88	45.22	43.81	43.18	41.33
25.0	45.86	45.18	44.57	43.25	42.65	40.89
30.0	45.35	44.65	44.08	42.83	42.26	40.57
35.0	45.00	44.28	43.73	42.54	41.99	40.36
40.0	44.75	44.04	43.51	42.35	41.82	40.24
45.0	44.64	43.91	43.39	42.26	41.74	40.20
50.0	44.60	43.88	43.37	42.26	41.75	40.23
55.0	44.65	43.94	43.43	42.33	41.83	40.34
60.0	44.78	44.08	43.58	42.48	41.98	40.51
65.0	45.00	44.31	43.80	42.71	42.21	40.75
70.0	45.30	44.63	44.12	43.02	42.52	41.05
75.0	45.68	45.05	44.53	43.41	42.91	41.43
80.0	46.19	45.57	45.05	43.92	43.40	41.88
85.0	46.83	46.21	45.69	44.54	44.00	42.42
90.0	47.63	47.00	46.48	45.29	44.74	43.06
95.0	48.62	47.96	47.43	46.21	45.62	43.81

Table XI. (continued)

<u>°C</u>	<u>1.0031</u>	<u>1.2633</u> m	<u>1.3894</u> m	<u>1.6030</u> m	<u>1.8019</u> m	<u>1.9980</u> m
0.0	43.30	41.64	40.87	39.58	38.35	37.07
5.0	42.29	40.76	40.06	38.88	37.78	36.66
10.0	41.46	40.03	39.37	38.29	37.29	36.29
15.0	40.80	39.44	38.81	37.80	36.88	35.97
20.0	40.27	38.97	38.37	37.40	36.54	35.70
25.0	39.87	38.61	38.04	37.10	36.28	35.49
30.0	39.58	38.36	37.80	36.89	36.09	35.34
35.0	39.40	38.20	37.65	36.77	35.99	35.25
40.0	39.30	38.13	37.59	36.72	35.95	35.23
45.0	39.28	38.14	37.61	36.75	35.99	35.27
50.0	39.34	38.22	37.70	36.85	36.10	35.38
55.0	39.46	38.36	37.85	37.02	36.27	35.55
60.0	39.64	38.57	38.07	37.24	36.50	35.79
65.0	39.89	38.83	38.33	37.52	36.79	36.08
70.0	40.20	39.14	38.65	37.85	37.13	36.44
75.0	40.56	39.50	39.01	38.22	37.52	36.85
80.0	40.99	39.91	39.41	38.63	37.94	37.32
85.0	41.49	40.36	39.85	39.06	38.40	37.83
90.0	42.07	40.86	40.33	39.52	38.88	38.38
95.0	42.72	41.41	40.84	39.99	39.38	38.96

Table XII. Isothermal Compressibilities of KI solutions
vs Temperature and Concentration ($K \times 10^6 \text{ atm}^{-1}$)

<u>°C</u>	<u>Water</u>	<u>0.1005 m</u>	<u>0.2002 m</u>	<u>0.4010 m</u>	<u>0.5877 m</u>	<u>0.7995 m</u>
0.0	51.89	50.97	50.31	49.04	47.93	46.75
5.0	50.15	49.27	48.70	47.60	46.63	45.59
10.0	48.66	47.92	47.42	46.45	45.58	44.65
15.0	47.48	46.86	46.41	45.53	44.75	43.90
20.0	46.56	46.05	45.64	44.83	44.11	43.32
25.0	45.86	45.44	45.05	44.30	43.62	42.89
30.0	45.35	45.00	44.63	43.91	43.27	42.57
35.0	45.00	44.69	44.34	43.65	43.03	42.37
40.0	44.75	44.50	44.16	43.49	42.89	42.25
45.0	44.64	44.44	44.07	43.41	42.84	42.22
50.0	44.60	44.39	44.05	43.42	42.85	42.26
55.0	44.65	44.44	44.12	43.49	42.95	42.37
60.0	44.78	44.57	44.25	43.64	43.11	42.54
65.0	45.00	44.77	44.46	43.86	43.34	42.79
70.0	45.30	45.05	44.75	44.17	43.66	43.11
75.0	45.68	45.43	45.15	44.58	44.07	43.51
80.0	46.19	45.94	45.67	45.11	44.59	44.01
85.0	46.83	46.60	46.33	45.78	45.23	44.61
90.0	47.63	47.43	47.18	46.61	46.03	45.35
95.0	48.62	48.49	48.24	47.64	47.00	46.23

Table XII. (continued)

<u>°C</u>	<u>0.9985 m</u>	<u>1.2133 m</u>	<u>1.4025 m</u>	<u>1.5995 m</u>	<u>1.8015 m</u>	<u>1.9935 m</u>
0.0	45.73	44.74	43.95	43.24	42.63	42.16
5.0	44.67	43.77	43.04	42.36	41.74	41.24
10.0	43.82	42.99	42.31	41.66	41.05	40.54
15.0	43.14	42.38	41.74	41.12	40.53	40.02
20.0	42.62	41.90	41.30	40.71	40.15	39.66
25.0	42.23	41.55	40.99	40.43	39.90	39.43
30.0	41.95	41.31	40.78	40.25	39.75	39.30
35.0	41.77	41.17	40.66	40.16	39.69	39.26
40.0	41.68	41.11	40.62	40.15	39.70	39.30
45.0	41.67	41.12	40.66	40.21	39.77	39.39
50.0	41.73	41.20	40.76	40.32	39.90	39.53
55.0	41.85	41.34	40.91	40.49	40.08	39.72
60.0	42.04	41.54	41.12	40.71	40.31	39.95
65.0	42.29	41.80	41.38	40.97	40.58	40.23
70.0	42.61	42.11	41.78	41.29	40.90	40.56
75.0	43.01	42.49	42.06	41.65	41.27	40.95
80.0	43.48	42.94	42.49	42.08	41.70	41.41
85.0	44.04	43.46	42.99	42.56	42.20	41.96
90.0	44.71	44.07	43.56	43.12	42.78	42.61
95.0	45.51	44.77	44.21	43.75	43.46	43.40

K vs temperature, t , for water, 2 m KF and 2 m KI are shown in Fig. (32). The changes in the K vs t curves with increasing concentration are slight and gradual. The effects of KI and KF on the compressibility of water are most noticeable when comparing the K vs t curve of water with the K vs t curves of the most concentrated salt solutions.

The computed values of the isothermal compressibilities are good approximations to the correct values but are not precise for either the KI or KF solutions because of the use of heat capacity data at a particular temperature for the determination of the conversion factors over a large range of temperatures.

The values for the isothermal compressibilities, K for all solutions of each salt at each temperature were fit to an equation of the form,

$$K = a + bm + cm^2 + dm^3 \quad (44)$$

where m is the molality and a , b , c , and d are adjustable parameters. All of the resultant equations were differentiated giving

$$\bar{K} = \frac{dK}{dm} = b + 2cm + 3dm^2$$

from which \bar{K} , the partial molal isothermal compressibility of each salt at each of the 20 temperatures and eleven

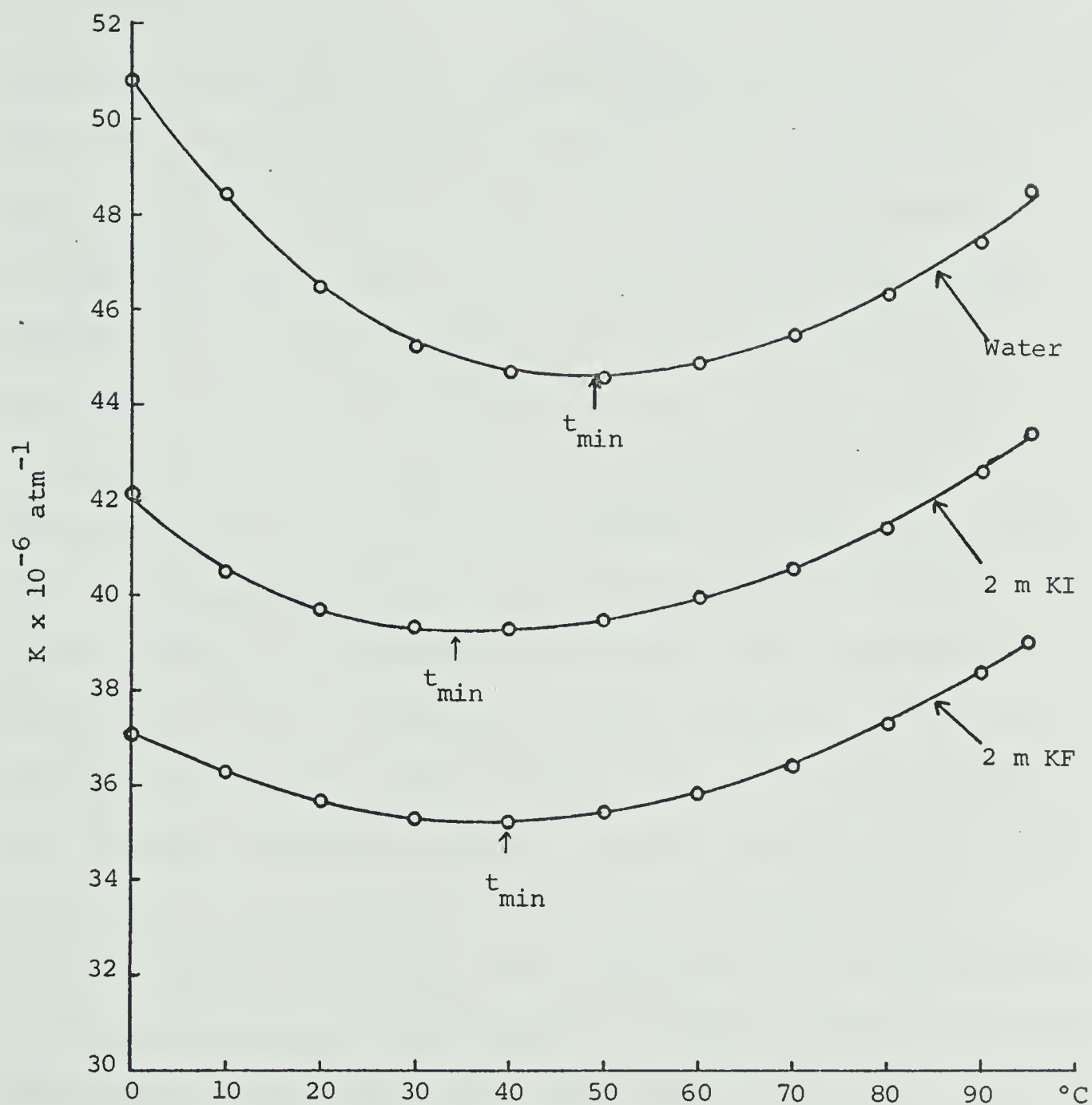


Fig. 32: Isothermal Compressibilities, K , of water and 2 m KI and 2 m KF solutions vs. temperature.

concentrations and also at infinite dilution were determined. These results are shown in Figs. (33,34).

5 - Discussion

Stokes and Robinson (58) discuss the use of compressibility measurements to estimate hydration numbers. The basic idea in this approach to the problem of hydration numbers is that hydrated water molecules are compressed to their maximum extent by the intense electrical forces around the ion and are thus not able to contribute to the compressibility of the fluid. By finding the loss of compressibility caused by introducing ions into water an estimation of the hydration number of the ions is made. But as Stokes and Robinson say, "The compressibility method gives some unexpected results; those (hydration numbers) for the lithium salts are in good agreement with figures obtained by other methods, but the sodium salts give higher hydration numbers, whilst the potassium salts are shown as hydrated to a surprisingly high extent."

It would appear that the above approach to the phenomenon of compressibility, while paying careful attention to the electrostrictive effect of ions in water, neglects the structure-breaking effect of the ions. Since the breakdown of water structure is accompanied by a decrease in the relaxational compressibility of water, as discussed

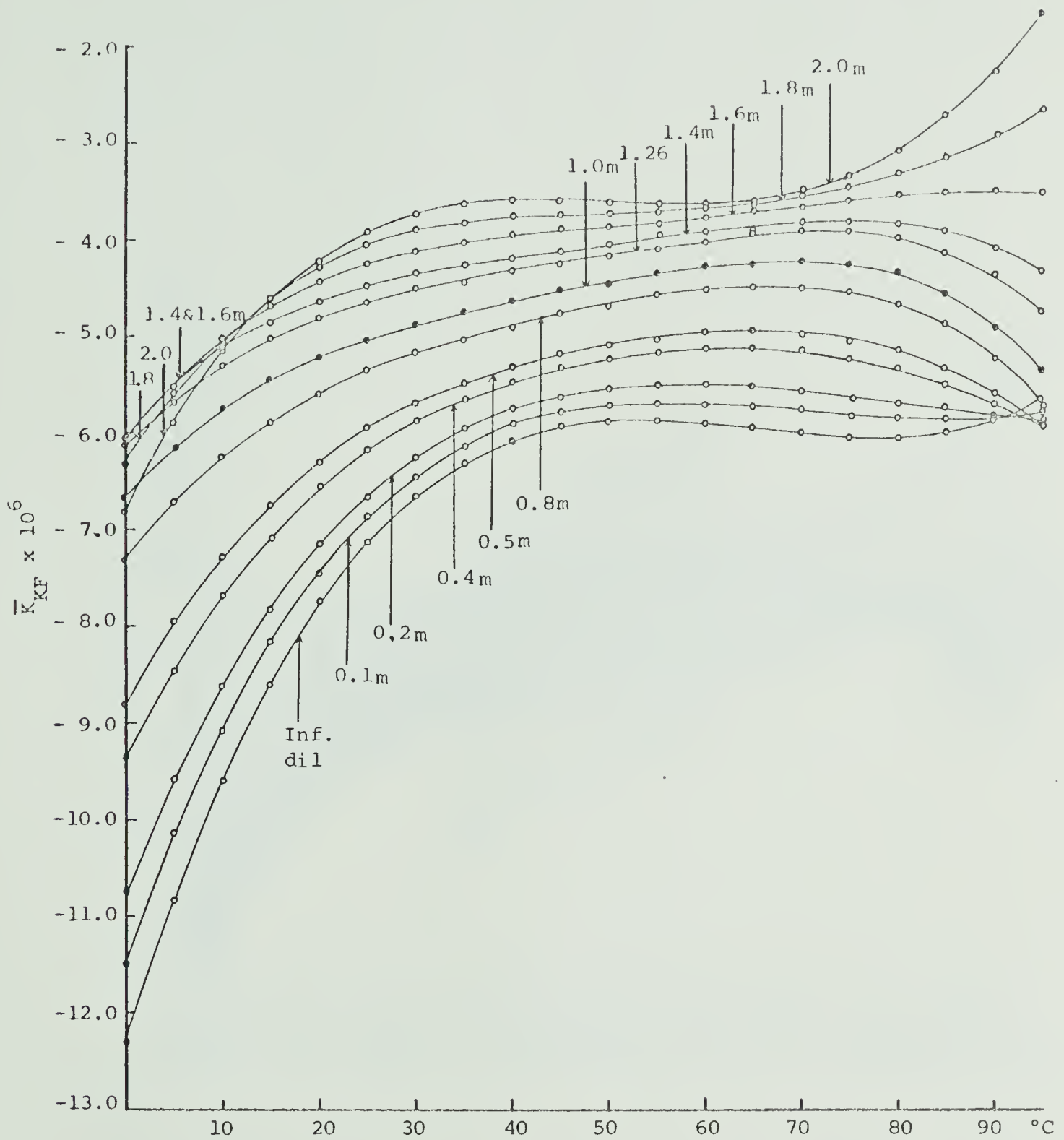


Fig. 33: Partial molal compressibilities of KF, $\bar{\kappa}_{KF}$ vs temperature.

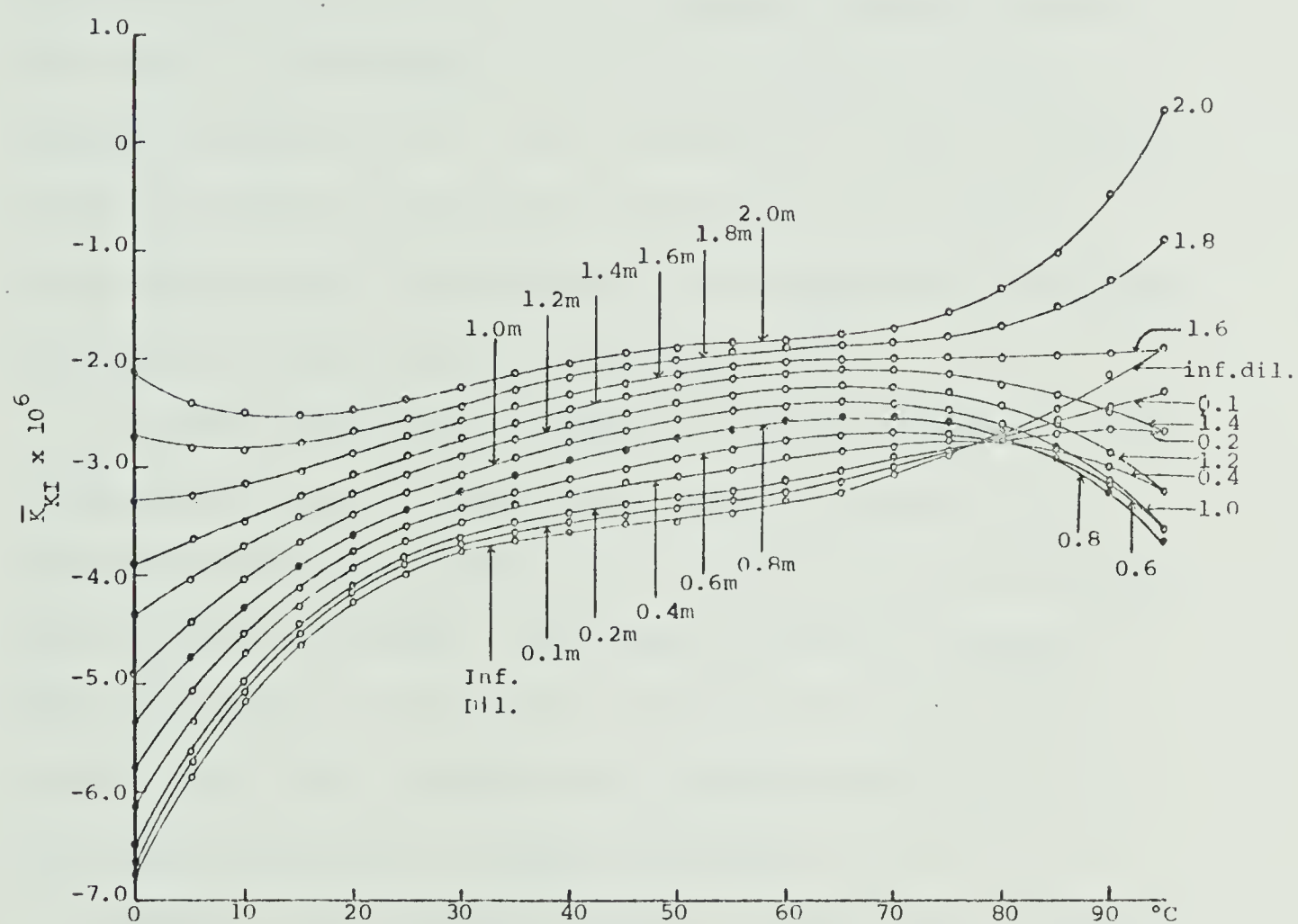


Fig. 34: Partial Molal Iso. Compressibility of KI, $\bar{\kappa}$, vs. Temperature for KI.

in Chapter II, this effect should be considered. Frank's calculations indicate that the sodium ion is a mild structure breaker ($\Delta S^{\text{st}} \text{Na}^+ = 4.0 \text{ e.u.}$) (38) and the potassium ion is an even stronger structure breaker ($\Delta S^{\text{st}} \text{K}^+ = 12.0 \text{ e.u.}$). (38) Thus the breakdown of compressible structures, caused by these ions, will result in a decrease in the compressibility of water. If a part of the compressibility decrease of water, caused by these ions is now attributed to the structure-breaking effect as well as to the hydration effect, it is then easy to understand the experimental findings discussed by Frank and by Robinson. (58)

As was discussed in Chapter II, the minimum in the compressibility vs temperature curve of water is attributed to the relaxational compressibility of water and is proof of bulky, structured species in water. Thus the minima in the K vs t curves of 2 m KI and 2 m KF Fig. (32) indicate the presence of bulky structured species in these solutions.

However, the negative slopes of the K vs t curves of 2 m KI and 2 m KF, Fig. (32) are far less steep than the negative slope of the K vs t curve of water. This indicates that there are fewer structured species in the salt solutions than in pure water.

Fig. (32) also indicates that the compressibilities of 2 m KF are less than those of 2 m KI. The comparatively low compressibilities of the KF solutions are likely caused by the larger proportion of water molecules in the KF solution which are part of highly compressed 'water of hydration' as compared to the proportion of water molecules in the KI solution. This is in agreement with the idea that the F^- ion is more strongly hydrated than the I^- ion.

The curves for the partial molal compressibilities of the KI and KF solutions as a function of temperature, \bar{K}_{KF} vs t and \bar{K}_{KI} vs t , are shown in Figs. (33,34). One of the most striking features of these curves is the strongly negative values for \bar{K}_{KF} and \bar{K}_{KI} in the low temperature region (0° to 35°) and at low concentrations (0 m to 1.0 m). This means that at these temperatures and concentrations a small addition of salt causes a comparatively large decrease in the compressibility of the solution. This behaviour is an indication of the breakdown of H_2O_I by the salts.

As was outlined previously, the simplest explanation of the parts of the \bar{V}_{KI} vs t and \bar{V}_{KF} vs t curves having negative slopes, Figs. (26,27) appears to be that H_2O_{II} is broken down by ions and that this effect increases

with increasing temperature. It appears that this same effect provides the simplest explanation of the parts of the \bar{K}_{KI} vs t and \bar{K}_{KF} vs t curves which have negative slopes.

It seems necessary then to consider three effects in understanding the decreased compressibility of water in salt solutions which are; the electrostrictive effect, \bar{K}^{es} ; the breakdown of H_2O_I , $\bar{K}^{st(I)}$; and the breakdown of H_2O_{II} , $\bar{K}^{st(II)}$. The term \bar{K}^{es} decreases in magnitude with increasing temperature since hydration decreases with increasing temperature. Also the concentration of H_2O_I decreases with increasing temperature, so that it is likely that the breakdown of H_2O_I and thus $\bar{K}^{st(I)}$, also decreases in magnitude with increasing temperature. It is necessary to postulate that $\bar{K}^{st(II)}$ increases with increasing temperature to explain the shape of the \bar{K} vs t curves.

If we assume that in solution the K^+ , F^- , I^- ions have no intrinsic compressibility, it is possible to write

$$\bar{K} = \bar{K}^{es} + \bar{K}^{st(I)} + \bar{K}^{st(II)} \quad (44)$$

\bar{K} will be a negative quantity since \bar{K}^{es} , $\bar{K}^{st(I)}$ and $\bar{K}^{st(II)}$ are all negative quantities.

Generally, the curves for \bar{K} vs t for each successive concentration lie above each other for both salts up to 75° which indicates that the sum of \bar{K}^{es} , and $\bar{K}^{st(I)}$ and $\bar{K}^{st(II)}$ becomes smaller in magnitude with increasing concentration; the strong positive slopes for both \bar{K}_{KF} (1.8 m and 2.0 m) vs t and \bar{K}_{KI} (1.8 m and 2.0 m) vs t above 75° could be due to a sharp decrease in both \bar{K}^{es} and $\bar{K}^{st(II)}$ at these temperatures and concentrations.

At high temperatures and low concentrations the \bar{K}_{KI} vs t curves follow a complex pattern. Above 70° the \bar{K}_{KI} vs t curve for the infinitely dilute solution has a strongly positive slope. As the concentration of KI is increased, the \bar{K}_{KI} vs t curves above 70° have decreasingly positive slopes until the \bar{K}_{KI} vs t curve of 0.4 m KI has a slight negative slope, and the \bar{K}_{KI} vs t curve of 0.8 m KI has the most negative slope of all the solutions; with increased concentration above 0.8 m the \bar{K}_{KI} vs t curves have decreasingly negative slopes so that the slope of the \bar{K}_{KI} vs t curve of the 1.6 m KI solution is the same as that of the 0.2 m KI solution. This would suggest that above 70° , $\bar{K}_{KI}^{st(II)}$ has the most negative values at 0.8 m concentration. Thus it would follow once again that there is a large breakdown of H_2O_{II} at fairly high concentrations of KI when further KI is added to the solution.

5 - Conclusions

This study of the compressibility of salt solutions tends to confirm the findings of the study of the specific volumes of the same solutions in that consideration of both electrostriction and breakdown of H_2O_{II} are necessary to the understanding of the findings. Strictly speaking, it is not necessary to consider the breakdown of H_2O_I in explaining the compressibility results but there is nevertheless evidence for its existence in the \bar{K} vs t curves at low temperatures and salt concentrations.

The findings of Chapters III and IV also agree in both indicating the presence of structured species of water at salt concentrations above 2.0 m, which lends further support to the postulate that salt concentrations of above 3 m of 1:1 electrolytes are needed to completely breakdown water structure above 0°.

The unexpected dependence of the breakdown of H_2O_{II} by KI on the concentration of KI was observed in the studies on both specific volume and compressibility.

The findings of the compressibility study are in accord with the model of water put forward in Chapter I, especially in regard to the existence of H_2O_{II} and its increasing breakdown with increasing temperature.

A general conclusion arising from this study is that data on the specific volumes and compressibilities of KI and KF solutions over the temperature range 0° - 95° and the concentration range 0-2.0 m provides evidence which can only be interpreted simply in terms of the presence of definite structured species in liquid water. Studies on thermodynamic data for pure liquid water indicate that a minimum of three distinct species must be considered. Whether the correct picture of the structure of water requires three species or the infinite number of species postulated by believers in the continuum model of liquid water remains to be determined. However, careful studies of properties such as the specific volume, specific heat, specific viscosity and compressibility of a wide variety of salt solutions ranging from 0.0 m to 5.0 m between the temperatures of 0° and the critical temperature would do much toward a complete understanding of the structure of water and ion-water interactions.

Bibliography

1. Frank, H. S., Federation Proceedings, 24, S-1 (1965).
2. Kavanau, J. L., 'Water and Solute-Water Interactions,' Holden-Day Inc., San Francisco (1964).
3. Rontgen, W. K., Ann. Phys. Chem., (Weid) 45, 91 (1892).
4. Bernal, J. D., and Fowler, R. H., J. Chem. Phys., 1, 515 (1933).
5. Leonard-Jones, T. E., and Pople, J. A., Proc. Roy. Soc. London, A205, 155 (1951).
6. Frank, H. S., and Wen, W.-Y., Disc. Faraday Soc., 24, 133 (1957).
7. Frank, H. S., Proc. Roy. Soc. London, A247, 481 (1958).
8. Pauling, L., in "Hydrogen Bonding." (D. Hadzi and H. W. Thompson, eds.) Pergamon Press, London (1959), p. 1.
9. Frank, H. S., and Quist, A. S., J. Chem. Phys., 34, 604 (1961).
10. Grjotheim, K, and Krogh-Moe, J., Acta. Chem. Scand. 8, 1193 (1954).
11. Wada, G., Bull. Chem. Soc. Japan, 34, 955 (1961).
12. Davis, C. M., and Litovitz, T. A., J. Chem. Phys., 42, 2565 (1961).
13. Wicke, E., Angew. Chem. (International Ed.), 5, 106 (1966).
14. Pimentel, G. C., and McClellan, A. L., "The Hydrogen Bond", Freeman, New York, 1960, pp. 100, 226, 255.
15. Van Thiel, M., Becker, E. D., Pimentel, G. C., J. Chem. Phys. 27, 486 (1957).

16. Wall, T. T. and Hornig, J. Chem. Phys. 43, 2099 (1966).
17. Falk, M. and Ford, T. A., Can. J. Chem. 44, 1699 (1966).
18. Smithsonian Institute Tables, quoted in Handbook of Chemistry and Physics, 47th Ed. p.F-4 (1966-7).
19. Kell, G. S. and Whalley, E., Phil. Trans. Roy. Soc. (London), A258, 565 (1965).
20. Osborne, Stimson, and Ginnings - Bur. of Stand. J. Res. 23, 238 (1939) quoted in Handbook of Chemistry and Physics, 47th Ed. p.D-90 (1966-7).
21. Hall, L., Phys. Rev. 73, 775 (1948).
22. Bingham and Jackson, Bull. Bur. Stand. 14, 75 (1918), quoted in Handbook of Chemistry and Physics, 39th Ed. (1957-8) p. 2036.
23. Walrafen, G. E., J. Chem. Phys., 47, 114 (1967).
(a) Moore, W. J., in "Physical Chemistry", 3rd Edition Prentice Hall, (1964) p. 721.
24. Litovitz, T. A., and Carnevale, E. H., J. App. Phys. 26, 816 (1955).
25. Lieberman, L. N., Phys. Review 75, 1415 (1949).
26. Markham, J. J., Beyer, R. T., Lindsay, R. B., Rev. of Modern Physics 23, 253 (1951).
27. Marchi, R. P. and Eyring, H., J. Phys. Chem., 68, 221 (1964).
28. Nemethy, S., and Scheraga, H. A., J. Chem. Phys. 36, 3383, (1962).

29. (a) Handbook of Chemistry and Physics, 41st Ed. (1959-60)
p. 2260; (b) p. 2264; (c) p. 2314; (d) p. 2148; (e) p. 2246.
30. Eigen, M., and Wicke, E. Z., Electrochem. Angewan. Physik.
Chem. 55, 354 (1951).
31. Wicke, E., Eigen, M., and Ackerman, Th., Z. Physik. Chem.
N. F. 1, 340 (1954).
32. Ackerman, T., Z. Electrochem., Ber. Bunsenges., Physik.
Chem. 62, 411 (1958).
33. Bingham, E. C., J. Phys. Chem. 43, 885 (1941).
34. Latimer, W. M., Pitzer, K. S., and Slansky, C. M.,
J. Chem. Phys., 7, 108 (1939).
35. Jacobson, B., and Heedman, P. A., Acta Chem. Scand. 7,
705 (1953).
36. Scatchard, G., Kavanagh, G. M., Ticknor, J. Am. Chem.
Soc. 74, 3714 (1952); 74, 3724 (1952).
37. Breenberg, L., and Nissan, A. H., Trans. Faraday Soc.,
45, 125 (1949).
- 37a. Walrafen, G. E., J. Chem. Phys. 48, 244 (1968).
- 37b. Bonner, O. D., and Woolsey, G. B., J. Chem. Phys.
72, 899 (1968).
- 37c. Narten, A. H., Danford, M. D., and Levy, H. A.,
Diss. Far. Soc. 43, 97 (1967).
- 37d. Collie, C. H., Hasted, J. B., and Ritson, D. M.,
Proc. Phys. Soc., London B60, 145 (1948).
- 37e. Frank, H. S., Federation Proceedings 24, S-1 (1965).

38. Frank, H. S. and Evans, M. W., J. Chem. Phys. 13, 507 (1945).
39. Buijs, K. and Choppin, G.R., J. Chem. Phys., 39, 2042 (1963).
40. Bingham, E. C., J. Phys. Chem., 43, 885 (1941).
41. Millero, F. J., Rev. Sci. Intr., 38, 1441 (1967).
42. Mukerjee, P., J. Phys. Chem., 65, 740, 744 (1961).
43. Benson, S. W. and Copeland, C. S., J. Phys. Chem., 67, 1194 (1963).
44. Padova, J., J. Chem. Phys., 39, 1552 (1963), 40, 691 (1964).
45. Whalley, E., J. Chem. Phys. 38, 1400 (1963).
46. Harris, F. E. and O'Konski, C. T., J. Phys. Chem., 61, 310 (1957).
47. Ritson, D. M. and Hasted, J. B., J. Chem. Phys. 16, 11 (1948).
48. Fuoss, R. M. and Accasina in "Electrolytic Conductance", Interscience (1959) p. 208.
49. Grahaeme, D. C., J. Chem. Phys., 18, 903 (1950).
50. Bolt, G. H., J. Colloid Sci. 10, 206 (1955).
51. Timmermans, J., "Physico-Chemical Constants of Binary Systems", Vol. 3, Interscience (1960).
52. Diaz Pena, M. and McGlashen, M. L., Trans. Faraday Soc. 55, 2018 (1959).

53. Tyrer, D., J. Chem. Soc. 105, 2534 (1914).
54. Newman and Searle, "The General properties of matter", (Arnold, 1957) p. 133.
55. Bridgman, Amer. J. Sci., 10, 359 (1925).
56. U. S. Bureau of Standards, NSRDS-NBS2, 48 (1965).
57. Jauch, Zeitschrift fur Physik 4, 441 (1921) as quoted in International Critical Tables V, p. 124 (1933).
58. Stokes, R. H. and Robinson, R. A., Electrolyte Solutions (Butterworths 1959) p. 61.

B29902